Atomic Energy Control Board
P.O. Box 1046
Ottawa, Canada
K1P 5S9

Commission de contrôle de l'énergie atomique
C.P. 1046
Ottawa, Canada
K1P 5S9

INFO-0169

CRACK AND FRACTURE BEHAVIOUR IN TOUGH DUCTILE MATERIALS

by

R.D. Venter and D.W. Hoeppner
University of Toronto

A report prepared for the

Atomic Energy Control Board
Ottawa, Canada

October, 1985

REPORT

86-02011/

CRACK AND FRACTURE BEHAVIOUR IN TOUGH DUCTILE MATERIALS

A report prepared by R.D. Venter and D.W. Hoeppner, Structural Integrity Fracture and Fatigue Research Laboratory (SIFFRL), Department of Mechanical Engineering, University of Toronto, under contract to the Atomic Energy Control Board.

SUMMARY

The report describes various approaches and developments pertaining to the understanding of crack and fracture behaviour in touch ductile materials. The fundamental elastic fracture mechanics concepts based on the concepts of energy, stress field, and displacement are introduced and their interrelationships demonstrated. The extension of these concepts to include elasto-plastic fracture mechanics considerations is reviewed in the context of the preferred options available for the development of appropriate design methodologies.

The recommendations of the authors are directed towards the continued development of the J-integral concept. This energy-based concept, in its fundamental form, has a sound theoretical basis and as such offers the possibility of incorporating elasto-plastic fracture mechanics considerations in the crack and fracture behaviour of tough ductile materials. It must however be emphasized that the concise definition of J becomes increasingly suspect as the crack length increases. J is not a material property, as is J_{IC}, but emerges as a useful empirical parameter which is dependent upon the particular geometry and the loading imposed on the structure. It is proposed that 'lowest bound' J-resistance curves and the associated J-T curves be experimentally developed and employed in the design process.

Improvements to these 'lowest bounds' can be developed through extensive analysis of the twin J-CTOA criteria and validation of this approach through near full scale tests.

RÉSUMÉ

Le présent rapport décrit les différentes approches et améliorations relatives à la compréhension du comportement des fissures et des fractures dans les matières ductiles. Les concepts fondamentaux de mécanique des fractures élastiques fondés sur les principes d'énergie, de champ de contrainte et de déplacement sont présentés et leurs rapports sont expliqués. La portée de ces concepts qui comprennent des considérations sur la mécanique des fractures élastoplastiques est examinée à la lumière des options disponibles préférées pour le perfectionnement des méthodes de conception appropriées.

Les recommandations des auteurs visent surtout le perfectionnement du concept de l'intégrale «J». Ce concept basé sur l'énergie, dans son essence, repose sur une base théorique solide et offre, à ce titre, la possibilité d'inclure des considérations sur la mécanique des fractures élastoplastiques dans le comportement des fissures et des fractures dans les matières ductiles. Il faut insister, cependant, sur le fait que la définition de «J» devient de plus

en plus douteuse à mesure que la longueur de la fracture s'étend. «J» n'est pas une propriété matérielle, comme «J_{IC}» par exemple, mais apparaît comme un paramètre empirique utile qui dépend des proportions géométriques particulières et du chargement de la structure. On propose de développer expérimentalement les courbes de résistance «J» les plus basses et les courbes «J-T» associées, et de les utiliser dans la conception.

Il est possible d'améliorer les courbes les plus prudentes par une analyse poussée des critères mixtes «J-CTOA» et une validation de cette approche par des épreuves près de la grandeur réelle.

DISCLAIMER

The Atomic Energy Control Board is not responsible for the accuracy of the statements made or opinions expressed in this publication and neither the Board nor the authors assume liability with respect to any damage or loss incurred as a result of the use made of the information contained in this publication.

ACKNOWLEDGMENT

The authors wish to acknowledge the considerable contributions made by Drs. D. McCammond, A.N. Sinclair, P. Sooley and G.I. Ogundele of the Structural Integrity, Fracture and Fatigue Research Laboratory in the Department of Mechanical Engineering. Their involvement in the preparation, compilation and assessment of the material presented in this report was invaluable.

A special note of thanks is also due to Dr. J. Pachner and Mr. J.K. Pereira of AECB for their active participation during the term of this project.

TABLE OF CONTENTS

A. INTRODUCTION.....1

B. LINEAR ELASTIC FRACTURE MECHANICS.....7

1. General.....7

2. Strain Energy Release Rate, G.....7

3. Stress Intensity Factor, K.....8

4. Crack Opening Displacement, δ.....9

5. Discussion.....9

C. ELASTIC PLASTIC FRACTURE MECHANICS.....17

1. General.....17

2. J-Integral.....17

3. Crack Tip Opening Displacement (CTOD)/Crack Tip Opening Angle (CTOA).....22

4. R-6 Assessment Method and Modifications.....24

5. Discussion.....25

D. STABLE CRACK GROWTH.....35

1. General.....35

2. The J-Integral and Its Derivatives.....36

2.1 J-Integral Resistance Curve.....36

2.2 Tearing Modulus.....37

3. Crack Tip Opening Angle, CTOA.....37

4. J-Integral Crack Driving Force Contours.....38

5. The J-T Approach.....40

6. Summary.....40

E. DUCTILE FRACTURE OF PIPES.....51

1. General.....51

2. Pipe Design Methodology.....51

2.1 J-R Assessment Method.....51

2.2 COD Assessment Method.....53

2.3 R-6 Assessment Method.....54

3. Summary.....55

F. DISCUSSION.....57

G. RECOMMENDATIONS.....60

REFERENCES.....62

NOMENCLATURE.....67

APPENDICES

EVALUATION OF STRUCTURAL COMPONENTS BY J-INTEGRAL TECHNIQUES.....APPENDIX A

FATIGUE CRACK PROPAGATION.....APPENDIX B

A. INTRODUCTION

A CANDU nuclear power plant features three principal closed-loop water systems: the moderator circuit, the primary heat transport (PHT) system, and the steam-feedwater (or secondary) system, as shown in Figure 1-1. Of these three, only the latter two are high pressure circuits with water close to saturation conditions. Structural integrity of the PHT system, which contains on the order of 200 Mg of D_2O, is of crucial concern, as this coolant prevents the reactor core from overheating, with attendant fuel damage. Although the secondary (light water) system does not come into direct contact with the reactor core, a major break in the secondary system could imperil the feedwater supply to the boilers, and thereby lead to a loss of heat sink for the primary coolant. Table 1-1 provides some details and conditions characteristic of large diameter piping employed in a CANDU power plant.

One of the hypothetical accident scenarios evaluated in the safety analysis of every CANDU reactor is a large Loss of Coolant Accident (LOCA). Recently, evidence has been gathering that the assumption of a sudden total break of a large diameter, thin-walled ferritic steel pipe may not be realistic under anticipated plant operating conditions. Such a break would be consistent with a Linear Elastic Fracture Mechanics (LEFM) model, in which there is very little plastic deformation preceding fracture. This model is applicable to components whose "large" thickness, B, prevents any significant distortion in the thickness direction, and confines strain largely to directions perpendicular to the crack front (plane-strain constraint).

The graphs of 'fracture' stress versus crack length in Figure 1-2 illustrate the dependence of crack growth and fracture for each of three specimens with thicknesses B_1, B_2 and B_3 where $B_3 > B_2 > B_1$. These representative conditions for specimen thicknesses B_1, B_2 and B_3 are referred to as plane stress, mixed mode and plane strain fracture respectively. Typically, the specimen of large thickness, i.e. B_3, will fail catastrophically when the stress intensity factor, K_c, at the tip of a crack of size A_1 attains the critical value of K_{Ic}. This is represented by point "O" on the K_{Ic} curve of Figure 1-2. The conservative approach to safety analysis used in CANDU power plants has been to assume that any major pipe failures would occur in such a manner.

However, as shown by Table 1-1, some piping in a CANDU plant is sufficiently thin that significant plastic flow may occur parallel to the front of a hypothetical crack. The fracture mechanism is then a complex mixture of elastic and plastic processes, and an appreciable amount of stable crack extension may take place before final fracture of the component. In Figure 1-2, this is illustrated by the specimen of thickness B_2 with crack size A_1: there is a "pop-in" from points "O" to "P", followed by stable crack growth to "Q", and finally fracture at a significantly higher stress intensity factor than that for the specimen of thickness B_3. Extending this concept even further, for a very thin specimen of thickness B_1, deformation would be predominantly plastic leading to fracture at a stress intensity of $(K_c)_{B_1}$. This is represented by the stable crack growth from point "O" to "R".

For the piping described in Table 1-1, Elastic-Plastic Fracture Mechanics (EPFM) corresponding to thickness B_2 is believed to be appropriate. Unfortunately, methods of analysis are less firmly developed than for fully elastic (B_3) or fully plastic (B_1) fracture modes. An added complication is the possibility of section yielding, as shown in Figure 1-2, where, for a crack of length A_2 in a thin component, yielding can precede the plane stress fracture condition defined by the curve $(K_c)_{B_1}$.

The concepts inherent in analyzing the subcritical growth of an initial flaw and its ultimate fracture are presented in Figure 1-3. This figure clearly illustrates that a considerable database is required which describes the material properties, load history, environment, and inspection standards. This report will concentrate on the row labelled "Associated Conceptual Step", to indicate how the database can be used to predict the likelihood of pipe failure, and failure mode - whether linear elastic, fully plastic, or elastic-plastic.

An elastic-plastic fracture mechanism could provide advance warning of imminent pipe fracture, as the pipe would develop a leak via a through-wall crack well before the crack grew to a critical size. Leak detection devices would then indicate when plant shut-down and pipe inspection were required. Although such an analysis might be applicable to many of the different pipes in a power plant, it is the larger-diameter pipes that are of major concern, as these have the potential for widespread destruction of neighbouring systems, following a sudden pipe fracture. Also, in many cases, the integrity of the large-diameter pipes is more crucial to the controlled cooling of the reactor core than most of the very small pipes such as sample lines. This report, therefore, will concentrate on piping with dimensions, temperatures, and pressures typical of those shown in Table 1-1 for CANDU main PHT pipes, and the main steam pipes on the secondary side of the plant.

Several potential methods of analyzing elastic-plastic fracture in such pipes can be viewed as extensions of linear-elastic theory. A brief review will therefore be provided of LEFM in Chapter B, with an emphasis on the limitations of such methods. The discussion of elastic-plastic fracture mechanics will begin in Chapter C with an outline of the various analysis methods considered for use around the world, followed by a study of crack propagation and instability in Chapter D. In Chapter E, EPFM theory will be applied to the fracture of thin-walled, ferritic steel piping. The discussion and recommendations of Chapters F and G will assess current capabilities and optimum methods for modelling elastic plastic fracture.

Table 1-1: Characteristic Large Diameter Piping in a CANDU Power Plant

1.	Main Heat Transport Pipes (Darlington)	
	material	ASME SA106 carbon steel, grade B, Section III
	outer diameter	24" (.61 m)
	wall thickness	1.53" (3.89 cm)
	operating pressure	9.7 MPa
	operating temperature	20°C - 300°C
2.	Main Steam Feed-Water Pipes (Darlington)	
	material	ASME A-516, code B31.1, grade 70
	operating pressure	5 MPa
	operating temperature	260°C
	outer diameter	30" (.762 m)
	wall thickness	1" (2.54 cm)

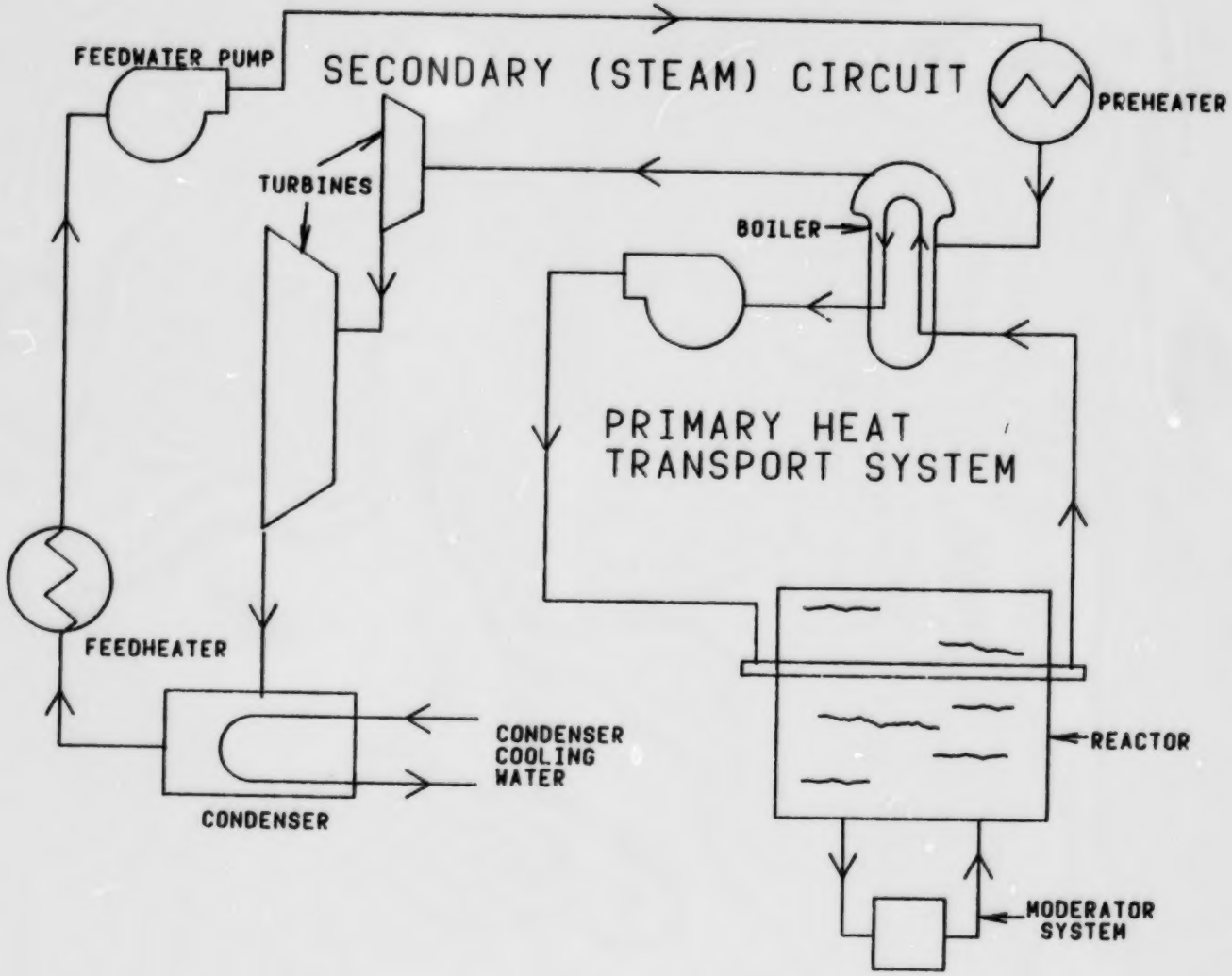

FIGURE 1-1: SIMPLIFIED CANDU SCHEMATIC FLOW DIAGRAM.

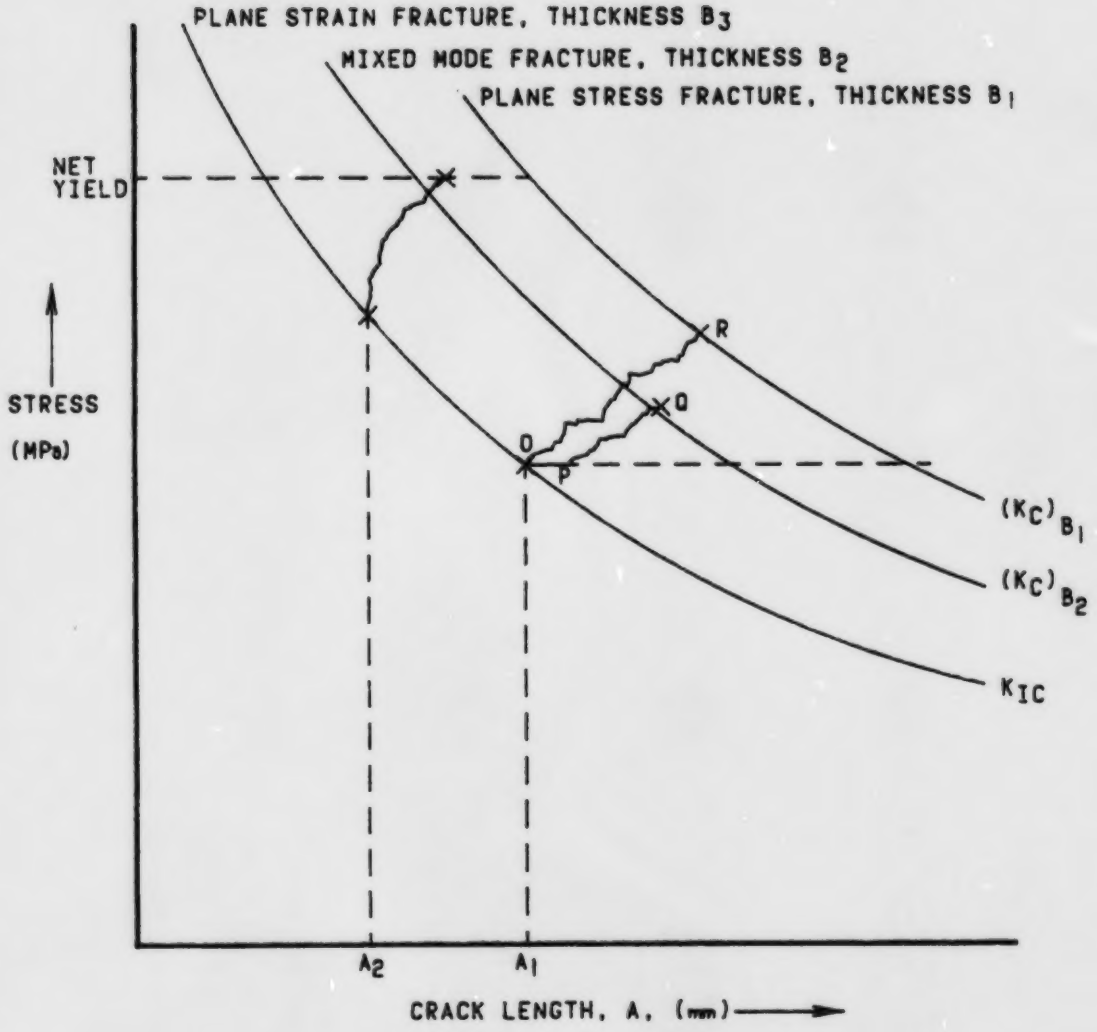

FIGURE 1-2: THE EFFECT OF THICKNESS AND INITIAL CRACK LENGTH ON STABLE CRACK GROWTH DURING PLANE STRESS AND MIXED MODE FRACTURE.

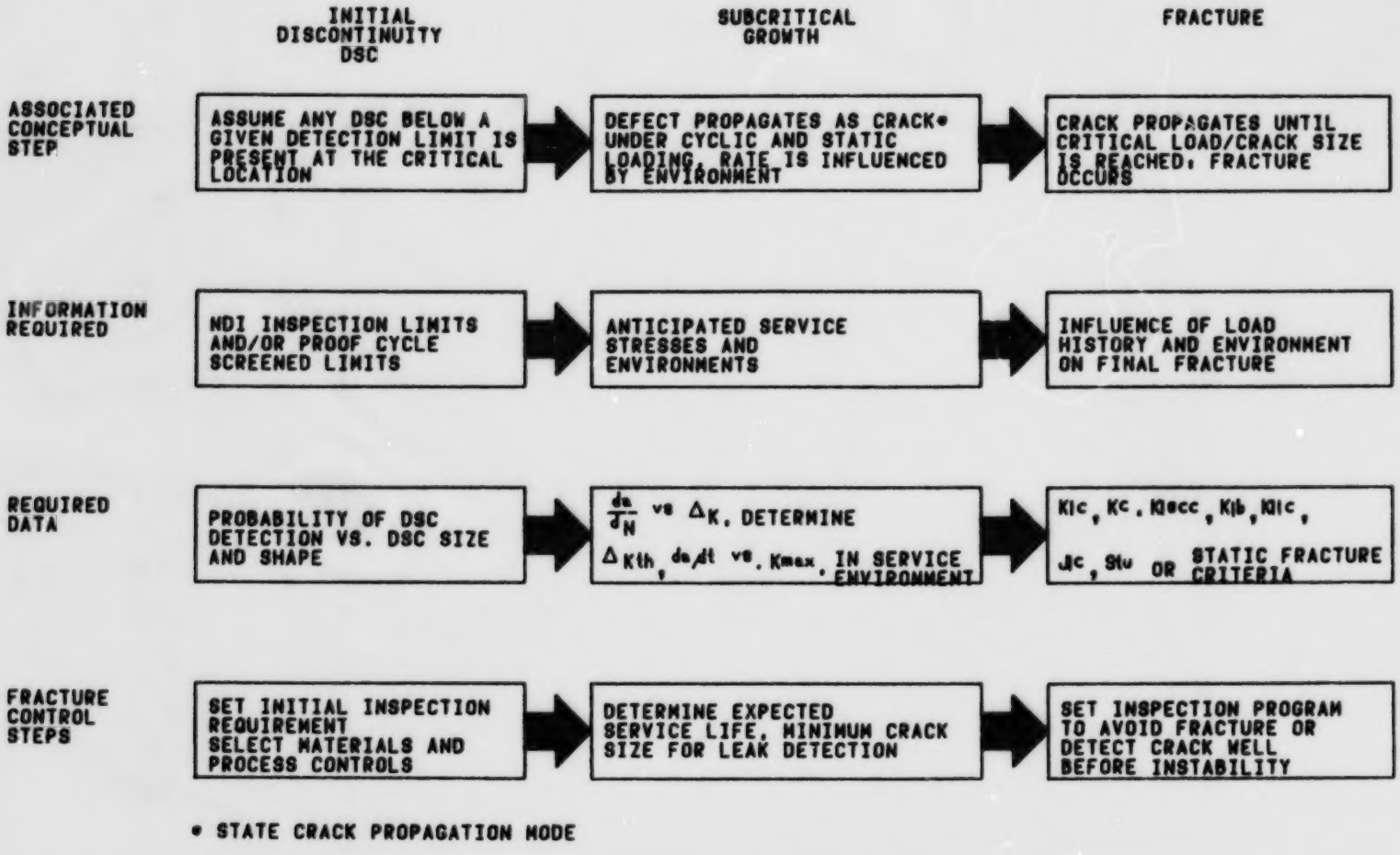
INITIAL DISCONTINUITY DSC
SUBCRITICAL GROWTH
FRACTURE
ASSOCIATED CONCEPTUAL STEP
ASSUME ANY DSC BELOW A GIVEN DETECTION LIMIT IS PRESENT AT THE CRITICAL LOCATION
DEFECT PROPAGATES AS CRACK* UNDER CYCLIC AND STATIC LOADING, RATE IS INFLUENCED BY ENVIRONMENT
CRACK PROPAGATES UNTIL CRITICAL LOAD/CRACK SIZE IS REACHED; FRACTURE OCCURS
INFORMATION REQUIRED
NDI INSPECTION LIMITS AND/OR PROOF CYCLE SCREENED LIMITS
ANTICIPATED SERVICE STRESSES AND ENVIRONMENTS
INFLUENCE OF LOAD HISTORY AND ENVIRONMENT ON FINAL FRACTURE
REQUIRED DATA
PROBABILITY OF DSC DETECTION VS. DSC SIZE AND SHAPE
da/dN vs ΔK, DETERMINE
ΔKth, da/dt vs. Kmax, IN SERVICE ENVIRONMENT
KIc, Kc, Klscc, Kb, KIc,
Jc, Stu OR STATIC FRACTURE CRITERIA
FRACTURE CONTROL STEPS
SET INITIAL INSPECTION REQUIREMENT
SELECT MATERIALS AND PROCESS CONTROLS
DETERMINE EXPECTED SERVICE LIFE, MINIMUM CRACK SIZE FOR LEAK DETECTION
SET INSPECTION PROGRAM TO AVOID FRACTURE OR DETECT CRACK WELL BEFORE INSTABILITY

* STATE CRACK PROPAGATION MODE

FIGURE 1-3: CONCEPTUAL FRACTURE MECHANICS CONSIDERATIONS.

B. LINEAR ELASTIC FRACTURE MECHANICS, LEFM

1. General

Fracture analysis techniques have been developed extensively since the energy analysis published by Griffith (Ref. 1) in 1920. Griffith considered an infinite elastic plate of thickness t, containing a through thickness centre crack of length 2a, subjected to tensile loading (see Figure 2-1), and defined the total energy of the system, U_T, by

$$U_T = U_\ell + U_e + U_s \qquad 2\text{-}1$$

where

U_ℓ = work done by the traction forces at the boundaries
U_e = the strain energy due to the stress field
U_s = the surface energy of the crack surface

Substitution for U_ℓ, U_e and U_s yields

$$U_T = -\frac{\pi a^2 \sigma^2 t}{E} + 4\gamma a t \qquad 2\text{-}2$$

where

σ = applied tensile stress
γ = surface energy
E = Young's Modulus

Minimum energy considerations suggest that a critical stress σ_c will result when $\frac{\partial U_T}{\partial a} = 0$, i.e

$$\sigma_c = \sqrt{\frac{2\gamma E}{\pi a}} \qquad 2\text{-}3$$

Equation 2-3 successfully predicted the strength of glass from a knowledge of surface energy (surface tension), modulus and flaw size but grossly underpredicted the strength of even the most brittle of engineering materials. It was evident that other energy dissipative mechanisms, such as plastic deformation, must be included in the analysis and that their contributions were considerably larger than that of the surface energy term. Subsequent research has been directed at identifying parameters, associated with the stress/strain displacement fields containing the crack tip, which could adequately predict crack propagation or fracture.

2. Strain Energy Release Rate, G

An advantage of the energy approach for predicting the onset of unstable crack growth is that the uncertainty of dealing with the stress field singularity at the crack tip is avoided. This concept is utilized by introducing a quantity, G_c, which represents the total energy (plastic,

surface, etc.) associated with unit length of crack. Equation 2-3 then becomes

$$\sigma_c = \sqrt{\frac{G_c E}{\pi a}} \qquad 2\text{-}4$$

where G_c, the critical strain energy release rate, is a material property. Recognition that three modes of crack opening could occur, Figure 2-2, led to the need for three such parameters, G_{Ic}, G_{IIc}, and G_{IIIc}, to describe a general crack geometry.

3. Stress Intensity Factor, K

The elastic solution of the two-dimensional stress field at the tip of a mode I opening crack (Figure 2-2) can be described by (Ref. 2)

$$\sigma_{ij} = \frac{K_I}{\sqrt{2\pi r}} f_{ij}(\theta) + \ldots \qquad 2\text{-}5$$

where K_I, the stress intensity factor, is given by

$$K_I = \psi\sigma\sqrt{\pi a} \qquad 2\text{-}6$$

and ψ is a function of loading and crack geometry (and equals unity for the geometry considered in Section 1). The remaining terms are dependent upon component geometry but are dominated by the $\frac{1}{\sqrt{r}}$ singularity in the first term.

K_I may be regarded as a single parameter which provides a measure of the magnitude of the stress field around a crack tip and has been regarded as a strong candidate for a fracture correlation parameter. It is postulated that fracture will occur when K_I attains some critical value, K_{Ic}. Equation 2-6 becomes,

$$\sigma_c = \frac{K_{Ic}}{\psi\sqrt{\pi a}} \qquad 2\text{-}7$$

Critical values for mode II and III cracks, K_{IIc} and K_{IIIc}, can also be defined.

In the elastic regime, G_I and K_I are uniquely related by

$$G_I = \frac{K_I^2}{E'} \qquad 2\text{-}8$$

where $E' = E$ for plane stress

$= \frac{E}{1-\nu^2}$ for plane strain, where ν is Poisson's ratio.

4. Crack Opening Displacement, δ

In addition to the energy and stress field parameters described in the previous sections, a displacement parameter, Crack Opening Displacement (COD), has been proposed as a fracture parameter. The term COD, when used as a fracture parameter, refers to the displacement at the base (tip) of the crack and is sometimes called the Crack Tip Opening Displacement, CTOD. To make the confusion complete, the crack opening deflection measured at the line of load application is sometimes refered to as COD. These various deflections are illustrated in Figure 2-3. Again it is postulated that crack growth occurs when δ reaches a critical value, δ_c.

The COD approach recognizes the existence of a plastic zone at the crack tip and therefore has potential application beyond the limits of LEFM. When limited to small scale yielding, it has been shown that

$$G_{Ic} = \alpha \sigma_Y \delta_{Ic} \qquad 2\text{-}9$$

where δ_{Ic} is the critical crack opening displacement in mode I
$\alpha = \pi/4$, (Ref. 3)
$= 1$, (Ref. 4)
and σ_Y = yield strength.

5. Discussion

The three parameters, based on energy, stress field and displacement, described in the previous sections are uniquely related for elastic behaviour by Equations 2-8 and 2-9. In real materials, the stress field singularity cannot be attained and yielding will occur. The size of the plastic zone, r_y, can be described by

$$r_y = \frac{1}{2\pi} \left(\frac{K_I}{\sigma_Y}\right)^2 \quad \text{for plane stress}$$

$$r_y = \frac{1}{6\pi} \left(\frac{K_I}{\sigma_Y}\right)^2 \quad \text{for plane strain} \qquad 2\text{-}10$$

In the presence of this plastic zone, the crack tip becomes "blunt" and crack opening can occur without crack extension. A correction proposed is to include the plastic zone as part of the crack dimension such that Equation 2-6 becomes

$$K_I = \psi \sigma \sqrt{\pi(a + r_y)} \qquad 2\text{-}11$$

Reference to Equation 2-10 reveals that the plastic zone size at a crack tip is not constant through the thickness of the material since the surfaces are in a condition of plane stress, while the interior may be in plane strain, Figure 2-4. It is clear that the energy to fracture and the toughness measured will therefore be dependent on the specimen thickness, Figure 2-5. Consideration of the "worst case" has led to the lower asymptote being used as the fracture toughness parameter. K_{Ic} as a material property, is defined

as the plane strain fracture toughness. In order to ensure that a fracture toughness measurement is on the lower plateau shown in Figure 2-5, specimens of appropriate thickness must be tested. LEFM is considered applicable providing the plastic zone, as defined by r_y, is much smaller than either the region dominated by the first term of Equation 2-5 or any of the specimen dimensions, e.g. crack length, specimen width, etc.

The testing procedures and specimen geometries permitted for approved K_{Ic} measurements are defined in ASTM:E399-83. Plane strain conditions are assured by requiring that specimen thickness and crack length exceed

$$\left(\frac{K_{Ic}}{\sigma_Y}\right)^2$$

This is equivalent to restricting the plastic zone size such that, even at the surface

$$B \text{ or } a > 15r_y \qquad 2\text{-}12$$

A discussion of the limitations, advantages and disadvantages of the parameters described in sections 2 to 4, together with several other methods of fracture analysis* has been condensed and is presented in Figure 2-6.

---

* R.B. Scarlin and M. Shakeshaft, Metals Technology, "Limitations of Some Methods of Establishing Fracture-toughness Data", Vol. 8, 1981.

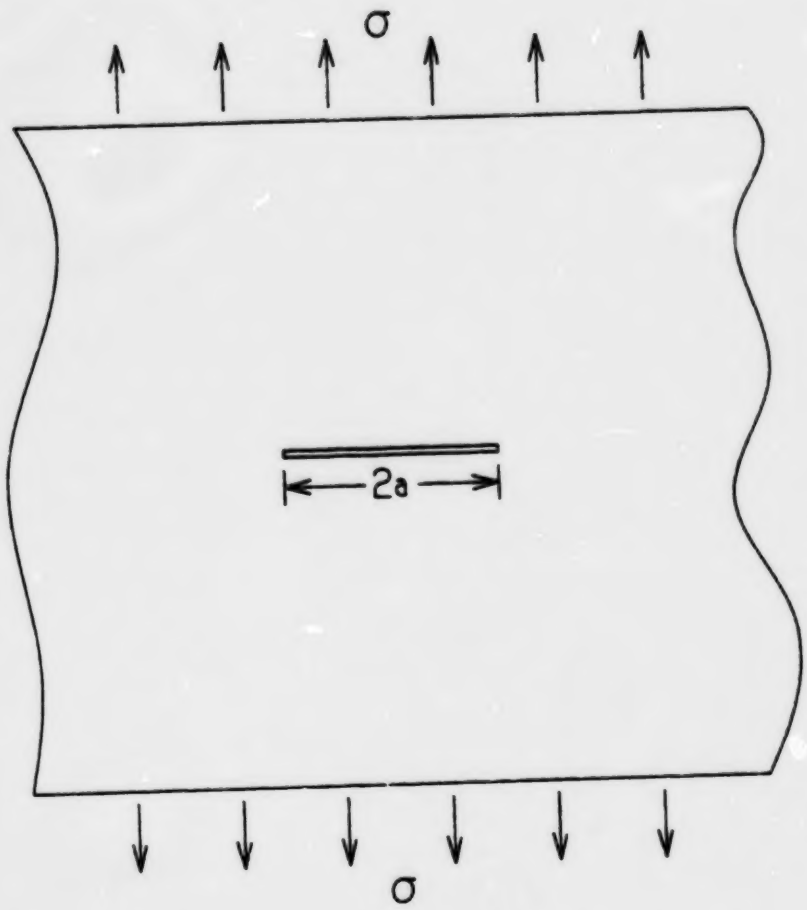

FIGURE 2-1: INFINITE, CENTER CRACKED PLATE.

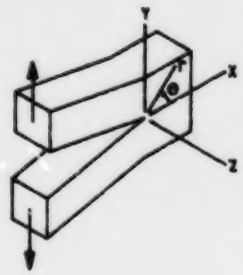

MODE I

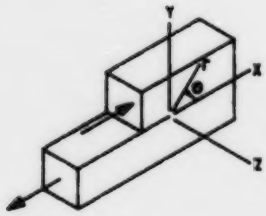

MODE II

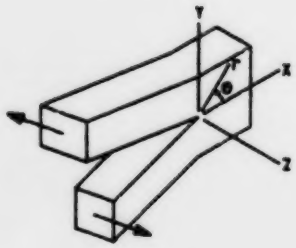

MODE III

FIGURE 2-2: FRACTURE MODES.

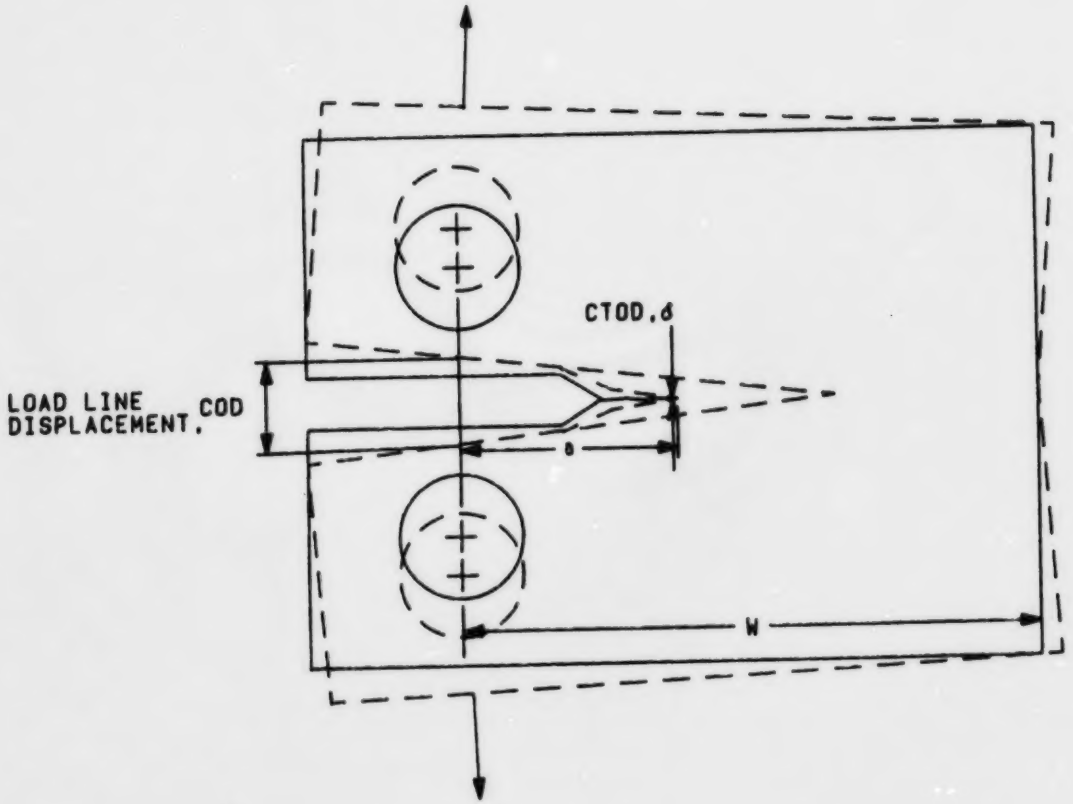

FIGURE 2-3. DEFINITIONS OF COD AND CTOD.

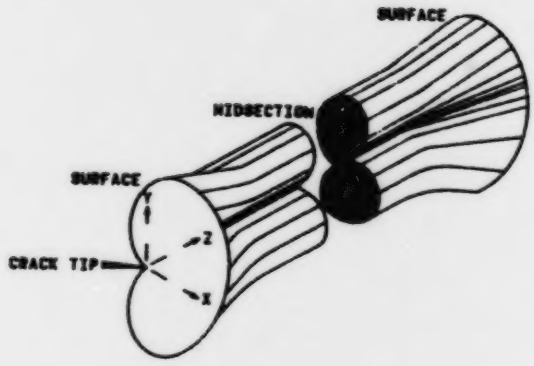

FIGURE 2-4: PLASTIC ZONE VARIATION THROUGH THICKNESS.

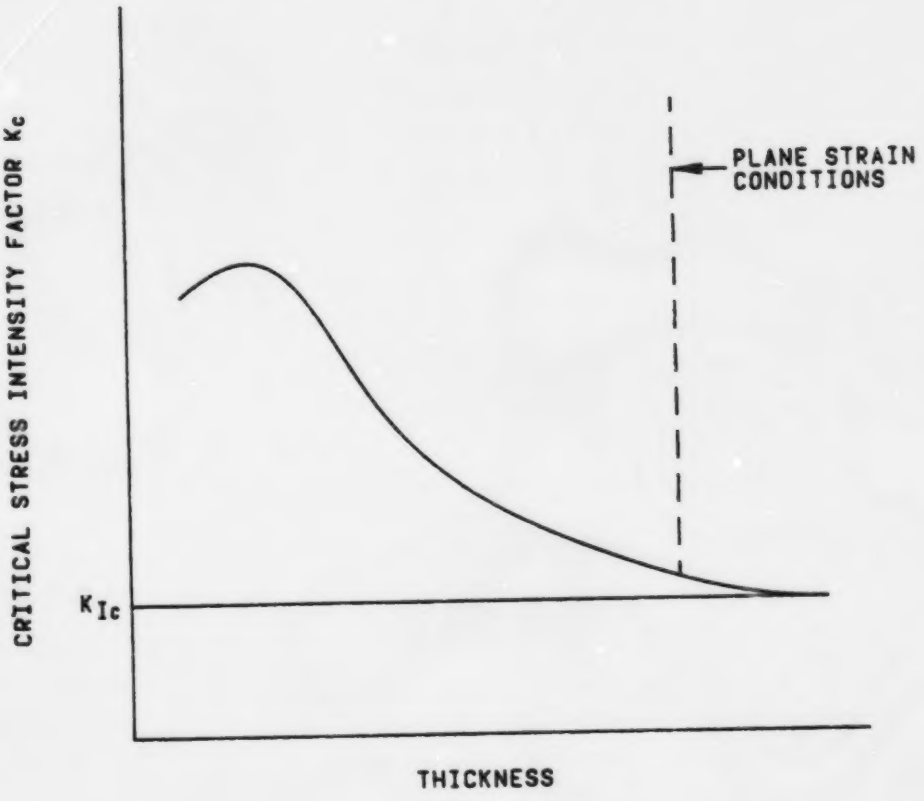

FIGURE 2-5: EFFECT OF THICKNESS ON CRITICAL STRESS INTENSITY FACTOR.

NO	NAME OF METHOD	MATHEMATICAL CONCEPTS
1.	K_{IC} ASTM E 399	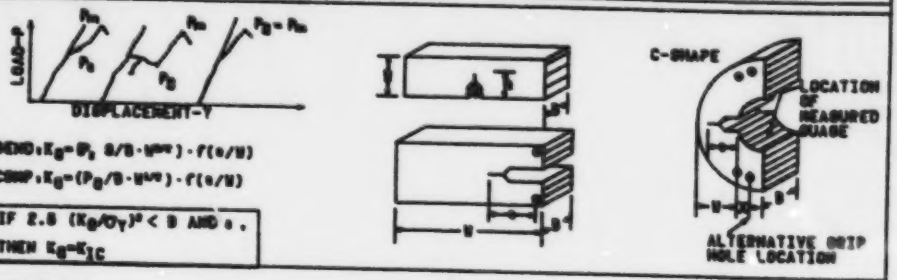 BEND: $K_Q = P_Q S/B \cdot W^{3/2}) \cdot f(a/W)$ COMP: $K_Q = (P_Q/B \cdot W^{1/2}) \cdot f(a/W)$ IF 2.5 $(K_Q/\sigma_Y)^2 < B$ AND a, THEN $K_Q = K_{IC}$
2.	J-INTEGRAL ASTM E 813-81	$J = 2U/B(W-a)$ J_{IC} = THE POINT OF THE FIRST CRACK EXTENSION, = K_{IC} $K_J = \sqrt{J_{IC} E/(1-\nu^2)}$ - FOR PLANE STRESS $K_J = \sqrt{J_{IC} \cdot E}$ FOR PLANE STRESS $r_p = (1/2\pi) \cdot (K/\sigma_Y)^2$ - PLASTIC ZONE SIZE FACTOR 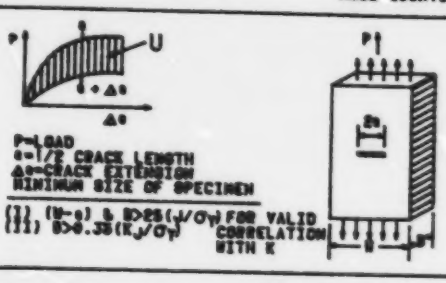 P=LOAD a=1/2 CRACK LENGTH Δa=CRACK EXTENSION MINIMUM SIZE OF SPECIMEN (I) $(W-a)$ & $B \geq 25(J/\sigma_Y)$ FOR VALID (II) $B \geq 0.35(K_J/\sigma_Y)^2$ CORRELATION WITH K
3.	C.O.D. BRITISH STANDARD (I) BS DD 19 (II) ASK-AAN-220	$K_{COD} = (r \sigma_Y E \cdot \delta)$ r = CONSTANT = 1 TO 2 δ = CRITICAL CRACK OPENING DISPLACEMENT AT THE CRACK TIP WHEN THE FIRST CRACK EXTENSION OCCURS (ANALOGOUS TO J-INTEGRAL) 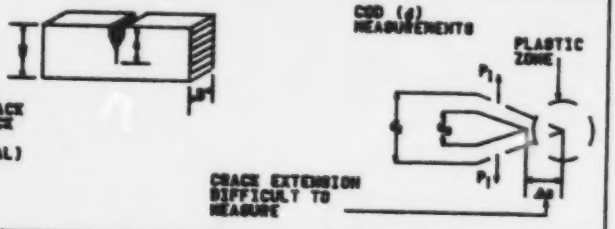
4.	SIMPLE EQUAL-ENERGY	$K_{EE} = \frac{b^{1/2} \cdot P_Q}{B \cdot D^{1/2}} \cdot f(a/W)$ b = RATIO OF AREAS UNDER RATIONALIZED LOAD-DEFLECTION CURVE AT A CRITICAL POINT. P_Q = CRITICAL LOAD $f(a/W)$ = SPECIMEN COMPLIANCE FUNCTION
5.	INSTRUMENTED CHARPY IMPACT TESTING	·ANALYSIS OF LOAD-DISPLACEMENT ·DIAGRAMS ·FOR VALID K_{ID}: ·$B_{MIN} > 0.2(K_{ID}/\sigma_Y)^2$ K_{ID} = DYNAMIC FRACTURE TOUGHNESS 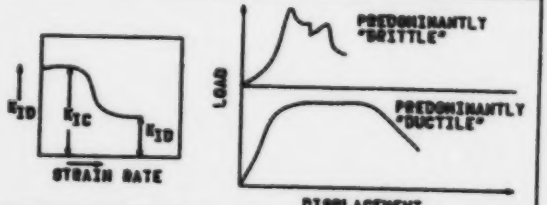
6.	EMPIRICAL METHODS PER BEGLEY & LOGSDON	EMPIRICAL RELATIONSHIP BETWEEN K_{IC} & CHARPY ABSORBED ENERGY V. TEMPERATURE CURVE: $K_{IC} = \sigma_Y \left(\frac{5.66 \Delta I - 0.0063}{\sigma_Y}\right)^{1/2}$ FOR BCC BRITTLE APPEARANCE ΔI = ENERGY ABSORBED IN CHARPY IMPACT TESTS (JOULES) σ_Y = YIELD STRENGTH (N/m^2) $K_{IC} = 0.071 \sigma_Y$ FOR LOW TEMPERATURE AND BCC BRITTLE APPEARANCE. 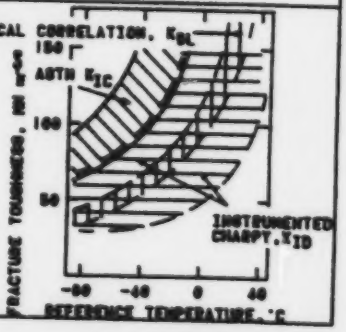

FIGURE 2.6: COMPARISON OF FRACTURE MECHANIC ANALYSIS AND TESTING METHODS (CONDENSED FROM "LIMITATIONS OF SOME METHODS OF ESTABLISHING FRACTURE-TOUGHNESS DATA" BY R.B.SCARLIN & M. SHAKESHAFT, METALS TECHNOLOGY, JAN. 1981 VOLUME 8 PART 1)

NO	NAME OF METHOD	DISADVANTAGES
1.	K_{IC} ASTM E 399	1 HIGH COST OF TESTING LARGE SPECIMENS REQUIRED FOR HIGHER TEMPERATURE TENDS TO REDUCE THE NUMBER OF DATA POINTS FOR THE ASSESSMENT. 2 LINEAR EXTRAPOLATION FROM VALID KIC AT LOWER TEMPERATURE TO HIGHER TEMPERATURE PRODUCES EXCESSIVE CONSERVATISM. 3 NO VALID KIC VALUES AT HIGHER TEMPERATURE. OTHER METHODS (J-INT., COD & EQ.-EN.) WITH SMALLER SPECIMENS CAN BE USED TO GET VALID DATA AT HIGHER TEMPERATURE.
2.	J-INTEGRAL ASTM E 813-81	1 J-INT IS NOT ABLE TO EVALUATE IRREGULAR CRACK PROPAGATION DUE TO RESIDUAL STRESS OR AT H.A.Z. NEAR WELDS. 2 NOT ACCURATE ENOUGH AT LOW TEMPERATURE. 3 MEASUREMENTS ARE INACCURATE DUE TO IRREGULAR CRACK FRONTS. 4 NOT VALID FOR THIN MATERIALS WHERE K_J IS 2.5 K_{IC}. 5 WHEN HEAT TINTING IS USED, THE ADDITIONAL NUMBER OF SPECIMENS ADDS TO TESTING COSTS.
3.	C.O.D. BRITISH STANDARD (I) BS DD 19 (II) ASK-AAN-220	1 VARIATIONS IN THE MEASUREMENT OF δ RESULTS IN VARIATIONS OF K_{IC} OF UP TO A FACTOR OF 2. 2 COD METHOD RESTRICTED TO TEMPERATURES ABOVE -60 °C.
4.	SIMPLE EQUAL-ENERGY	1 LIMITATIONS ARE SIMILAR TO THOSE FOR J-INTEGRAL. 2 THIS METHOD IS MORE EMPIRICAL IN NATURE, SO THAT THE J-INTEGRAL TESTING IS PREFERRED.
5.	INSTRUMENTED CHARPY IMPACT TESTING	1 INSTRUMENTED-CHARPY & EMPIRICAL METHODS CAN PROVIDE EXTREMELY PESSIMISTIC VALUES, PARTICULARLY AT HIGHER TEMPERATURES. 2 FRACTURE TOUGHNESS (K_{IC}) IS SLIGHTLY UNDER-ESTIMATED AT LOW TEMPERATURES, BUT CONSIDERABLE SCATTER OF MEASUREMENTS EXISTS ABOVE BRITTLE-TRANSITION TEMPERATURE WITHIN FACTOR OF 3. THIS SCATTER IS DUE TO SMALL SIZE OF SPECIMENS. 3 DIFFICULTY IN SEPARATING THE CRACK-INITIATION & CRACK-PROPAGATION COMPONENTS OF THE FRACTURE PROCESS.
6.	EMPIRICAL METHODS PER BEGLEY & LOGSDON	2 THIS METHOD CANNOT GIVE INFORMATION RELEVANT TO SMALL REGIONS SUCH AS H.A.Z. AT WELDS, CASTINGS, OR MATERIALS OTHER THAN THE FERRITIC STEELS.

FIGURE 2-6: (CNT.)

NO	NAME OF METHOD	ADVANTAGES
1.	K_{IC} ASTM E 399	1 THIS METHOD IS THE MOST RELIABLE TO GET FRACTURE TOUGHNESS VALUES AT LOWER TEMPERATURES. THE SUCCESS OF ALL OTHER METHODS WAS JUDGED/COMPARED TO THEIR ABILITY TO GIVE DATA COMPARABLE TO THIS METHOD.
2.	J-INTEGRAL ASTM E 813-81	1 J-INTEGRAL, COD & EQUAL-ENERGY METHODS PROVIDE FRACTURE-TOUGHNESS VALUES WHICH AGREE WITH ASTM K_{IC} METHOD. 2 J-INTEGRAL, COD & EQUAL-ENERGY METHODS YIELD REALISTIC FRACTURE-TOUGHNESS DATA AT HIGHER TEMPERATURES. 3 J-INT. METHOD POSSESSES THE ADVANTAGE (OVER COD & EQ.-EN.) OF HAVING SOUND THEORETICAL BASIS, WHICH PERMITS EVALUATION OF THE STABLE CRACK GROWTH. 4 DETERMINATION OF dJ/da IS A MEASURE OF THE RESISTANCE TO CONTINUED CRACK PROPAGATION. 5 TESTING OF MANY SMALL J-SPECIMENS PROVIDES AN INDICATION OF MATERIAL TOUGHNESS VARIATION THROUGHOUT, FOR EXAMPLE, A LARGE FORGING OR CASTING.
3.	C.O.D. BRITISH STANDARD (I) BS DD 19 (II) ASK-AAN-220	3 COD RESULTS HAVE SHOWN GOOD CONSISTENCY AND COMPARABILITY WITH TOUGHNESS VALUES CALCULATED USING OTHER METHODS. 4 SIMULTANEOUS MEASUREMENTS OF COD & J-INT. IS POSSIBLE FOR A MINOR EXTRA COST.
4.	SIMPLE EQUAL-ENERGY	3 TOUGHNESS DATA ARE IDENTICAL OR CLOSELY SIMILAR TO J-INTEGRAL DATA.
5.	INSTRUMENTED CHARPY IMPACT TESTING	1 INSTRUMENTED-CHARPY, IMPACT & EMPIRICAL METHODS REQUIRE SMALL SPECIMENS. 2 CHARPY TESTING IS PRACTICALLY SUITED FOR DETERMINATION OF TOUGHNESS VARIATIONS IN SMALL REGIONS OF COMPLEX PARTS, IN H.A.Z. OF WELDS & OTHER LOCALLY EMBRITTLED ZONES. 3 ERROR IN K_{IC} IS SMALL (IN COMPARISON WITH ASTM K_{IC}) FOR PREDOMINANTLY BRITTLE FAILURE.
6.	EMPIRICAL METHODS PER BEGLEY & LOGSDON	2 EMPIRICAL METHOD OFFERS A RAPID & AN INEXPENSIVE TECHNIQUE TO ESTIMATE FRACTURE-TOUGHNESS (K_{IC}) FOR WROUGHT FERRITIC STEELS. 3 THIS METHOD INDICATES THAT CHARPY K_{IC} VALUES ARE SCATTERED AND LIE ENTIRELY BELOW ASTM K_{IC} DATA, CONSERVATIVE BY A FACTOR OF UP TO 3. 4 K_{IC} BY THIS METHOD PROVIDES NARROW SCATTER BAND WITH THE RESULTS BELOW ASTM K_{IC} BY A FACTOR OF 2.

FIGURE 2-6: (CNT.)

C. ELASTIC PLASTIC FRACTURE MECHANICS

1. General

Elastic-plastic fracture mechanics (EPFM) can be viewed as a development of Linear Elastic Fracture Mechanics (LEFM), providing crack tip solutions which predict fracture in structures with small and large scale plasticity.

A prime fracture parameter in this regime is the J-integral. This method of approach retains many of the assumptions of LEFM; in fact, the only one relaxed is the assumption of linear elasticity, small strain non-linear elasticity being allowed (Ref. 5).

Another approach is the COD method which in the linear elastic regime can be related to G_{Ic} and K_{Ic} (see Chapter B., 3.). This approach has been successful in correlating cleavage fracture in both notched bars and standard fracture toughness specimens. The COD method attempts to provide a measure of the critical plastic strain to fracture for materials under more 'ductile' non-cleavage failure mechanisms (Ref. 4). This method is considered viable in cases where large amounts of plastic deformation accompany fracture, i.e. well above the transition temperature in the case of body-center-cubic (bcc) materials such as ferritic steels (Ref. 5).

The failure assessment diagram approach referred to as the R-6 method, has also been developed to integrate the LEFM parameter, K, and plastic collapse parameter, S_r. Essentially, this method attempts to describe the validity limits of LEFM based on the calculations of the ratios of the linear elastic stress intensity factor to the plane strain fracture toughness and the applied load to the plastic collapse load.

The following sections provide amplification of these fracture correlating parameters and discuss the assumptions inherent in their formulation, their ease of determination and their limitations.

2. J-integral

An elastic-plastic crack tip solution for power hardening solids under symmetric opening loads was first proposed by Hutchinson (Ref. 6) and Rice and Rosengren (Ref. 7), and is often referred to as the HRR solution. It was shown that the HRR stress and strain fields approach a $\frac{1}{r}$ singularity as $r \to o$. For stationary cracks, the HRR field equations are (Ref. 8)

$$\sigma_{ij} = \sigma_Y \left[\frac{EJ}{\sigma_Y^2 I_n r}\right]^{\frac{1}{n+1}} \tilde{\sigma}_{ij}(\theta,n)$$

3-1

$$\varepsilon_{ij} = \frac{\sigma_Y}{E} \left[\frac{EJ}{\sigma_Y I_n r}\right]^{\frac{1}{n+1}} \tilde{\varepsilon}_{ij}(\theta,n)$$

where n and σ_Y are the flow parameters, strain hardening and yield stress, respectively; r and θ are polar coordinates centered at the crack tip; I_n is

an integration constant which is a function of n only, and $\tilde{\sigma}_{ij}$ and $\tilde{\varepsilon}_{ij}$ are dimensionless functions of θ and n only.

The amplitude of the asymptotic crack-tip singularity fields given by Equation 3-1 is J, which was defined in a later work by Rice (Ref. 9) for any closed contour surrounding a crack tip. Rice (Ref. 9) showed that J is a path independent integral which characterizes the stress-strain field surrounding a notch tip in two-dimensional deformation fields of linear or non-linear elastic materials. The J-integral is expressed mathematically as (refer to Figure 3-1)

$$J = \oint_{\Gamma} \left(Wdy - \hat{T}_i \frac{\partial \hat{u}_i}{\partial x} ds\right) \qquad 3\text{-}2$$

where W is the strain energy density, $\hat{T}_i$ is the traction vector defined by the outward normal, n, along the arc Γ, $\hat{T}_i = \sigma_{ij} n_j$, $\hat{u}_i$ is the displacement vector and s is the arc length along Γ.

Furthermore, it can be shown that the J-integral is precisely path independent for nonlinear elastic materials conforming to deformation plasticity theory (Figure 3-2(a)) and substantially path-independent for numerical solutions of incrementally plastic materials conforming to flow theory (Figure 3-2(b)) (Ref. 10).

Since the energy line integral reflects the crack tip deformation field, Rice further interpreted J as the potential energy difference between two identically loaded bodies of unit thickness with slightly different crack sizes, and stated mathematically that

$$J = -\frac{\partial U}{\partial a} \qquad 3\text{-}3$$

where U is the potential energy and a is the crack size.

If the contour Γ is chosen to fall within the region dominated by the K-field for small scale yielding, J is simply equal to G, the crack driving force, i.e.

$$J_I = G_I = \frac{K_I^2}{E'} \text{ (linear elastic)} \qquad 3\text{-}4$$

where K_I is the mode I stress intensity factor (see Figure 2-2) and E' is defined in Equation 2-8.

In the general elastic-plastic problem, where deformation is not reversible, J loses its physical significance as a crack driving force. Hence the energy interpretation of J-integral cannot be applied to the process of crack extension. In this respect J as a fracture correlating parameter is restricted to crack initiation rather than propagation.

A number of expressions for J developed recently but following the pioneering work of Rice (Ref. 9) are summarized in Table 3-1. Included in

the table are the various assumptions on which the derivations are based. All of the above works generally endorsed the use of J integral for applications involving small and large scale plastic deformations. A review of Table 3-1 illustrates the difficulty associated with the accurate evaluation of the J parameter. Begley and Landes (Ref. 16) were the first to successfully develop an experimental evaluation of J for two alloy steels, NiCrMoV rotor steel and A533B pressure vessel steel. In the same work, a critical value of J, J_{Ic}, was defined as a fracture criterion referring to crack initiation under plane strain conditions from elastic to fully plastic behaviour. Later experimentation by Landes and Begley (Ref. 17) determined J_{Ic} from measurement of the critical value of load-line displacement. Both works (Refs. 16,17) recognized that defining crack initiation and determining its onset make measurement of J_{Ic} difficult. However, consistent results were found with the J_{Ic} and LEFM interpretation of G_{Ic} using Equation 3-4. A summary of the experimental procedure due to Bucci et. al (Ref. 12) is presented in Figure 3-3. For a typical test specimen configuration (Figure 3-3(a)), load-displacement (P-δ) records are obtained for a number of constant crack lengths as shown in Figure 3-3(b).

For given values of deflection, δ, the area under each load-displacement record, U (the pseudo-potential energy) is normalized per unit thickness to yield U/B. This is then plotted against crack length, a (Figure 3-3(c)). This permits evaluation of a J versus δ relationship for a given crack size as shown in Figure 3-3(d).

Utilizing this approach, Griffis (Ref. 18) constructed a material resistance curve (J versus crack extension, Δa), as shown in Figure 3-4. The J-Δa curve was generated from J-integral values obtained from the P-δ curve according to

$$J = \frac{2U}{B(W-a)} \qquad 3\text{-}5$$

where B is the specimen thickness and W-a is the length of the uncracked ligament.

The J-Resistance curve provides valuable data from which a critical value of J, J_{Ic}, is defined by the intersection of the resistance curve with the ordinate $\Delta a = 0$. Griffis (Ref. 18) also verified experimentally that a minimum size (thickness) requirement for J_{Ic} is

$$B,\ W-a,\ a > 50\ \frac{J_{Ic}}{\sigma_y} \qquad 3\text{-}6$$

In addition to the above measurements, other estimation procedures for J are summarized in Table 3-2. Because of the geometry dependence of J, and assuming that method 1 (experimental compliance technique) in Table 3-2 gives an accurate estimate of the contour integral J, Chipperfield, (Ref. 19), uses a deviation parameter, R_n:

Table 3-1

J-INTEGRAL ANALYTICAL EXPRESSIONS

AUTHOR(S)/YEAR	J-INTEGRAL EXPRESSION	ASSUMPTIONS/ASSERTIONS	FURTHER REMARKS	REFERENCE NO.
Rice (1968)	$J = \int_\Gamma \left(W dy - \vec{T} \frac{\partial \vec{u}}{\partial x} ds \right)$ $W = W(\varepsilon) = \int_0^\varepsilon \sigma_{ij} d\varepsilon_{ij}$	- Homogeneous body - Linear and non-linear elastic material - Two-dimensional deformation, i.e. plane strain, generalised plane stress, anti-plane strain - Stress-strain singularity for large scale yielding at crack tip	- Parameter is path independent	9
	$J = \int_\Gamma W dy$	- Path close to notch tip - Smooth-ended notch T = 0	- Integral depends on local field	
	$J = \frac{1-\nu^2}{E} K_I^2$	- Small scale yielding under plane strain, purely elastic loading		
	$J = \frac{1-\nu^2}{E}\left(K_I^2 + K_{II}^2\right) + \frac{1+\nu}{E} K_{III}^2$	- Small scale yielding - Linear isotropic elastic material - Generalised loading	- Small non-linear zone at a notch tip negligibly affects overall compliance of a notched body	
	$J = -\frac{\partial U}{\partial a}$	- Energy considerations - Potential energy of identically loaded body of different crack length		
Blackburn (1972)	$J^* = \lim_{\rho \to 0} \int \left(\frac{1}{2} \sigma_{ij} \frac{\partial u_j}{\partial x_1} dx_2 - T_i \frac{\partial u_i}{\partial x_1} ds \right)$	- Non-homogeneous, non-elastic material	- Path independent	11
	$J^* = J$	- Linear elastic material		
Bucci et al (1972)	$J = -\partial(U/B)/\partial a$ $U/B = \iint_A W dx dy - \int_{L_\sigma} \vec{T} \cdot \vec{u} \, ds$	- U/B is the potential energy normalised per unit thickness - elastic-plastic material		
	$J = -\frac{\delta}{B} \frac{\partial P}{\partial a}$	- Limit load approach providing rigid plastic expression for J - That J can be evaluated from single load-displacement curve	- For rigid plasticity, J is linearly related to δ	12
Merkle and Corten (1974)	$J = \frac{2}{b} \int_0^\Delta \left(\frac{P}{B} \right) d\Delta$	- Using compact specimen, b is size of uncracked ligament	- (Δ) includes elastic and plastic displacement of load	13
Sumpter and Turner (1976)	$J = J_e + J_p$ $= \frac{\eta_e U_e}{(W-a)B} + \frac{\eta_p U_p}{(W-a)B}$	- Applicable to any geometry - Separates elastic and plastic components	- Requires knowledge of elastic compliance and limit load - η_e and η_p are geometry dependent	14
Derbalian (1983)	$J_{\substack{\text{gen.} \\ \text{plas.}}} = -\frac{1}{kB} \frac{\partial k}{\partial a} \int f \, d\delta$	- Energy based derivation for general plasticity - Good approximation achieved for all geometries - Tolerates small amount of plasticity	- Limited to linear regions of load-displacement curve - Need load/load-line displacement record - Requires determination of the elastic stress intensity	
	$J_{\substack{\text{cont.} \\ \text{plas.}}} = \left(\frac{\delta}{\delta_e} \right)^2 \frac{K^{*2}}{E'}$	- "contained" plastic zone - Rigid plastic circumstances - Assumes linear load versus displacement relationship - Good for small displacements only	- Requires good approximation of the elastic stiffness with respect to crack geometry - Not valid at onset of yielding	15

Table 3-2

J-INTEGRAL ESTIMATION PROCEDURES

METHOD NO.	MATHEMATICAL EXPRESSION	ASSUMPTIONS/ASSERTIONS	LIMITATION	SPECIMEN TYPE	AUTHOR(S)	REFERENCE NO.
1.	$J = -\frac{1}{B}\left(\frac{\partial U}{\partial a}\right)$	- Demonstrates J-integral as a failure criterion - Compliance relationship - Can be a source of comparison with other methods - Needs load versus displacement	- Expensive and tedious - Subject to error - Requires 5 to 10 specimens - Difficult to assess crack growth initiation point	CT, SEN, CCT	Begley and Landes (1972)	16
2.	$J = -\frac{1}{B}\left[\frac{\partial(\int P d\Delta)}{\partial a}\right]_{\Delta}$	- Requires measurement of load versus displacement - Based on elastic compliance and slip line field considerations - Can obtain J_c using single specimen	- Requires knowledge of σ_y, σ_w, E of test material	CT, SEN, CCT	Bucci et al (1972)	12
3a.	$J = \frac{2U_p}{B(W-a)}$	- For deeply cracked bend bars $0.5 < a/W < 0.75$	- Must account for load point indentation and test machine - Requires knowledge of energy component of uncracked ligament	CT, SEN	Rice, Paris and Merkle (1973)	
3b.	$J = \frac{2U}{B(W-a)}$	- Assumes small compliance of uncracked ligament - Equivalent to #3a when $a/W \geq 0.5$				20
4.	$J = J_e + J_p$ $= \frac{\eta_e U_e}{B(W-a)} + \frac{\eta_p U_p}{B(W-a)}$	- Not restricted to deeply notched specimen - Avoids limitations introduced by #3a - Good for $0.2 < a/W < 0.7$	- Need to determine u_e and u_p - Values of η_e and η_p given in reference 19	SEN, CT	Sumpter and Turner (1976)	14
5.	$J = \frac{2}{B(W-a)}\left[\eta_1 Pa + \eta_2 U\right]$	- Includes contributions of tension and bending - Good for $a/W \geq 0.5$ - Values of η_1 and η_2 in Ref. (17)	- Tends to give high values	CT	Merkle and Corten (1974)	13
6.	$J = \frac{Pa - 2U_{el}}{B(W-a)}\left[1 + \alpha\left(\frac{P}{P_{max}}\right)^2\right]$ $J = \frac{Pa}{B(W-a)}\left[1 + \alpha\left(\frac{P}{P_{max}}\right)^2\right]$	- Requires only measurement of load, P_1-load point deflection $\alpha = 0.35$ for plane stress $\alpha = 0.12$ for plane strain		SEN	Rice, Paris, Merkle (1973)	20
7.	$J = J_e + J_p$ $J_e = \left(\frac{P\sigma_y^{0.2}}{B\sqrt{W}}\right)^2\left(\frac{1}{E'}\right)$ $J_p = \frac{2P_{GY}}{B(W-a)}\left[\frac{W}{a + r(W-a) + Z}\right]\left(\frac{V_p}{P_{GY}}\right)$ $r = 0.45$ $(a/W \leq 0.45)$ $r = 0.4$ $(a/W > 0.45)$ P_{GY} = limit load E' = E for plane stress or $E/(1-\nu^2)$ for plane strain V = crack opening	- Separates elastic and plastic components - Requires load versus clip gauge record - Assumes rigid body rotation - Not restricted to deeply notched specimens		SEN	Sumpter and Turner (1976)	14
8.	$J = \frac{\eta_e U_e}{B(\sigma_0 W - a)} + \frac{U_p}{B(W-2a)}$	- An alternative approach to number 4 - η_e values given in reference (19)		CCT		19
9.	$J = \frac{K^2}{E'} + \frac{2U_p - Pa_0}{B(W-2a)}$ $K = \frac{P}{B\sqrt{W}}\sqrt{\pi a \sec\left(\frac{\pi a}{W}\right)}$	- An alternative approach to number 8 - Provides conservative value for J		CCT		19

$$R_n = \frac{J_n - J_1}{J_1} \times 100\%$$

where n refers to the method in Table 3-2 being compared. He then comments that:

1. For CT specimens, method 4 is preferable in the linear elastic region and would provide a less conservative value for J than method 3 for $0.5 < a/W < 0.7$.

2. For SEN Bend specimens, all the methods tend to overestimate the value of J. However, methods 6b and 7 are preferable for $a/W > 0.5$.

3. For CCT specimens, method 9 (or method 9 in conjunction with method 8) is preferable.

These geometries are illustrated in Figure 3-5. In recognition of the difficulties in establishing the parameter J and especially J_{Ic}, a standard testing procedure is contained in ASTM E813-81 (Ref. 21).

3. Crack Tip Opening Displacement (CTOD)/Crack Tip Opening Angle (CTOA)

The use of the crack opening displacement (COD) as a crack length correlating parameter in elastic-plastic fracture mechanics has been extensively investigated. Chapter B., Section 4 commented on some definitions of COD and these are illustrated in Figure 2-3. Tracey (Ref. 22) has suggested that the CTOD be measured at the point of intersection of the deformed crack profile and a 45 degree ray emanating from the crack tip. Thus, the measurements may be related to actual processes involving crack propagation which occur in the region of the crack tip.

A number of investigators have developed relations which attempt to describe the CTOD as a function of crack surface displacement at specified distances from the crack tip (Refs. 22,23). In general, experimental findings tend to confirm a logarithmic dependence of displacement on distance from the crack tip for crack extension in an elastic, perfectly plastic material.

It has been found that the initiation of crack growth can be characterized by a critical value of the CTOD and under certain conditions, this value may in fact be a material property. This may be considered to be a direct consequence of the interrelationship between J and CTOD for small scale plastic deformation. An experimental relation that has been investigated has the following form:

$$CTOD = d_n \frac{J}{\sigma_y} \qquad 3\text{-}7$$

where d_n = numerical constant, and
σ_y = material yield strength

This relation generally holds true for small amounts of crack growth. Subsequent resistance to crack extension may be characterized by a CTOD-Resistance curve.

For the situation of large scale plastic deformation occurring in the region of the crack tip, it has been found that the angle between the crack surfaces under load may be used as a crack propagation correlating parameter. The opening angle may be described by use of two definitions: the crack opening angle (COA) and the crack tip opening angle (CTOA). The COA is an average angle based on the original crack position and CTOA is a measure of the actual slope of the crack faces close to the crack tip, as shown in Figure 3-6. Shih et. al (Ref. 8), in Figure 3-7, illustrate the crack opening angles associated with deformation and flow theories of plasticity. It was shown that there is good agreement between the angles calculated via the two theories and this suggested a possible relationship between COA and slope of the J-integral resistance curve.

The COA lacks a practical relationship to the processes occurring at the crack tip which governs crack propagation. The CTOA, however, may be related to processes such as cavity formation and linkage between inclusion particles which occur at the crack tip. Thus, this term has been more thoroughly investigated for use as a fracture parameter and will be considered in some detail.

It has been found using both experimental and theoretical techniques that the CTOA becomes constant after an initial period of variation as a crack extends under conditions of extensive plastic deformation (Refs. 24-29). Specifically, de Koning (Ref. 24) presented results for center-cracked 2024-T3 aluminum in which he showed by both direct measurement using visual methods and by finite element analysis that the CTOA becomes constant. He suggested that the crack grows when the value of CTOA becomes greater than some critical value. Green and Knott (Ref. 25) investigated fracture behaviour in a mild steel of varying thicknesses to determine the effect of change in stress state on stable crack growth. The experimental results showed that crack propagation may occur at crack tip opening displacements which are lower than those which occurred at initiation of crack growth. An explanation for the finding of a constant CTOA for stable crack growth referred to a process of crack propagation by linkage of inclusions and the resultant constant geometry present at the crack tip.

Further examples describing the use of a CTOA parameter have also been presented in the literature (Refs. 26,27). Kanninen et al (Ref. 27) reported that the CTOA measured in fracture of A533B steel was essentially independent of specimen geometry and fracture type which was either of a flat or slant type. Following an initial transient, the CTOA was constant for large amounts of crack growth. The reported disadvantages of using CTOA were the problems of direct measurement of this parameter and the fact that the precise definition in a finite element or other analysis is somewhat arbitrary. Shih et al (Ref. 8) showed reasonable correlation for subcritical crack growth in A533B steel and 316 stainless steel using an appropriately defined CTOA obtained from finite element results based on deformation and flow theories.

Other findings include those reported by Emery et al (Ref. 29) in which CTOA was investigated as a dynamic fracture criterion. A finite element model was used to predict dynamic fracture in 316 stainless steel and A533B pipe material. Substantial reductions in terminal crack velocities under large-scale yielding were found. Also, results reported by Hermann and Rice (Ref. 30) on four compact tension specimens support the hypothesis that a geometrically similar near tip crack profile is maintained during stable crack growth. This implies that the ductile fracture processes consisting of microcracking and nucleation of voids were confined to the near crack tip region.

4. R-6 Assessment Method and Modifications

A method for analyzing the problem of ductile fracture by use of a failure assessment approach was developed by the Central Electricity Generating Board (CEGB) of the United Kingdom. The R-6 failure assessment approach was derived from the CEGB two-criteria approach suggested by Dowling and Townley (Ref. 31). Harrison et al (Ref. 32) reformulated this approach into a failure assessment diagram with the two coordinates S_r and K_r. The coordinates of an assessment point on this diagram are calculated by use of the following two equations:

$$K_r = K_I/K_{Ic} \qquad 3\text{-}8$$

$$S_r = \sigma/\sigma_i \qquad 3\text{-}9$$

where K_I = the stress intensity factor for the structure
K_{Ic} = fracture toughness of the material
σ = the applied stress on the structure
σ_i = the plastic collapse stress based on the material flow stress taken as the average of the yield and ultimate strengths

The basis of the R-6 approach is shown in Figure 3-8. The relation between the parameters is such that for $K_r=0$, $S_r=1$. For a particular flaw size, structure, and material under consideration, the coordinates(S_r', K_r') of the flaw being assessed are calculated and the point is plotted. If the point lies on or outside the failure assessment line, the structure will fail. If the point lies inside the curve, the assessment will indicate that the structure with the flaw will be safe.

The use of the R-6 failure assessment method leads to inaccuracies when used for crack growth predictions because it is based on the assumption that structures behave as strip models (that is, modelled as elastic-perfectly plastic center-cracked infinite plates). A modification using a deformation plasticity approach has eliminated this assumption and accounts for both strain hardening and geometry effects (Ref. 33). The short-coming of this approach is that a separate failure assessment curve is required for each cracked structure and each material. However, a simpler approach has been suggested which combines some geometry and material effects into a few simple-to-use failure assessment curves which represent most geometries of interest (Refs. 33,34). The resulting curves are presented in Figure 3-9. The curves are limited to use for conditions of i) low alloy steel, ii)

plane strain, and iii) the location of flaws must be remote from any discontinuities in the structure. Application of the curves is similar to use of the R-6 assessment curve except that the net section collapse is based on a yield strength of 60 ksi.

As shown in Figure 3-9, the parameter a/t, the ratio of the crack depth to pipe wall or pressure vessel wall thickness, has a major influence on determination of whether the structure is safe with the assumed flaw under the known loading conditions. Flaw characterization and required material properties, when not available, are assumed to be given in Section XI of the ASME code. The assessment point (S_r', K_r') is determined by use of Equations 3-8 and 3-9 with the quantity σ_i based on the material yield strength only. The appropriate a/t curve on the diagram is then used to determine the severity of the flawed structure. In calculating the assessment point, a distinction is made between primary and secondary stresses. The primary stresses are those due to mechanical loading such as that due to internal pipe pressure whereas the secondary loading is due to thermal and/or residual stresses. The assessment curves assume that the time-averaged stresses due to the secondary stresses is zero and no account is made of them. Thus, in cases where the secondary stresses are compressive, the curves would be conservative in their estimations while tensile secondary stresses would result in nonconservative estimates. Also, no account is made for crack growth due to fatigue or environmental effects. These have to be considered by use of other assessment methods.

The use of these methods for assessing a flawed pipe will be considered in a later chapter of the report.

5. Discussion

The J-integral method has proved to be a successful parameter for predicting onset of crack growth in regimes ranging from linear elastic to fully plastic behaviour in low to intermediate strength steels. Essentially, J and CTOD have been used to characterize the initiation of crack growth (e.g. $J = J_{Ic}$) for stationary cracks under monotonically increasing proportional loading in plane strain. For nonstationary cracks, subsequent crack extension can be analysed with J-resistance curves.

The use of J (or CTOD) is restricted by the underlying assumptions inherent in HRR solutions (Equation 3-1) and the energy release rate definition of J (Equation 3-2) (Ref. 10). This includes the condition that material behaviour conforms to the deformation theory of plasticity. This assumption, to a good approximation, is valid for a stationary crack subject to a monotonically increasing load. However, for growing cracks, where regions of nonproportional plastic flow will be embedded in the J-dominated field, behaviour is not modelled by deformation theory.

Similar to the case of K in LEFM, J analysis is plagued with size limitations which unlike K, can vary markedly in different specimen geometries. Experiments have further shown that J and CTOD are geometry and constraint dependent. A comparison between these methods is summarized in Table 3-3.

Generally in analyzing crack tip fields for rigid/perfectly plastic bodies under fully yielding conditions, Ritchie (Ref. 10) stated that no unique, configuration-independent parameter which is a measure of crack tip deformation is currently available. Cautious application of the single parameters described herein is therefore important.

Table 3-3: A Comparison of Some Fracture Parameters (Ref. 8)

	J* J-INTEGRAL	COD* CRACK-OPENING DISPLACEMENT	CTOA LOCAL CRACK-OPENING ANGLE
Measure of Near-Tip Field	Yes	Yes	Yes
Constant During Crack Extension	No	No	Yes
Independence of Specimen Geometry	Mildly Dependent	Mildly Dependent	Mildly Dependent
Applicability to Instability Analyses	+Yes	+ Yes	+ Yes
Generalizable to Mixed Mode Fracture	Probable	Uncertain	Uncertain
Ease of Computation	Simple	Moderately Simple	Moderately Difficult
Sensitivity to Mesh, Process Zone and Increment Size	No	Mildly	Mildly
Computation Cost (Estimated Ratio)	1	1	1
Direct Local Measurement	No	Possible	Difficult
Direct Global Measurements	Yes	Possible	No

* J and COD are employed as resistance parameters.

\+ For limited crack extension.

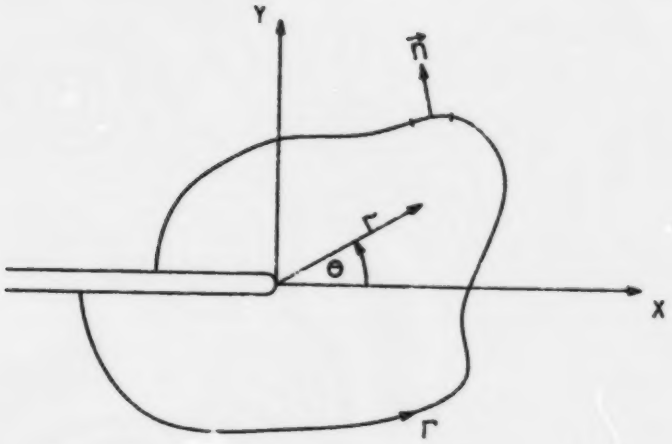

FIGURE 3-1: TWO-DIMENSION DEFORMATION FIELD AROUND A CRACK TIP.

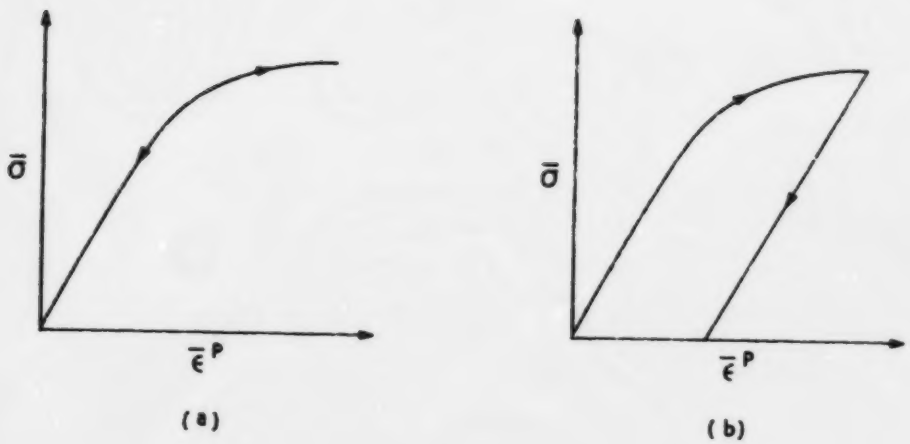

FIGURE 3-2: IDEALIZED CONSTITUTIVE BEHAVIOR, OF EQUIVALENT STRESS $\bar{\sigma}$ AS A FUNCTION OF EQUIVALENT PLASTIC STRAIN $\bar{\epsilon}^p$, FOR (a) NONLINEAR ELASTIC MATERIAL CONFORMING TO DEFORMATION PLASTICITY THEORY, AND (b) INCREMENTALLY-PLASTIC MATERIAL CONFORMING TO FLOW THEORY OF PLASTICITY. (REF. 10)

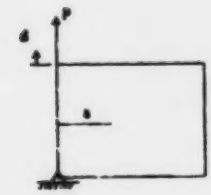

(a) TEST SPECIMEN CONFIGURATION

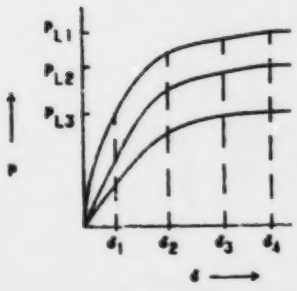

(b) LOAD DISPLACEMENT RECORDS

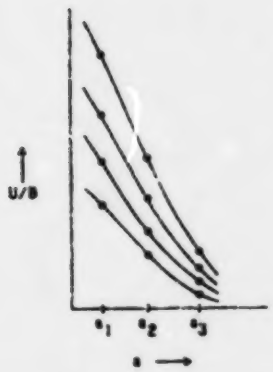

(c) ENERGY PER UNIT THICKNESS vs. CRACK LENGTH FOR CONSTANT DEFLECTION

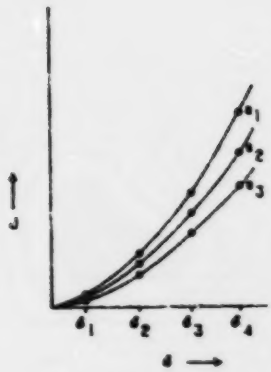

(d) J vs. δ FOR SPECIMENS OF DIFFERENT INITIAL CRACK LENGTH

FIGURE 3-3: SCHEMATIC DIAGRAM OF J VERSUS δ EVALUATION EMPLOYING A FAMILY OF LOAD DISPLACEMENT RECORDS. (REF. 12)

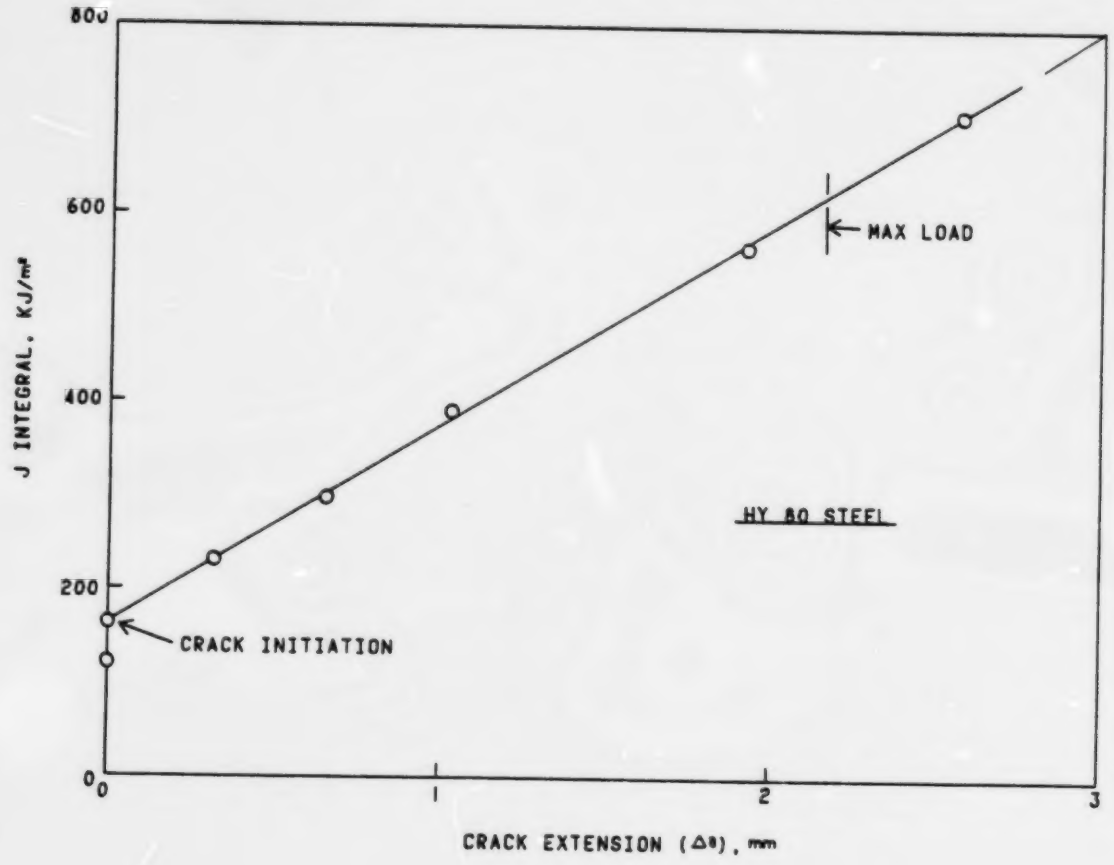

FIGURE 3-4: J-INTEGRAL AS A FUNCTION OF MEASURED CRACK EXTENSION (Δa) FOR B = 53 mm (J - RESISTANCE CURVE). (REF. 18)

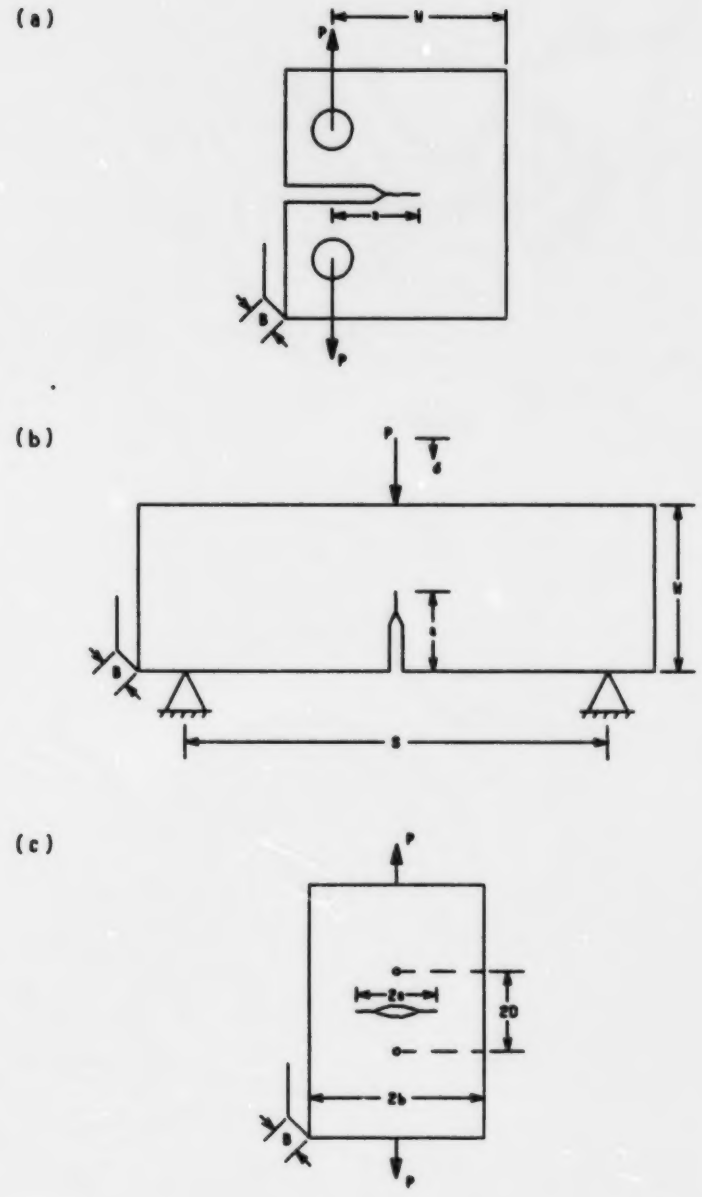

FIGURE 3-5: TEST SPECIMEN CONFIGURATION
(a) COMPACT TENSION SPECIMEN (CT)
(b) SINGLE EDGE NOTCH THREE POINT BEND BAR (SEN)
(c) CENTER CRACKED TENSION PANEL (CCT)

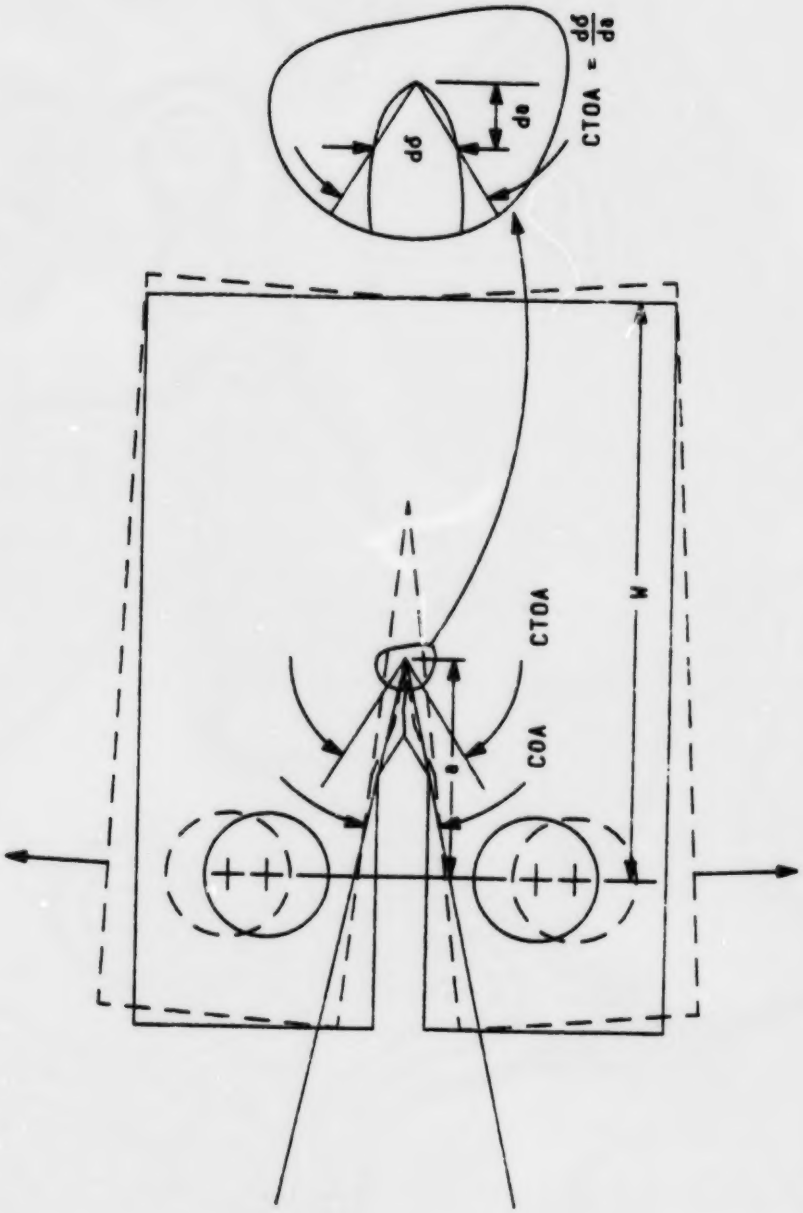

FIGURE 3-6: DEFINITIONS OF COA AND CTOA.

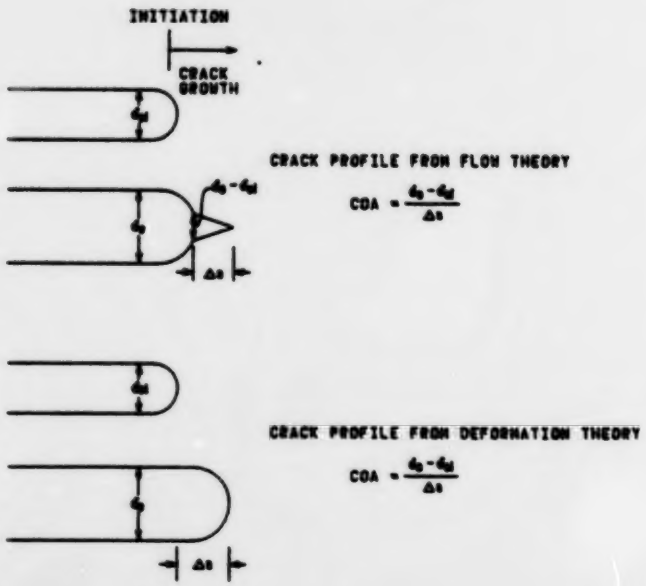
INITIATION
CRACK GROWTH
CRACK PROFILE FROM FLOW THEORY
COA = $\frac{\delta_0 - \delta_i}{\Delta a}$
CRACK PROFILE FROM DEFORMATION THEORY
COA = $\frac{\delta_0 - \delta_i}{\Delta a}$

FIGURE 3-7: CRACK-OPENING ANGLES FOR CRACK PROFILES ASSOCIATED WITH FLOW AND DEFORMATION THEORIES OF PLASTICITY. (REF. 8)

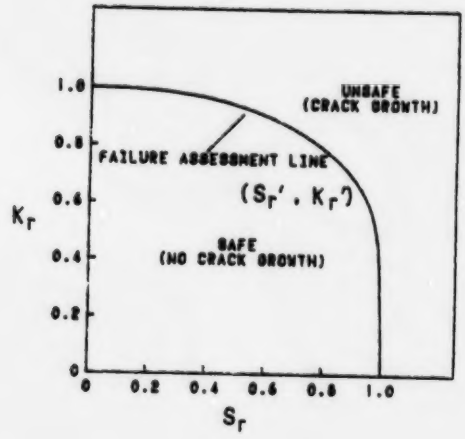

FIGURE 3-8: R-6 FAILURE ASSESSMENT DIAGRAM. (REF. 35)

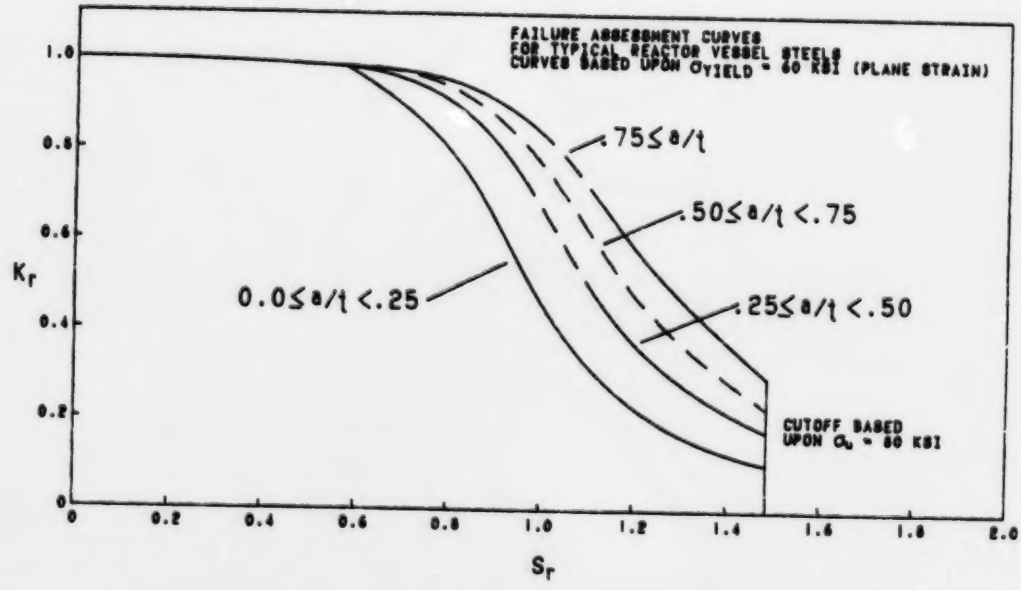

FIGURE 3-9: TYPICAL UPGRADED FAILURE ASSESSMENT DIAGRAM FOR LOW ALLOY STEELS. (REF. 35)

D. STABLE CRACK GROWTH

1. General

Plastic fracture mechanics techniques have been developed to accommodate the extensive plastic deformation and stable crack growth which can occur prior to fracture instability in tough ductile materials. The four dominant stages of crack extension and growth which can therefore lead to ductile fracture are schematically presented in Figure 4-1. It can also be immediately observed from Figure 4-1 that the maximum load carried by the structure can be appreciably higher than the load which first causes the initiation of growth. This resistance to fracture afforded by the material is a complex mechanism and relates directly to the crack tip plasticity assumptions and considerations from which appropriate parameters to describe stable crack growth must emerge. A number of requirements for a suitable parameter are presented below (Ref. 8).

(1) The parameter must be a measure of the stress and deformation state in the vicinity of the crack tip.

(2) The critical value of the parameter must be independent of initial crack length and specimen geometry.

(3) The parameter must be employable in an instability analysis.

(4) The parameter should be applicable to three-dimensioanl crack geometries such as an elliptic surface flaw.

(5) The parameter should be generalizable to mixed mode fracture, though the critical value will depend on the relative ratio of shear to flat fracture.

(6) The parameter should remain constant during crack extension. This is an attractive but not an essential feature. In an R-curve approach, the resistance parameter will increase with crack extension.

(7) The parameter must be relatively insensitive to finite element modeling, to mesh size, process zone size, and load/ displacement increment size.

(8) The parameter should be computable within reasonable computational cost.

(9) The parameter should be obtainable in laboratory tests from global measurements remote from the crack, but if this is not possible, it must be obtainable from easily discernible local measurements near the crack tip.

(10) The parameter must have physical relevance and ease of applicability.

2. The J Integral and Its Derivatives

From the literature, it is evident that the J integral approach can be viewed as a very useful extension of LEFM and has gained wide acceptance as a criterion for crack growth initiation which can be extended to include a limited amount of stable crack growth. However, it is also evident that crack growth instability is dependent on the total system of which the cracked member is but the weakest link of that particular system. Clearly, no single material property or parameter can define this point of instability as might be possible for crack growth resistance during stable growth. The difficulties are to define the parameter(s) which are applicable after a limited amount of stable crack growth, at which the validity of J is exceeded, through to an instability condition which is dependent on the system, and to assess when the crack driving forces exceed the material's resistance to controlled crack growth.

For stable crack growth, in excess of what can be justifiably defined as J-controlled crack growth, elastic unloading takes place in the 'wake' of the plastic region caused by the advancing crack tip. This growth is accompanied by an increasing inelastic process which basically invalidates the fundamentals of the J integral concepts. Once this condition arises, resistance curves specific to the given geometry under consideration provide the only means by which a representative J parameter can be employed.

2.1 J Integral Resistance Curves

J-resistance curves can be experimentally developed for a test specimen of particular geometry. These resistance curves are generally accepted to represent far field values. J-resistance curves can also be evaluated at different contours using finite element techniques. The J integral evaluated from near field contours tends to flatten with increasing crack extension whereas far field contours show increasing resistance with crack growth. For the near field results, with constant J at increasing crack extension, the results indicate a measure of steady state fracture energy dissipation rate. This is a useful concept which bears some correlation with the CTOA resistance curves discussed later.

While these differences between near and far field J-resistance curve determinations do exist, of even greater concern is the fact that it would appear that J-resistance curves are not independent of the specimen geometry and as such cannot be considered to be representative of the resistance of a material to stable crack growth.

Figures 4-2 and 4-3 serve to clearly illustrate this behaviour. Figure 4-2 shows the J-resistance curves evaluated at different contours or paths of integration for a compact tension specimen. J_{nf} and J_{ff} are termed the near and far field respectively. It would appear that the far field values which are generally more representative of experimentally measured J-resistance curves must include an energy dissipation associated with events remote from the fracture site. Figure 4-3 provides a comparison of J-resistance curves experimentally determined for different specimen geometries. These results show three important results, namely, i) reasonably consistent J values for limited crack growth, ii) considerable variation in J as crack growth

increases, and iii) confirmation that experimentally determined J-resistance curves more closely coincide with a far field evaluation of J (see Figure 4-2).

2.2 Tearing Modulus

From the resistance curves of J_R as a function of crack extension, the parameter T_R which defines the rate of change of J_R with respect to 'a' can be defined. Given that $T_R = \frac{dJ_R}{da}$ or non-dimensionalized to $T_R \equiv \frac{E}{\sigma_Y^2}\frac{dJ_R}{da}$, it has been demonstrated that this rate of change of the J-resistance curve coupled with a dimension of the component can provide some insight as to when the J dominance in stable crack growth might cease to exist.

For the J domain to exist, it is required that $\omega \equiv \frac{b}{J}\frac{dJ}{da} \geq 1$. It has been suggested that ω is about 40, and stable crack growth would be restricted to but a very small percentage of the ligament length, b. This consideration would again emphasize the need to determine a J-resistance curve specific to the particular geometry under consideration and as such, no J_R resistance curve can be interpreted as a material property. A further consideration which supports this argument arises from the appreciation of the importance of triaxiality and its influence upon a material's crack resistance. Two materials cracking at the same J_R value might offer different resistance to crack growth as a result of different imposed constraints. Similarily, a material with a high J_R resistance curve does not necessarily offer greater resistance to fracture than one with a lower J_R resistance curve.

A J_R resistance curve, while based on the J integral concept, cannot be considered to be a material property. At best, it can be developed to provide a representation of crack resistance for a given geometry. Under these circumstances, stability will exist when $J \leq J_R(a)$ and $dJ/da < dJ_R/da$. In terms of the tear modulus, this latter condition can be expressed by:

$$T \equiv \frac{E}{\sigma_Y^2}\frac{\partial J}{\partial a} < \frac{E}{\sigma_Y^2}\frac{dJ_R}{da} \equiv T_R \qquad 4\text{-}1$$

For instability to occur, J must be greater than J_R. However $T \geq T_R$ is not a sufficient condition for instability unless $J = J_R$. Figure 4-4 provides an illustration of the transformation of data from a J_R resistance curve to J-T space.

3. CTOA

A general equivalence between J and COD can be defined for J control which implies limited crack growth conditions. For larger amounts of crack growth, the viability of J, as described above, loses much of its fundamental elegance; under these conditions, the parameter CTOA requires independent assessment. Resistance curves of CTOA indicate a constant CTOA level as a function of increasing crack growth - a trend confirmed by finite element calculations. The distinct difference between the J and CTOA resistance curves is illustrated in Figure 4-5.

Both curves were obtained from compact tension specimens and are therefore certainly applicable to this configuration. However, only for the CTOA data is there a clear implication that the resistance curve obtained from the CT specimen can be extended to other geometries, which would exhibit the same constant CTOA behaviour as a function of crack growth. This leads to the possiblity of using a twin criteria method, where J would apply to initiation and limited crack growth followed by the CTOA criteria for extended growth. This approach is consistent with the approach suggested at EPRI (Electric Power Research Institute).

In discussing this twin criteria, it is important to quote directly from Ref. 39.

"As evidenced by experimental and analytical work on laboratory test specimens, J is computationally convenient and has a more definite theoretical basis, but it exhibits geometry dependence after a small amount of crack growth. On the other hand, CTOA exhibits a constant resistance value after an initial transient which makes it highly attractive when large amounts of crack growth (stable or unstable) must be considered. But its experimental determination is difficult and a theoretical basis is lacking."

4. J Integral Crack Driving Force Contours

The utilization of J (or COD) resistance curves will require that the J integral crack driving force contours be evaluated such that the instability condition (or maximum load), as defined in Section 2.2, can be determined. This type of exercise can be both time consuming and expensive in terms of finite element capability and therefore alternative 'engineering design approaches', as detailed in Ref. 8, have been introduced. This approach is briefly summarised with respect to J resistance curves for the CCT and single edge cracked panel (SECP) geometries. These particular geometries have been selected since, if curvature effects are neglected, a through crack and circumferential crack in a flawed pipe can, in the limiting case, be represented by the CCT and SECP configurations respectively as illustrated in Figure 4-6.

The procedure presented in point form below has been applied to the case of a 4 inch diameter 304 stainless steel pipe (Ref. 8).

(1) Determine experimentally the true stress-strain curve for the material. The data is correlated according to the Ramberg-Osgood stress-strain law given by

$$\frac{\varepsilon}{\varepsilon_o} = \alpha \left[\frac{\sigma}{\sigma_o}\right]^n \qquad 4\text{-}2$$

(2) Determine the J integral crack driving force contours for the material properties obtained from (1) above, and the geometries for CCP or SECP as given in Figure 4-6 for a crack extension from a_o to a. These contours can be developed by finite element analyses for both constant load or displacement conditions as represented in Figure 4-7. An alternate but simpler approach would be to derive the crack driving

force contours from the function forms or estimation procedures of the J integral in terms of the elastic and plastic components, i.e.

$$J = J^e(a_{eff}P) + J^P(a,P,n) \qquad 4\text{-}3$$

where J^e is the adjusted elastic contribution, J^P the plastic contribution, and a_{eff} is the effective crack length adjusted to include Irwin's small scale yielding correction. J can therefore be evaluated from a knowledge of the material properties and catalogued J^e and J^P values from fracture handbooks.

(3) The J resistance curve, determined experimentally, can be superimposed on Figure 4-7. The extent of stable crack growth at the point of tangential intersection of the matching driving force curve and the material resistance curve can then be determined. At this point

$$J = J_R \text{ and } \frac{dJ}{da} = \frac{dJ_R}{da} . \qquad 4\text{-}4$$

(4) Repeat this procedure for a number of different crack length to width ratios and again determine the point of instability in each case.

(5) Plot the estimated values of σ (applied) at maximum load as a function of the cracked area as shown in Figure 4-8 for both plane stress and plane strain conditions as developed for the CCT specimen which is representative of the through crack condition. The equivalent results, developed for the SECP specimen, which are representative of the circumferential behaviour are also plotted on Figure 4-8 for comparative purposes.

It will be observed that the format of presentation of these results i.e. Figure 4-8, is very similar to that developed for the net section collapse criterion (Ref. 39, 48) which is summarised in Figure 4-9. From Figure 4-9 the value of the collapse stress is given by the intercept on the vertical axis and maintains a constant value for all crack initiation and maximum load conditions at different crack lengths.

Since the net section stress corresponding to varying amounts of crack growth determined from Figure 4-8 is also constant for a set of conditions, it would appear that some degree of compatibility exists between the load carrying capacity as determined by limit load analysis based on the ligament area and the fracture mechanics approach outlined above, provided of course, that an appropriate fracture or flow stress is employed.

An important conclusion from the results presented in Figure 4-9 is that the loads required to propagate a through crack along the circumference of the pipe are lower than those required to propagate a full circumferential crack in the radial direction. Through this approach it is also possible to incorporate in the analysis, the system compliance and/or pipe length and the type of loading, both of which exert a dominant influence on the crack stability condition. In broad terms it can be shown that larger or longer pipes are less stable. Also bending conditions in the pipe are more tolerable than direct tension loading conditions.

5. The J-T Approach

A convenient algorithm which is being increasingly employed to assess the margin against possible instability is the J-T diagram introduced in Figure 4-4. In Figure 4-10 a J-T diagram developed from the J resistance curve is presented with three J-T loci superimposed thereon to represent three distinct types of applied loading as identified in Ref. 45. When the applied J falls below J_{Ic}, crack stability is automatically assured. Should the applied J locus approach and intersect the J-T curve, instability is predicted. The instability points for each of the applied loci are indicated by points I on Figure 4-10.

6. Summary

A brief pictorial summary of the J and COD parameters is provided in Figure 4-11. It would appear that both the J integral and COD approach are viable parameters for predicting crack initiation and can be extended to stable crack growth through the use of the T and CTOA parameters. It must be emphasized that certain requirements must be satisfied to ensure that crack growth is characterizable by the J integral or COD approaches, namely:

(1) There should exist a sufficient constraint to ensure dominance of the HRR field. For CT and CCT specimens, this requires that both the ligament and thickness values must be greater than 25 J_{Ic}/σ_Y and 200 J_{Ic}/σ_Y respectively.

(2) The slopes of the resistance curves must be sufficiently large to ensure that $\frac{b}{J_{Ic}}\frac{dJ}{da}$ or $\frac{E}{\sigma_Y}\frac{d\delta}{da}$ are much greater than unity. It is evident from Figure 4-11(c) that the near field solution violates this condition.

It is also essential, when using either of these parameters, to ensure that the resistance curves developed do represent the real situation to which they are being applied. Resistance curves, as distinct from J_{Ic} or δ_{Ic}, cannot be considered as a material property but do depend on the geometry of the system under consideration and the constraint provided at the crack site.

For large amounts of crack growth it would appear that a twin criteria approach using J followed by CTOA offers considerable advantage in that the best of J is utilised for small crack growth followed by CTOA which appears to maintain a reasonably constant value with increasing crack length.

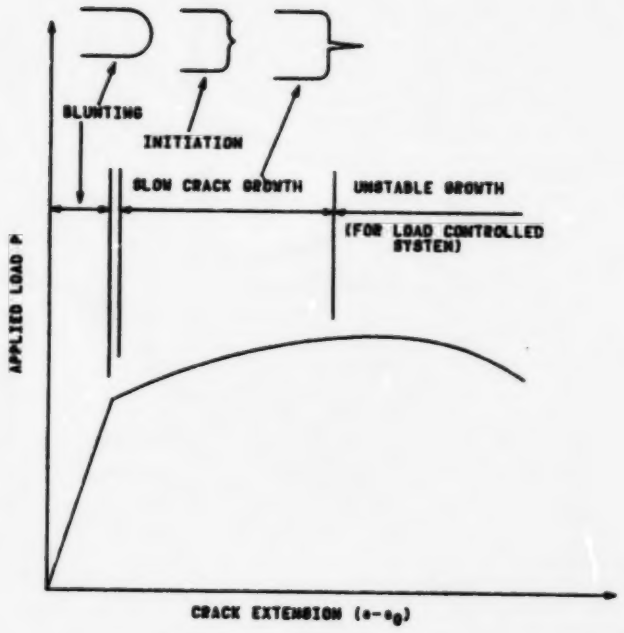

FIGURE 4-1: STAGES OF CRACK EXTENSION, SHOWING CRACK BLUNTING, INITIATION, AND GROWTH RELATED TO THE APPLIED LOAD. (REF. 8)

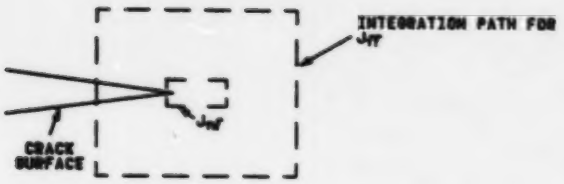

A. DEFINITIONS OF J-INTEGRAL

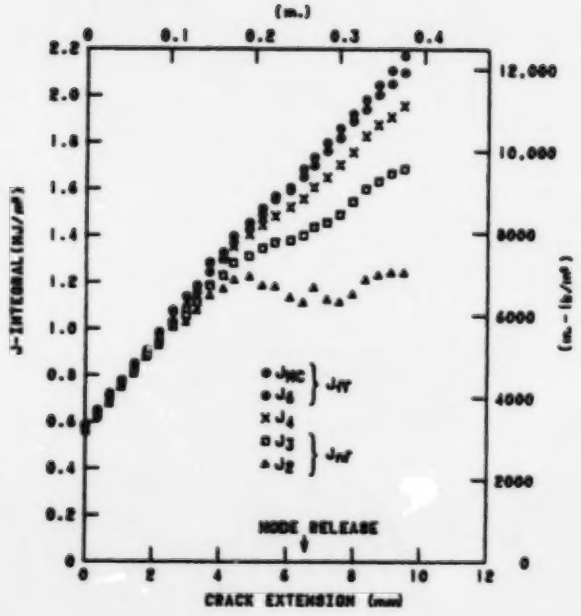

FIGURE 4-2: J-RESISTANCE CURVES EVALUATED AT DIFFERENT CONTOURS ON A-533B STEEL FOR A COMPACT TENSION SPECIMEN. (REF. 8)

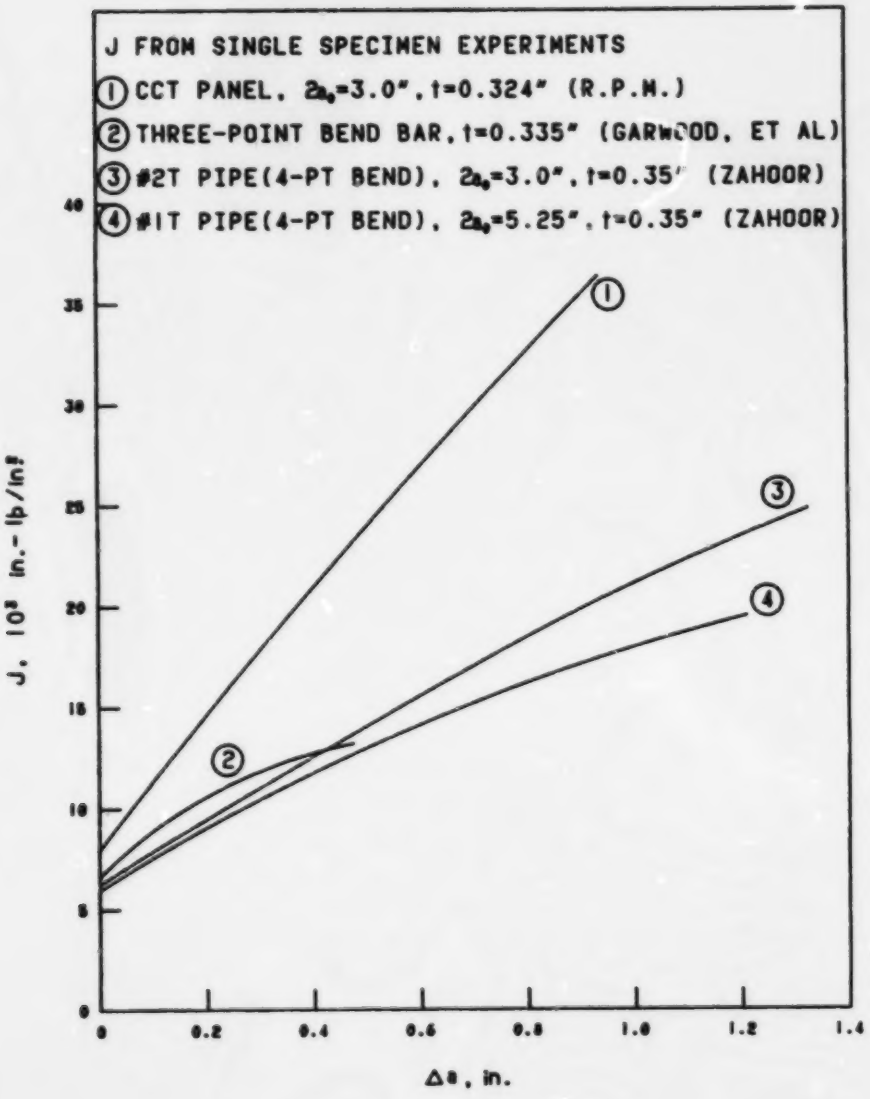

FIGURE 4-3: A COMPARISON OF J-RESISTANCE CURVES FOR TYPE 304 STAINLESS STEEL (REF. 48)

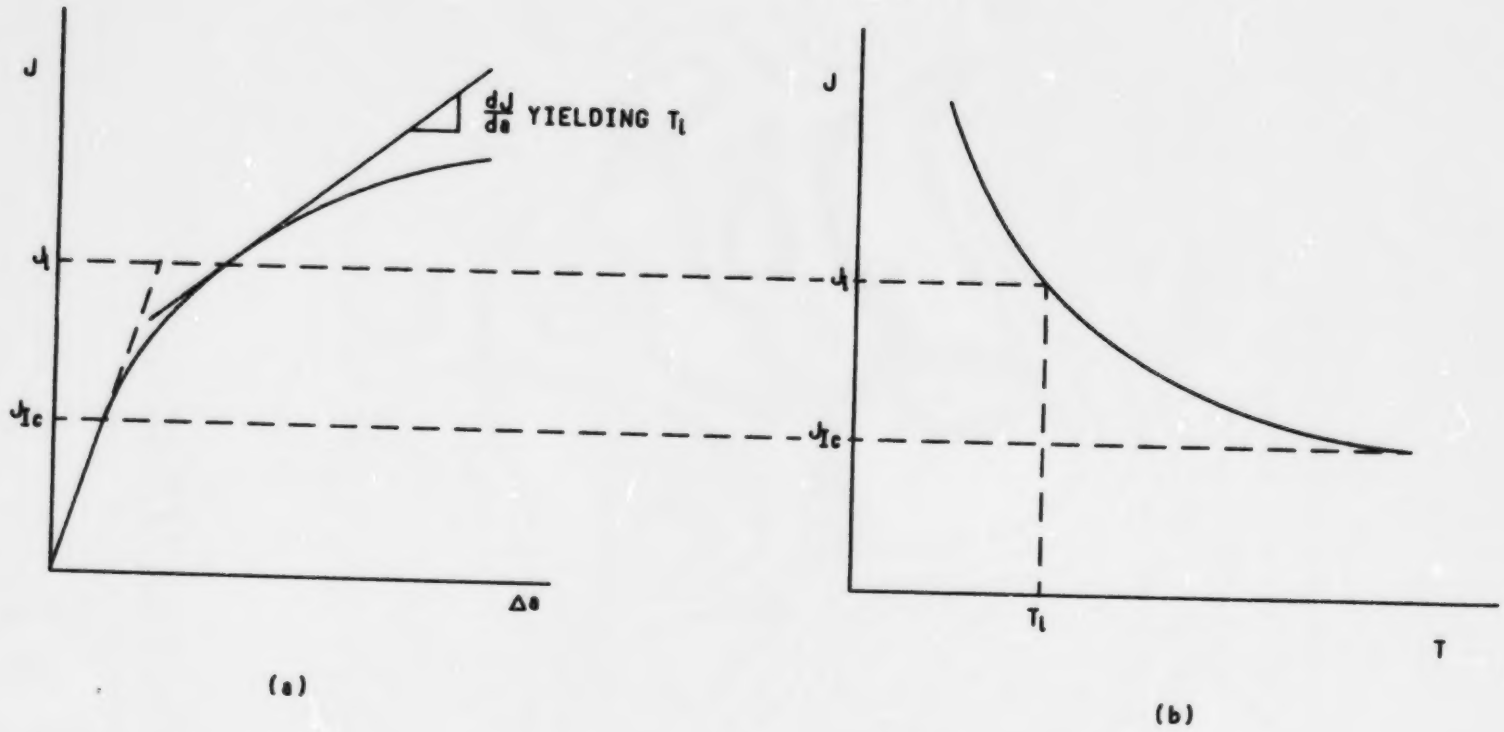

FIGURE 4-4: (a) TRANSFORMATION OF DATA FROM J-INTEGRAL R-CURVE. (b) J-INTEGRAL/TEARING MODULUS SPACE.

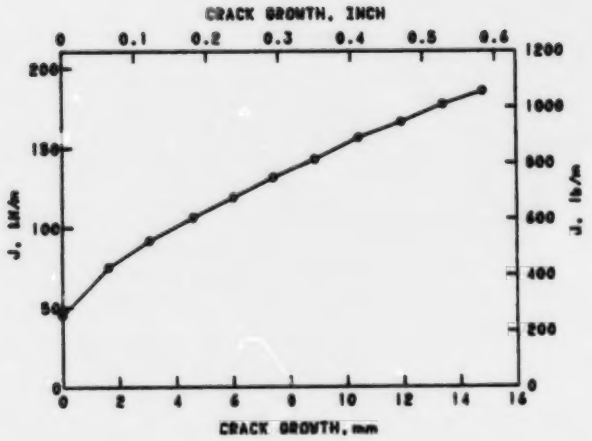

(A)

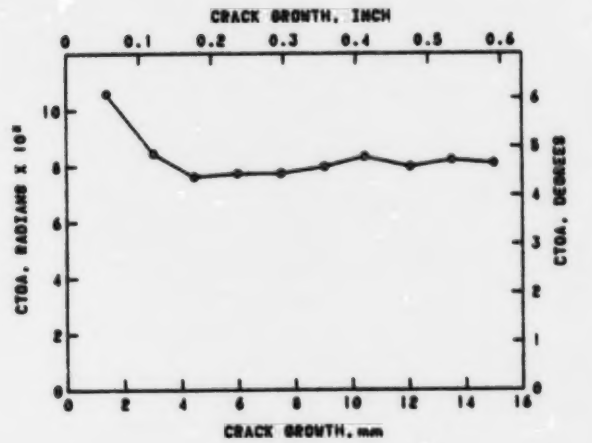

(B)

FIGURE 4-5: BATTELLE GENERATION-PHASE RESULTS FOR STABLE CRACK GROWTH IN A 2219-T87 ALUMINUM COMPACT-TENSION SPECIMEN (REF. 49); (A) J-RESISTANCE CURVE, (B) CTOA-RESISTANCE CURVE.

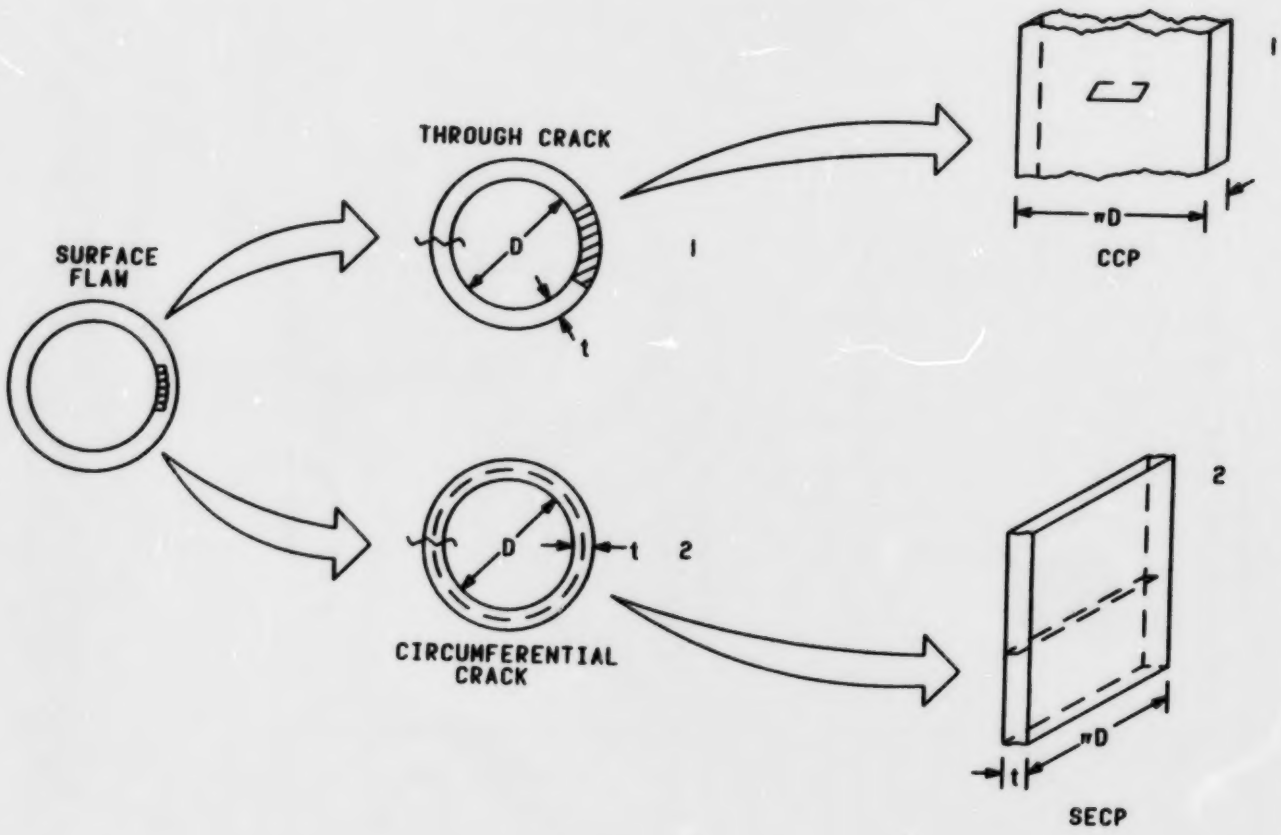

FIGURE 4-6: SURFACE FLAW IN PIPING REDUCED TO COMMON PLATE CONFIGURATIONS. (REF. 8)

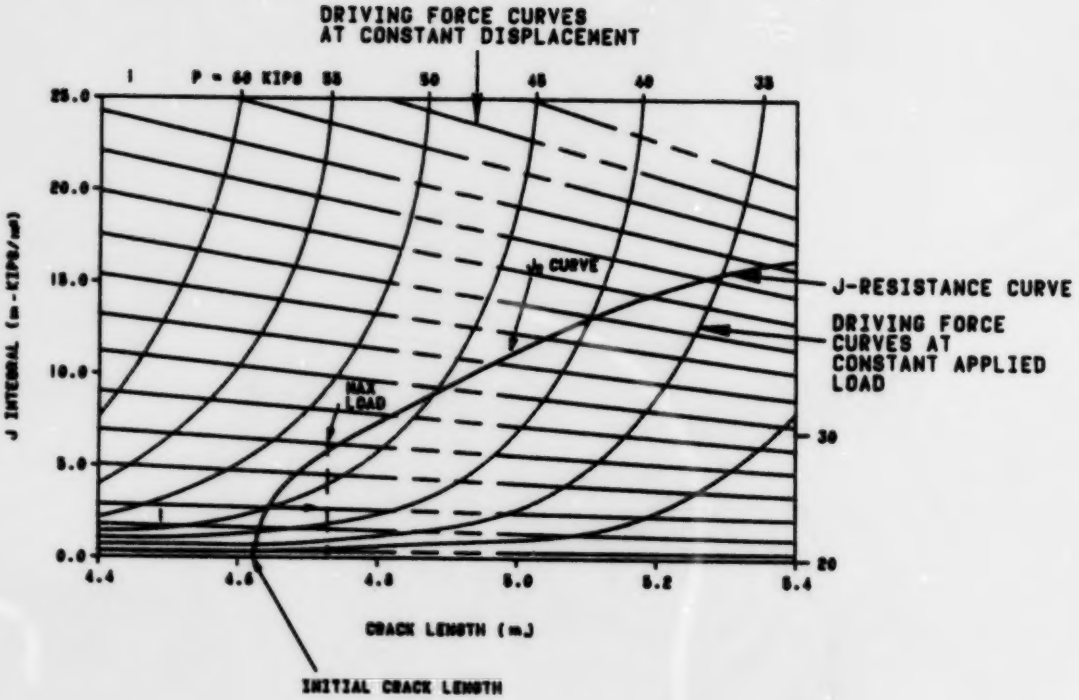

FIGURE 4-7: J-INTEGRAL CRACK STABILITY DIAGRAM FOR COMPACT SPECIMEN T-52. (REF. 8)

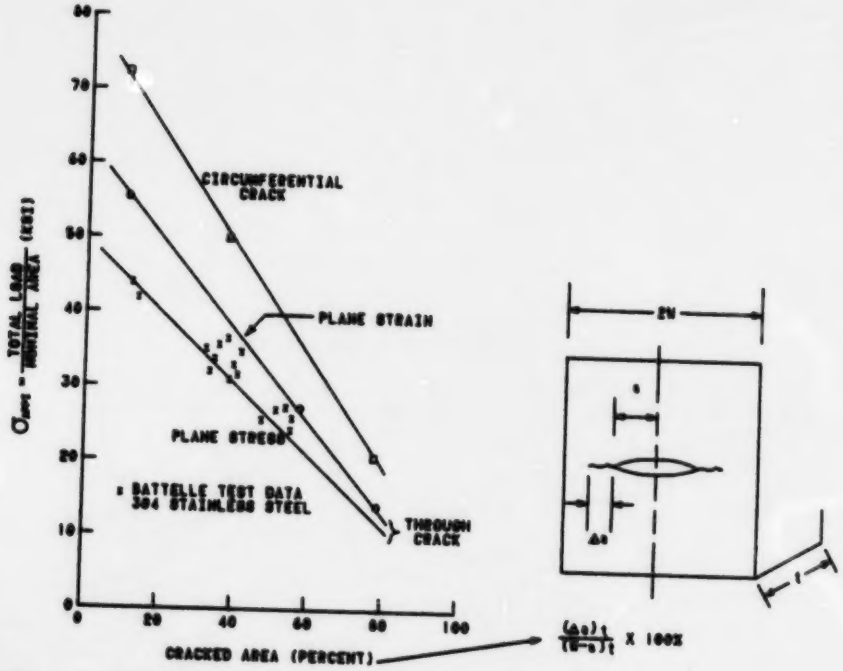

FIGURE 4-8: APPLIED NOMINAL STRESS AT MAXIMUM LOAD FOR SEVERAL RATIOS OF CRACKED AREA TO TOTAL AREA. (REF. 8)

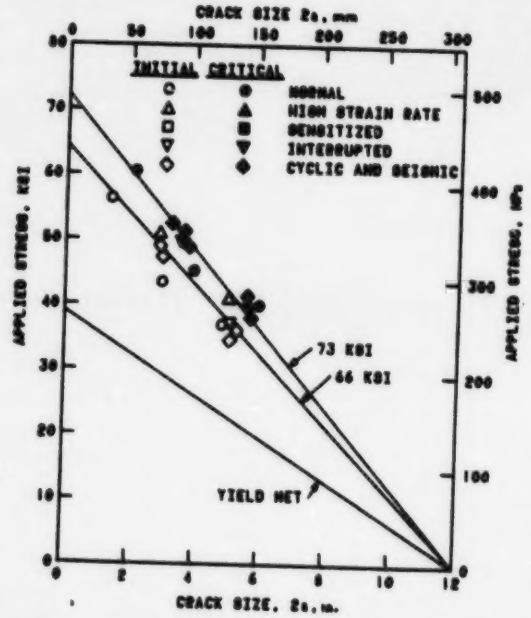

FIGURE 4-9: RESIDUAL STRENGTH AS A FUNCTION OF CRACK SIZE FOR TYPE 304 STAINLESS STEEL CENTER-CRACKED-TENSION PANELS. (REF. 48)

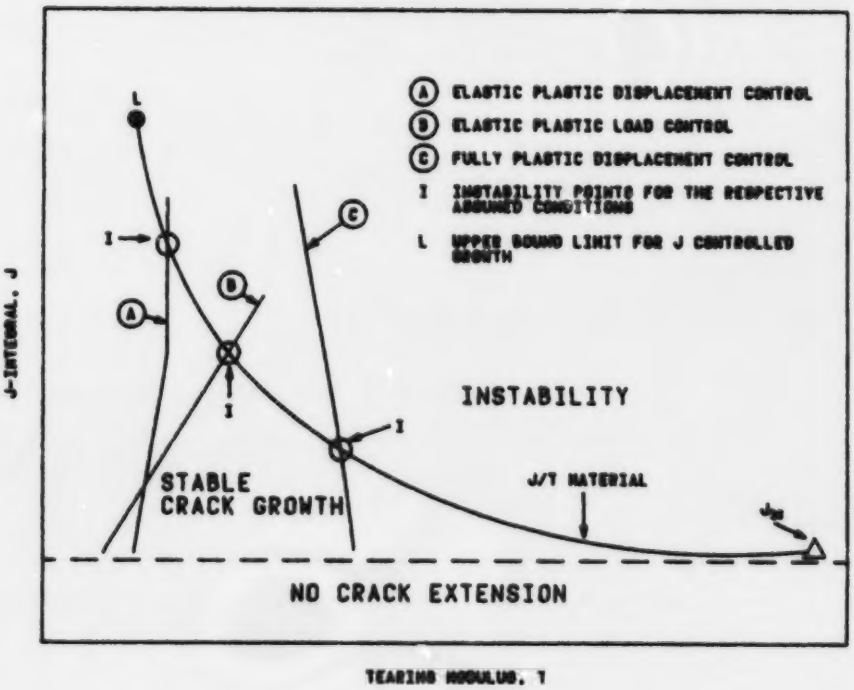
A ELASTIC PLASTIC DISPLACEMENT CONTROL
B ELASTIC PLASTIC LOAD CONTROL
C FULLY PLASTIC DISPLACEMENT CONTROL
I INSTABILITY POINTS FOR THE RESPECTIVE ASSUMED CONDITIONS
L UPPER BOUND LIMIT FOR J CONTROLLED GROWTH
INSTABILITY
STABLE CRACK GROWTH
J/T MATERIAL
NO CRACK EXTENSION
J-INTEGRAL, J
TEARING MODULUS, T

FIGURE 4-10: J-T PLOT. (REF. 45)

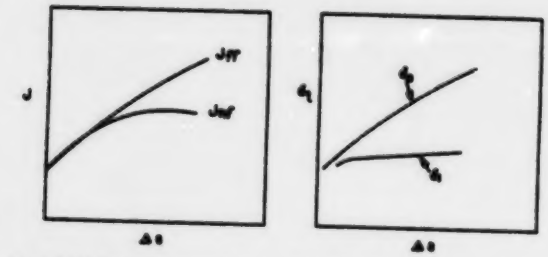

A) J-RESISTANCE CURVES FOR NEAR AND FAR FIELDS

B) COD-RESISTANCE CURVES BASED ON OPENING AT ORIGINAL CRACK TIP (δ_0) AND AT A FIXED DISTANCE BEHIND CURRENT TIP (δ_t).

δ_0 = COD SEE FIG. 2.3

δ_t = CTOD SEE FIG. 2.3

C) dJ/da DERIVED FROM NEAR AND FAR FIELD J.

D) COA'S α_0 AND α_t DERIVED FROM δ_0 AND δ_t.

α_0 = COA SEE FIG. 3.6

α_t = CTOA SEE FIG. 3.6

'INITIATION' PARAMETERS

- J
  - J_{nf} : EVALUATED IN REGION DOMINATED BY HRR SINGULARITES OR FIELDS
  - J_{ff} : EVALUATED ALONG A REMOTE CONTOUR, PROVEN ANALYTICALLY THAT THIS IS THE QUANTITY MEASURED IN EXPERIMENTAL INVESTIGATIONS USING LOAD-DISPLACEMENT RECORD
  - J_{Ic} : MATERIAL TOUGHNESS
- COD
  - δ_0 (COD) : OPENING DISPLACEMENT AT THE ORIGINAL CRACK TIP
  - δ_t (CTOD): OPENING DISPLACEMENT AT A FIXED DISTANCE BEHIND THE INSTANTANEOUS CRACK TIP
  - δ_{Ic} : MATERIAL TOUGHNESS

GROWTH PARAMETERS

- dJ_{ff}/da : CAN BE DETERMINED EXPERIMENTALLY
- dJ_{nf}/da : OBTAINED THROUGH THEORETICAL AND NUMERICAL CRACK GROWTH STUDIES
- $d\delta_0/da = \alpha_0$ (COA) : AVERAGE CRACK OPENING ANGLE, NOT A FUNDAMENTAL MEASURE OF THE CRACK FIELD
- $d\delta_t/da = \alpha_t$ (CTOA): LOCAL CRACK OPENING ANGLE, NOT EASILY MEASURED
- $T_J = \frac{E}{\sigma_Y^2}\frac{dJ}{da}$: MATERIAL TOUGHNESS
- $T_\delta = \frac{E}{\sigma_Y}\frac{d\delta}{da}$: MATERIAL TOUGHNESS

FIGURE 4-11: DEFINITIONS AND VARIATION OF SELECTED FRACTURE PARAMETERS WITH CRACK EXTENSION. (REF. 8)

E. DUCTILE FRACTURE OF PIPES

1. General

The evaluation of the structural integrity of piping materials used for nuclear power plant applications must consider the inherent ability of these materials to undergo extensive amounts of plastic deformation. The conventional fracture mechanics approach using stress intensity methods to evaluate the criticality of cracks in pipes under fatigue and static loading conditions results in very conservative predictions regarding their effects. In the ductile stainless steels and ferritic steels used in nuclear plants, considerable additional resistance to crack growth occurs due to the development of regions of plastic deformation at a crack tip. A stress intensity assessment ignores this increased crack growth resistance.

Several methods of assessing the increased load carrying capacity of flawed ductile tubes and the possibility of stable crack growth before final rupture have been investigated. These have recently been reviewed in the literature (Ref. 39). In addition, various studies utilizing both analytical and theoretical techniques have been completed to determine the applicability of several elastic-plastic correlating parameters to assess the fracture of full-scale flawed pipes (Refs. 36,37,40-44). Finally, the results of a major study have been recently published to set forth guidelines for use in designing pipes using a leak before break philosophy (Ref. 45). The results of these various investigations will be summarized briefly as follows.

2. Pipe Design Methodology

Current pipe design practice utilizes one of the following methods to assess the presence of flaws. These are the J-integral/Tearing Resistance (J-T) method, the crack opening displacement(COD) method, and the R-6 design curve approach. Each of these methods will be examined and examples of their applications will be discussed.

2.1 J-T Assessement Method

The J-T approach utilizes the assumption that stable crack growth will proceed when the J applied to a flaw in a pipe becomes greater than the J_{Ic} of the pipe material. The assessment of stable crack growth assumes that crack growth will continue until the crack driving force becomes greater than the material resistance to cracking. The crack driving force is a function of the current crack length and applied load only. The material resistance is a function of the amount of crack growth only. Expressed algebraically, crack growth is unstable when:

$$(\partial J/\partial a)_{\Delta_T} > dJ_R/da \qquad 5\text{-}1$$

where Δ_T = the total system displacement
$= \Delta + C_m P$
Δ = load point displacement through which P works

P = the applied load
C_m = the system compliance

In terms of another often used parameter, Equation 5-1 may be expressed in terms of tearing moduli defined as:

$$T_J = \frac{E}{\sigma_Y^2}\left(\frac{\partial J}{\partial a}\right)_{\Delta_T} \quad \text{and} \quad T_{JR} = \frac{E}{\sigma_Y^2}\left(\frac{dJ_R}{da}\right) \qquad 5\text{-}2$$

Thus, in terms of the tearing moduli, Equation 5-1 becomes:

$$T_J > T_{JR}$$

The design method utilizing a J integral approach for flaw assessment thus attempts to use material data obtained from typical laboratory specimens such as compact tension, single edge notched, and center cracked panel specimens in order to assess whether a known crack in a pipe will propagate. Various analytical studies have been presented in the literature which use finite element methods to predict crack propagation in flawed pipes using laboratory data. German and Kumar (Ref. 42) investigated the conditions governing stable crack growth and instability in flawed stainless steel piping. Although the main emphasis of this report is the analysis of ferritic steels, the results reported on the stainless steels are useful because of similar behaviour in these highly ductile materials. The German and Kumar investigation was mainly of an analytical nature in attempting to use specimen data to predict flaw behaviour in both 4 cm and 26 cm diameter pipe. The approach consisted of determining a crack force diagram in which different values of tension or bending were applied to a pipe. The material resistance curve is superimposed on this diagram. According to theory, stable crack propagation will occur at the crack tip when J_{Ic} is surpassed. Unstable crack growth will take place when the criterion given in Equation 5-2 is achieved. Another failure mechanism known as the plastic collapse criterion was also plotted. Failure of the tube may also occur when net section yielding takes place at the tip of the crack. For this case, crack propagation would not occur if this condition was satisfied. The results of their analysis showed that for the type 304 stainless steel studied, a pipe with a circumferential part-through crack loaded in tension would fail by plastic collapse and the crack initiation and tearing processes may not occur. For the case of the through wall crack, decreased pipe length, increased pipe diameter, and increased initial crack length reduce the likelihood of failure by tearing instability and increase the amount of stable crack growth. It is possible for plastic collapse to occur after some stable crack extension but prior to reaching the tearing instability condition. The results presented for the case of a pipe in bending indicated similar trends to that of the pipe in tension in terms of crack size effects and the length/diameter effects.

In the work discussed previously, no actual tests were performed to verify the finite element approach to applying specimen data in predicting failure of cracked pipes. One of the ongoing problems mentioned in utilizing a J-T approach in predicting the conditions for ductile fracture is whether the J-T curve is independent of specimen geometry and thickness. It has again

been recommended recently that the J-T curve ideally should be obtained from specimens whose thickness is equal to or greater than that of the pipe wall being analyzed and should allow for crack extensions up to an amount consistent with the J-T modulus conditions for the application (Ref. 45). Thus, it may be necessary in this approach to obtain data for the individual pipe/crack configuration to be analyzed. This may prevent the development of a "universal" crack propagation analysis graph for each material.

Recently, investigations have been carried out on full size pipes to back up the analytical predictions of crack propagation in ductile type 304 stainless steel (Refs. 40,41). In the first study, Zahoor and Kanninen (Ref. 40) performed tests on cracked pipes and planar specimens to determine the J-T resistance curves for the 304 material. The pipe thickness was about the same as for the CCT and three point bend bar specimens used. The resulting J-T curves indicated a marked difference among the four curves. The tearing modulus was approximately twice as high from the CCT specimen compared to the results from the pipe tests. This showed that the use of a CCT specimen generated J-T curve could predict that a cracked pipe was safe when instability was likely.

In the second paper, Wilkowski et al (Ref. 41) attempt to predict fracture in a cracked tube using a J-T approach utilizing the data from the pipe test results as reported above. Acknowledging the dependence of the J-T curve on specimen geometry, they stated that the curve consistent with the type of constraint experienced by the crack in the structure should be used in assessing instability. An experimental test setup was arranged to test a pipe in a mode in which failure would occur by instability after a limited amount of stable crack growth had occurred. Similar to the pipes tested in Ref. 40, the pipe was loaded in 4 point bending. The pipe diameter was 102 mm and a through wall crack with a length of 106 mm was used. The loading system utilized a high compliance spring to simulate a longer pipe than used in the tests.

The results were as follows. The estimation procedure using the pipe J-T results predicted that for the 106 mm crack, fracture instability should occur after approximately 15-22 mm of stable crack growth at each tip. In the actual experiment, fracture instability occurred after the load had decreased to 86% of the maximum load at an average of 19 mm of stable growth at each crack tip. The results of the test were significant even though it was mentioned that it was difficult to determine exactly when instability had occurred. This was believed to be the first assessment of the use of a J-T approach to predict instability in an actual structure.

2.2 COD Assessment Method

The second approach to be considered for the assessment of ductile fracture uses a COD type of analysis to determine conditions necessary for unstable crack growth. A standard has been written (Ref. 46) to assess the critical crack tip opening displacement (CTOD) occuring at the point of unstable fracture. Similar to the problems encountered with use of J-T approaches in assessing the possibility of unstable crack growth, the results of a test program on various pressure vessel steels showed a thickness dependency on the measured value of the critical CTOD (Ref. 43). The larger specimens

tested yielded a higher CTOD value and a higher apparent toughness. It was suggested that more tests would be required on small specimens to achieve a statistically valid population than that for larger specimens because there was more scatter in the test results for the smaller specimens. In addition, for strictly valid results, the specimens thickness should be equivalent to that of the actual structure to be analyzed.

The use of actual specimen data to predict fracture of cracked pipes using a COD approach has been attempted recently (Ref. 44). Wellman et al investigated the failure of pressure vessels constructed of A517 and A508 steel. The A517 pressure vessels were fabricated from 12.7 mm thick plate rolled to an inside diameter of 378 mm. The length of each vessel was 1.22 m. Longitudinal notches 381 mm in length were machined with a 45 degree cutter to depths from 1.9-4.57 mm. Specimen data for the CTOD was determined using 12.7 mm square bend type specimens. Water was used to pressurize the vessels to failure.

The A508 pressure vessel was forged and machined into cylindrical form with an inside diameter of 686 mm, an outside diameter of 991 mm, and a wall thickness of 152 mm. A longitudinal circular flaw of 127 mm radius was machined from the outer surface of the vessel to a depth of 51 mm and a length of 211 mm. The machined flaw was sharpened by fatigue precracking to a final semi-elliptical size having a depth of 64 mm and a length of 211 mm. The pressure vessel was pressurized at 0 degrees Celsius by use of triethyl phosphate.

The results of the burst tests on the pressure vessels were as follows. Using specimen data for the two types of steels used in the tests, predictions were made of the burst pressures for the different initial flaw sizes using a Burdekin-Dawes (Ref. 47) assessment. This procedure basically makes use of a design curve which compares a non-dimensionalized CTOD value with the flaw size and the yield strain of the material. The resulting prediction of the burst pressure is a very conservative estimate because of the method of determining the design curve. Using such an analysis, the actual burst pressures were overestimated between 22-43%. However, an extensive analysis using finite element methods was much more accurate. Both 2-D and 3-D non-linear finite element analyses were used to predict burst pressure for the five flawed pressure vessels. The FEM predicted the correct burst pressure within 7% of the actual measured burst pressures. In each case, the lowest CTOD value obtained in the laboratory testing of standard three point bend type specimens provided the better correlation with actual pressure vessel failure than did the average CTOD value. In particular, for the single A508 pressure vessel analyzed, the predicted burst pressure was less than 1% in error compared to the actual measured value. The lowest critical value of CTOD measured on the specimens corresponded very closely to that of the measured values off the pipe.

2.3 R-6 Assessment Method

The final method to be considered for use in assessing ductile failure of pipes is the R-6 type of prediction method. The procedure is based upon failure assessment curves derived for typical nuclear vessels and components. Calculations of the ratios of the linear elastic stress

intensity factor to the plane strain fracture toughness (K_r) and the applied load to the plastic collapse load (S_r) in the structure are used in conjunction with the curves to set the validity limits of linear elastic applicability. The limitation of the method is that only primary loads may be considered. Recent papers (Refs. 36,37) have detailed results of investigations to extend the original concepts to additional applications. An example of the use of this method described in Ref. 37 for assessing the structural integrity of a flawed pipe is summarized as follows.

Figure 5-1 shows the LEFM validity diagram which was used for assessing the effects of the flaw in this example. A 26 inch diameter pipe with a wall thickness of 1.3 inches was assumed. The operating pressure was 1200 psi. At the operating temperature, the fracture toughness was 150 ksi$\sqrt{in}$. A circumferential flaw with a crack depth of 0.65" was assumed resulting in a/t=0.5. The calculations show that the stress intensity factor is 15.8 ksi$\sqrt{in}$ which results in a $K_r' = 0.10$. The plastic collapse load was determined to be 3954 kips and the applied load 637 kips which resulted in a $S_r' = 0.16$. Thus, the point with coordinates $(S_r', K_r') = (0.16, 0.10)$ was plotted in Figure 5-1. The position of the point to the right of the LEFM limit line shows that the use of the LEFM failure criterion is invalid for this particular situation. Thus, an elastic-plastic assessment approach must be used to determine the severity of the flaw. The factor of safety for the initiation of stable crack growth for the given loading conditions is calculated by the ratio of the distances OB/OA.

3. Summary

In conclusion, various approaches have been utilized in attempts to analyze the effects of a flaw on the structural integrity of a pipe. Of the three approaches discussed, most effort appears to be directed toward utilizing the J-T assessment approach although the usefulness of the COD and R-6 methods have been the subject of recent investigations. The main problem in attempting to utilize these assessment methods is the strict necessity of requiring data from test specimens of the same thickness as the actual pipes to be analyzed. This in turn complicates the problem of utilizing laboratory data to analyze actual structures.

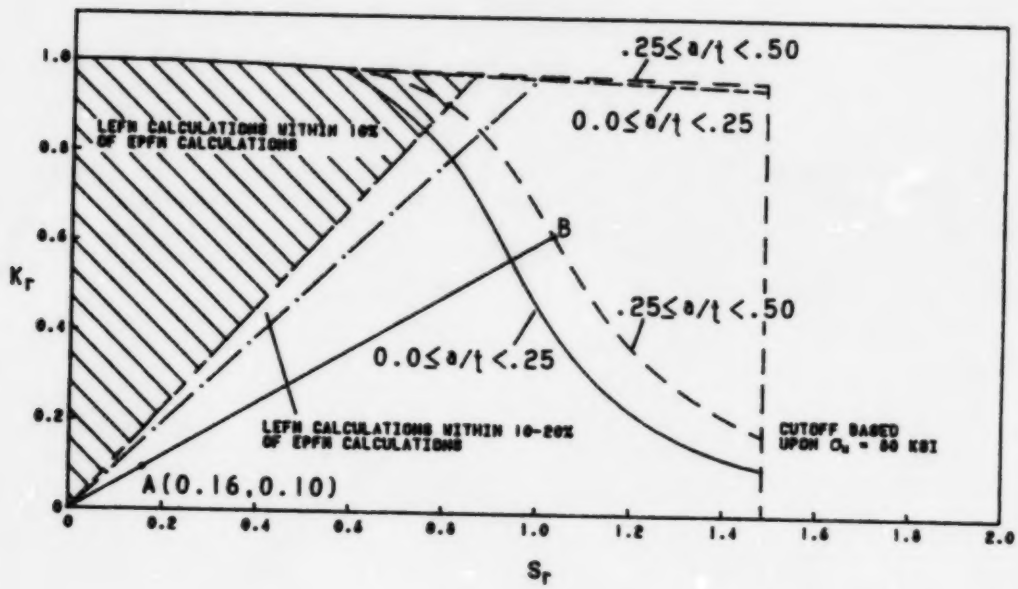

FIGURE 5-1: LEFM VALIDITY DIAGRAM. (REF. 5)

F. DISCUSSION

A vast amount of literature is available in the field of EPFM. This literature, like many other areas of endeavour, requires thoughtful interpretation to develop any meaningful focus.

In broad terms the thrust of fracture mechanics developments can be subdivided into three distinct categories. These are i) energy methods which have a logical theoretical formulation and incorporate the now well established J integral, ii) displacement methods which provide a more physical interpretation of crack growth behaviour and are encompassed in the family of COD measurements and iii) the basic stress field approach through which K_{Ic} has been defined as in LEFM and which convey a distinct empiricism.

To conveniently summarise these developments reference is made to the Venn diagram shown in Figure 6-1.

(1) The common intersection of the energy, stress field and displacement domains represents the area of LEFM where considerable interchangeability of the fracture parameters developed through energy, stress field or displacement concepts exist.

(2) Identification of developments common to any two of the three destructive approaches as it pertains to EPFM considerations, and

(3) Developments in EPFM which are particular to any individual concept.

For completeness, the Venn diagram is extended to include other possibilities such as the twin criterion linking J to CTOA and the empirical Charpy correlations to energy considerations.

While Figure 6-1 has served primarily to loosely categorise the current developments, it is evident that the bulk of the literature and indeed the potential direction or focus of EPFM is now directed towards a J integral based resistance curve or more specifically the J-T approach.

To employ the J-T approach first requires that the J resistance curve be developed. The J resistance curve is unfortunately not a material property, and there is now substantial evidence to suggest that these resistance curves are geometry dependent. Tests on compact tension, three point bending or centre cracked specimens yield considerably different results (8,39,50-52). It is important however to note that a lower bound plane stress J resistance curve is most likely to be obtained from compact tension and/or bend specimens (8), the latter probably being most conservative due to a high triaxial constraint.

To reliably employ J resistance curves will therefore require that these curves be developed from tests which closely approximate the 'near full scale' tests i.e. thickness etc. The J resistance curve will, under these conditions, yield a representative curve and will as such not conform to the strict definitions of J controlled crack growth usually associated with limited crack growth. For full scale tests which closely approximate the structure to be analysed this would be of lesser concern, provided of course

that sufficient data were available to adequately interpolate the results. In the event that such data are not available it would appear that J resistance curves obtained from three point bend specimens would yield a conservative estimate from which the J-T curve might be constructed. A representative evaluation of structural components by J-integral techniques is provided in Appendix A.

A logical extension of this approach, would be to combine the J resistance curve with the CTOA as a twin criterion. The significance of this approach is illustrated in Figure 4-5 where the CTOA assumes a constant value as a function of increasing crack length. While the CTOA is a difficult parameter to measure accurately it is proposed the CTOA values for selected geometries can be analytically determined and catalogued. These values can then be utilised to bound the J-T curves as constructed in Figure 4-4 at the higher value of J.

From the above discussion, it is apparent that there has been considerable development from the earlier application of LEFM to the present need to incorporate EPFM considerations into the analysis and design of structural components. While these developments have been considerable, the real shortcomings of the various approaches is the lack of a universal criterion which can separate the material parameters of characterization from the geometric and load considerations of a given application. To address this difficulty does require i) the need to undertake full scale testing of components or ii) to assess the merits of establishing a lower bound equivalent from laboratory test data which is less conservative than the approach offered by LEFM methods, but which avoids the excessive costs of full scale testing. A further concern associated with limited full scale testing would be the difficulty in transferal of this test data to other similar but geometrically different applications.

This issue is further complicated by the need to understand the mechanism of stable crack propagation rate under conditions of cyclic load. It must be emphasized that our ability to understand and predict this type of behaviour in the elasto-plastic context has little foundation at this time. Appendix B serves to provide an introduction to the current status on fatigue crack propagation.

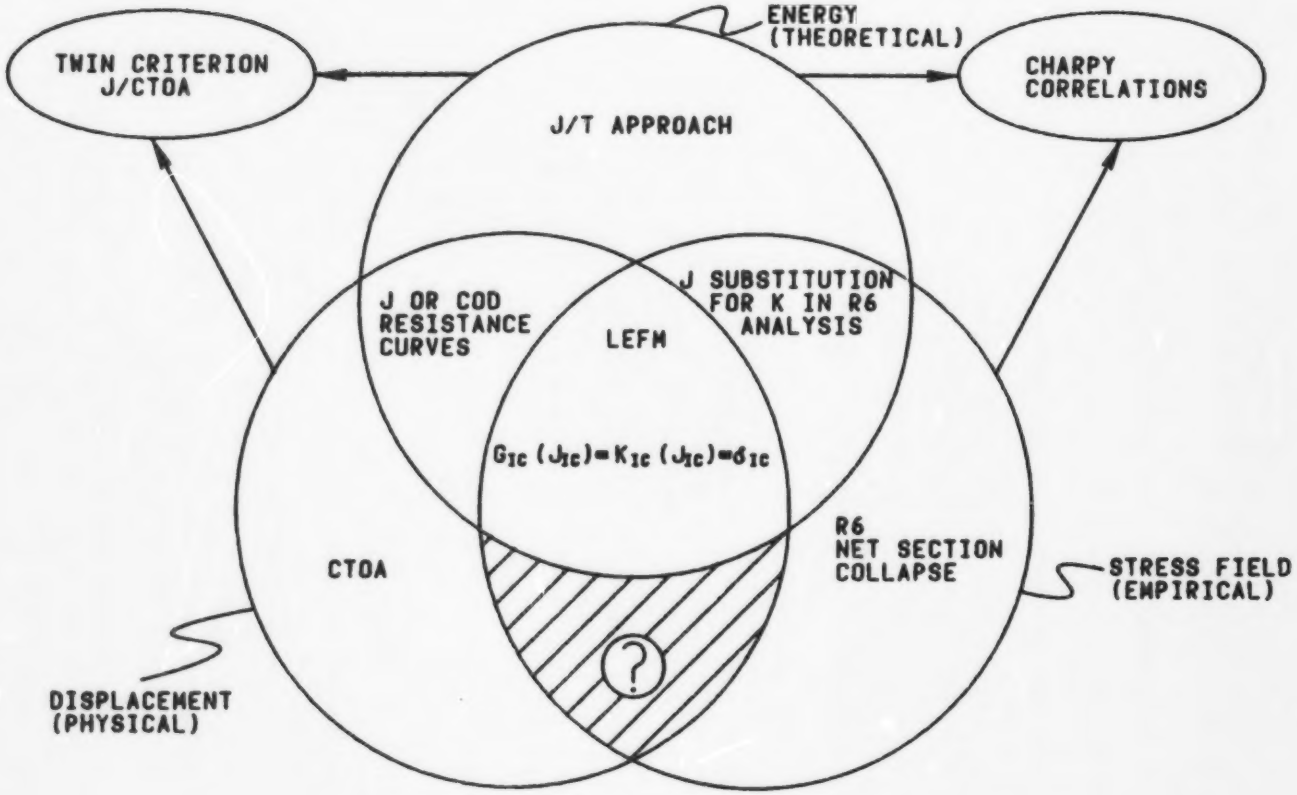

FIGURE 6-1. VENN DIAGRAM ILLUSTRATION OF RELATIONSHIPS BETWEEN ENERGY, STRESS FIELD AND DISPLACEMENT APPROACHES TO FRACTURE MECHANICS ANALYSES.

G. RECOMMENDATIONS

The following recommendations are presented for consideration. It is anticipated that these recommendations, if adequately developed, will enhance our capability in the design process. Subsequent developments, and we refer in particular to stable crack propagation, will in large measure depend upon the understanding which can be derived from the results which may follow from these recommendations.

(1) Experimental development of J-R (J-Resistance) curves.

(2) Utilization of the J-T approach.

(3) Development of the twin J/CTOA criteria.

(4) Investigation into near full scale tests to validate analysis techniques and confirm laboratory data obtained from specimens.

(5) Analysis of different crack configurations, i.e. circumferential longitudinal, angled cracks, through thickness, etc. to assess mixed mode configurations.

These recommendations do require further clarification. It is recommended that an extensive data base of J-resistance curves be developed experimentally using both compact tension and bend test specimens. It would appear from the literature that these specimen configurations will provide the lowest bound of J-resistance curves for a given material. It would be important to develop this compendium of data for a range of different thicknesses which correspond to the wall thicknesses of pipe currently in use. This lowest bound J-resistance curve can be employed in conjunction with the J-T approach to provide a conservative estimate of the fracture instability condition.

It should be realized that the lowest bound interpretation of J-resistance curves obtained from CT and bend test specimens does require confirmation. This can only be achieved by near full scale testing in which the J-resistance curves are compared with the lowest bound J-resistance curves. This type of test will serve to identify the degree of conservatism employed in the use of the lowest bound J-resistance curves obtained from the CT or bend test specimens. It is important to emphasize that no comprehensive data base is available from which it might be concluded that either the CT or bend test will give rise to the lowest bound J-resistance curves for all thicknesses of test specimens employed. It is however, clear from the literature that these configurations do yield J-resistance curves which are certainly more conservative than CCT specimens.

While near full scale tests would be exorbitantly expensive, it is unclear whether the results of small scale tests can be accurately extrapolated to full sized components. Experimental investigation of similitude effects would go a long way to improve the confidence level of the design approach. It would also be necessary to investigate the compliance behaviour of piping structures and to correlate these parameters with laboratory data. From a design standpoint, it would be sufficient to develop resistance curves which could be conservatively applied to a component of any size.

Similar approaches which require the establishment of a family of J-resistance curves leading to the definition of the lowest bound curve can be employed for both heat affected zones and weldments. In essence, it is appropriate to consider these areas of the piping as material distinctly different from the parent material. Data derived from such tests would exhibit more scatter and would consequently require a greater number of tests to account for specimen orientation, etc.

The development of the twin J/CTOA criterion will require extensive finite element analyses to determine the CTOA behaviour as a function of increasing crack length. It is necessary to determine this behaviour for a range of specimen geometries - pipe diameters, thicknesses, etc. to ascertain whether indeed the CTOA maintains a constant value as described within the report. Once data of this type are available, taking into account the apparent constant value of CTOA with increasing crack length, it could be possible to twin the J/CTOA results such that the lowest J-R bounds could be adjusted to incorporate the CTOA data.

It must be emphasized that the understanding of EPFM concepts and the utilization of these concepts are as yet in their infancy. Very little information is available to describe mixed mode configurations which more often than not represents the real situation. This is also true of our understanding of stable crack propagation rates where as yet one can only resort to LEFM approaches of solution.

It is, therefore, important to appreciate that the recommendations are in large measure based on the continued development and design of the J-integral concept. This concept, in its fundamental form, does have a sound theoretical basis and as such offers the means, albeit cautious in the EPFM domain, to interpret and extend results to other situations. This is in sharp contrast with strictly empirical approaches which will always require full scale validation.

REFERENCES

1. Griffith, A.A., "The Phenomena of Rupture and Flow in Solids", Philosophical Transactions, Royal Society of London, A221, p. 163, 1920.

2. Westergaard "Bearing Pressures and Cracks", J. Appl. Mech., 61, p. A49, 1939.

3. Wells, A.A., "Unstable Crack Propagation in Metals: Cleavage and Fast Fracture", Crack Propagation Symposium, Cranfield, England, 1961.

4. Burdekin, F.M. and Stone, D.E.W., "COD Approach to Fracture Mechanics in Yielding Materials", J. Strain Analysis 1, p. 145, 1966.

5. Nichols, F.A., "How Brittle is Brittle Fracture?", Engineering Fracture Mechanics, Vol. 12, pp. 307-316, 1979.

6. Hutchinson, J.W., "Singular Behaviour at the End of a Tensile Crack in a Hardening Material", J. of Mech. and Physics of Solids, Vol. 16, pp. 13-31, 1968.

7. Rice, J.R., and G.F. Rosengren, "Plane Strain Deformation near a Crack Tip in a Power-Law Hardening Material", J. of Mech. and Physics of Solids, Vol. 16, pp. 1-12, 1968.

8. Shih, C.F., Andrews, W.R., German, M.D., Van Stone, R.H. and Wilkinson, J.P.D. "Methodology for Plastic Fracture", EPRI Contract RP 601-2, combined 7th and 8th Quarterly Report prepared by General Electric Company, July 31, 1978.

9. Rice, J.R. "A Path Independent Integral and the Approximate Analysis of Strain Concentration by Notches and Cracks", J. of Appl. Mech., No. 6, pp. 379-386, 1968.

10. Ritchie, R.O., "Why Ductile Fracture Mechanics?", J. of Eng. Mater. and Technol., Vol. 105, pp. 1-7, Jan. 1983.

11. Blackburn, W.S. "Path Independent Integrals to Predict Onset of Crack Instability in an Elastic Plastic Material", Int. J. of Fracture Mech., Vol. 8, pp. 343-346, 1972.

12. Bucci, R.J., Paris, P.C., Landes, J.D. and Rice, J.R. "J-Integral Estimation Procedures", ASTM STP 514, pp. 40-69, 1972.

13. Merkle, J.G. and Corten, H.T. "A J-Integral Analysis for the Compact Specimen, Considering Axial Force as Well as Bending Effects", J. of Pressure Vessel Technol., No. 11, pp. 286-292, 1974.

14. Sumpter, J.D.G. and Turner, C.E. "Method for Laboratory Determination of J_c", ASTM STP 601, pp. 3-18, 1976.

15. Derbalian, G. "J-Integral Estimation Procedures", J. of Pressure Vessel Technol., Vol. 105, No. 11, pp. 299-308, 1983.

16. Begley, J.A. and Landes, J.D. "The J-Integral as a Fracture Criterion", ASTM STP 514, pp. 1-120, 1972.

17. Landes, J.D. and Begley, J.A. "The Effect of Specimen Geometry on J_{Ic}", ASTM STP 514, pp. 24-39, 1972.

18. Griffis, C.A. "Elastic-Plastic Fracture Toughness: A Comparison of J-Integral and Crack Opening Displacement Characterizations", J. of Pressure Vessel Technol., No. 11, pp. 279-283, 1975.

19. Chipperfield, C.G. "A Summary and Comparison of J Estimation Procedures", Journal of Testing and Evaluation, JTEVA, Vol. 6, No. 4, pp. 253-259, 1978.

20. Rice, J.R., Paris, P.C. and Merkle, J.G. "Some Further Results of J-Integral Analysis and Estimates", Progress in Flaw Growth and Fracture Toughness Testing, ASTM STP 536, pp. 231-245, 1973.

21. ASTM E813-81, Standard Test Method for J_{Ic}, A Measure of Fracture Toughness.

22. Tracey, D.M. "Finite Element Solutions for Crack-Tip Behaviour in Small-Scale Yielding", Journal of Engineering Materials Technology, Transactions of the ASME, Vol. 98, pp. 146-151, 1976.

23. Rice, J.R. and Sorensen, E.P. "Continuing Crack-Tip Deformation and Fracture for Plane-Strain Crack Growth in Elastic-Plastic Solids", in Journal of the Mechanics and Physics of Solids, Vol. 26, pp. 163-186, 1978.

24. de Koning, A.U. "A Contribution to the Analysis of Quasi-Static Crack Growth in Sheet Materials", in Fracture 1977, Vol. 3, ICF4, pp. 25-31, Waterloo, Canada, June 19-24, 1977.

25. Green, G. and Knott, J.F. "On Effects of Thickness on Ductile Crack Growth in Mild Steel", in Journal of the Mechanics and Physics of Solids, Vol. 23, pp. 167-183, 1975.

26. Kanninen, M.F., Rybicki, E.F., Stonesifer, R.B., Brock, D., Rosenfield, A.R., Marschall, C.W. and Hahn, G.T. "Elastic-Plastic Fracture Mechanics for Two-Dimensional Stable Crack Growth and Instability Problems", in Elastic-Plastic Fracture, eds. J.D. Landes, J.A. Begley and G.A. Clarke, ASTM STP 668, pp. 121-150, March 1979.

27. Kanninen, M.F. et. al. "The Development of a Plastic Fracture Methodology", Battelle's Columbus Laboratories, Final Report to EPRI on RP 601-1, 1980.

28. Rice, J.R., Drugan, W.J. and Sham, T.L. "Elastic-Plastic Analysis of Growing Cracks", in Fracture Mechanics, ASTM STP 700, pp. 189-221, 1979.

29. Emery, A.F., Kobayashi, A.S., Love, W.J. and Jain, A. "Dynamic Propagation of Circumferential Cracks in Two Pipes with Large Scale Yielding", in Journal of Pressure Vessel Technology, Vol. 102, pp. 28-32, 1980.

30. Hermann, L. and Rice, J.R. "Comparison of Experiment and Theory for Elastic-Plastic Plane Strain Crack Growth", Brown University, Technical Report No. 76 to the U.S. Department of Energy, February 1980.

31. Dowling, A.R. and Townley, C.H.A., "The Effects of Defects on Structural Failures: A Two-Criteria Approach", International Journal of Pressure Vessels and Piping, Vol. 3, pp. 77, 1975.

32. Harrison, R.P., Loosemore, K., and Milne, I., "Assessment of the Integrity of Structures Containing Defects", CEGB Report No. R/H/R6, Central Electricity Generating Board, 1976. Updated Revision 2, April 1980.

33. Bloom, J.M., "A Procedure for the Assessment of the Structural Integrity of Nuclear Pressure Vessels", Journal of Pressure Vessel Technology, Vol. 105, pp. 28-34, 1983.

34. Bloom, J.M. and Hechmer, J.L., "Limits of Linear Elastic Fracture Mechanics", Journal of Pressure Vessel Technology, Vol. 106, pp. 196-200, 1984.

35. Bloom, J.M. and Malik, S.N., "A Procedure for Assessment of the Integrity of Nuclear Pressure Vessels and Piping Containing Defects", EPRI Topical Report NP-2431, June 1982.

36. Bloom, J.M., "A Procedure for the Assessment of the Structural Integrity of Nuclear Pressure Vessels", Journal of Pressure Vessel Technology, Vol. 105, pp. 28-34, 1983.

37. Bloom, J.M. and Hechmer, J.L., "Limits of Linear Elastic Fracture Mechanics", Journal of Pressure Vessel Technology, Vol. 106, pp. 196-200, 1984.

38. Paris, P.C., Tada, H., Zahoor, A. and Ernst, H. "The Theory of Instability of the Tearing Mode of Elastic-Plastic Crack Growth", ASTM STP 668, pp. 5-36, 1979.

39. Kanninen, M.F., Popelar, C.H., and Broek, D., "A Critical Survey on the Application of Plastic Fracture Mechanics to Nuclear Pressure Vessels and Piping", Nuclear Engineering and Design, Vol 67, pp. 27-55, 1981.

40. Zahoor, A. and Kanninen, M.F., "A Plastic Fracture Mechanics Prediction of Fracture Instability in a Circumferentially Cracked Pipe in Bending - Part I: J-Integral Analysis", Journal of Pressure Vessel Technology, Vol. 103, pp. 352-358, 1981.

41. Wilkowski, G.M., Zahoor, A., and Kanninen, M.F., "A Plastic Fracture Mechanics Prediction of Fracture Instability in a Circumferentially Cracked Pipe in Bending - Part II: Experimental Verification on a Type 304 Stainless Steel Pipe", ibid. 2, pp. 359-365.

42. German, M.D. and Kumar, V., "Elastic-Plastic Analysis of Crack Opening, Stable Growth and Instability Behaviour in Flawed 304 SS Piping", Journal of Pressure Vessel Technology, Vol. 105, pp. 290-298, 1983.

43. Wellman, G.W. and Rolfe, S.T., "Engineering Aspects of CTOD Fracture Toughness Testing", Welding Research Council Bulletin, Bulletin 299, pp. 3-14, 1984.

44. Wellman, G.E., Rolfe, S.T., and Dodds, R.H., "Failure Prediction of Notched Pressure Vessels Using the CTOD Approach", ibid. 7, pp. 26-35.

45. Report of the U.S. Nuclear Regulatory Commission - Piping Review Committee, "Evaluation of Potential for Pipe Breaks", NUREG-1061, Vol. 3, Nov. 1984.

46. British Standards Institute, "Methods for Crack Opening Displacements Testing", BS5762:1979.

47. Burdekin, F.M. and Dawes, M.G., "Practical Use of Yielding and Linear Elastic Fracture Mechanics with Particular Reference to Pressure Vessels", I. Mech. E. Conference on the Practical Application of Fracture Mechanics to Pressure Vessel Technology, London, England, May 1971.

48. Kanninen, M.F. et al "Instability Predictions for Circumferentially Cracked Large-diameter Type 304 Stainless Steel Pipes Under Dynamic Loading. Second Semi-Annual Report to EPRI on RP2554-2 (June 1980).

49. Kanninen, M.F., et al "The Development of a Plastic Fracture Methodology, Battelle's Columbus Laboratories, Final Report to EPRI on RP601-1, 1980.

50. Albrecht, P., Andrews, W.R., Gudas, J.P., Joyce, J.A., Loss, F.J., McCabe, D.E. Schmidt, D.W. and VanDerSluys, W.A., "Tentative Test Procedure for Determining the Plane Strain J_I-R Curve", Journal of Testing and Evaluation, JTEVA, Vol. 10, No. 6, pp. 245-251, Nov. 1982.

51. Gudas, J.P. and Davis, D.A., "Evaluation of the Tentative J_I-R Curve Testing Procedure by Round Robin Tests of HY130 Steel", Journal of Testing and Evaluation, JTEVA, Vol. 10, No. 6, pp. 252-262, Nov. 1982.

52. Putatunda, S.K., Rigsbee, J.M. and Corten, H.T., "Effect of Size on Elastic-Plastic Fracture Toughness Parameters", Journal of Testing and Evaluation, JTEVA, Vol 13, No. 3, pp. 181-190, May, 1985.

53. Scarlin, R.B. and Shakeshaft, M., "Limitations of Some Methods of Establishing Fracture Toughness Data", Metals Technology, pp. 1-9, January 1981.

54. Hoeppner, D.W. and Krupp, W.E., "Prediction of Component Life by Application of Fatigue Crack Growth Knowledge", Engineering Fracture Mechanics, Vol. 6, pp. 47-70, 1974.

55. Hoeppner, D.W., "Estimation of Component Life by Application of Fatigue Crack Growth Threshold Knowledge", Fatigue and Creep of Pressure Vessels for Elevated Temperature Service, MPC-17, ASME, New York, N.Y., pp. 1-85, 1981.

56. Hoeppner, D.W., "Application of Damage Tolerance Concepts to Short Cracks", Invited Paper presented at International Committee on Aeronautical Fatigue Symposium, Toulouse, France, published in ICAF proceedings, May 1983.

57. Hoeppner, D.W., Ekvall, J.C., McCammond, D., Venter, R.D. and Poon, C., Aircraft Structural Fatigue, Course notes for course of same name prepared for U.S. Federal Aviation Administration, 1979.

58. Dowling, N.E. and Begley, J.A., "Fatigue Crack Growth During Gross Plasticity and J-integral", ASTM STP 590, pp. 82-103, 1976.

59. Dowling, N.E., "Geometry Effects and the J-Integral Approach to Elastic-Plastic Fatigue Crack Growth", ASTM STP 601, pp. 19-32, 1976.

60. El Haddad, M.H. and Mukherjee, B., "Elastic-Plastic Fracture Mechanics Analysis of Fatigue Crack Growth", ASTM STP 803, pp. II-689-707, 1983.

NOMENCLATURE

a	crack length
a_{eff}	effective crack length
b	size of uncracked ligament
B	specimen nominal thickness
C_m	system compliance
d_n	numerical constant
E	Young's modulus
f	load-displacement curve
G	strain energy release rate (also G_I, G_{II}, G_{III})
G_c	critical value of G
I_n	integration constant
J	J-integral
J_e	elastic component of J (also J^e)
J_{Ic}	critical value of J in plane strain
J_p	plastic component of J (also J^p)
k	elastic stiffness of cracked specimen
K_{Ic}	fracture toughness
n	strain hardening exponent
n_1	constant (also n_2)
P	load
P_L	limit load
P_{max}	maximum load
P_{GY}	general yield load
r	rotational constant, co-ordinate axis
r_y	size of plastic zone at crack tip
s	arc length along Γ

t	plate (or pipe) thickness
T	tearing force
$\mathbf{T}$	traction vector
T_R	tearing modulus
$\hat{u}$	displacement vector
U	total absorbed energy
U_c	energy component of U solely associated with the presence of a crack
U_e	elastic component of U
U_ℓ	work done by traction forces at specimen boundaries
U_{nc}	energy component of U resulting from the deflection of the unnotched test specimen
U_p	plastic component of U
U_s	surface energy of crack surface
V	total clip gage displacement
V_e	elastic component of clip gage displacement
W	specimen width
x	coordinate axis
y	coordinate axis
z	knife edge thickness, coordinate axis
α	constant
Δ	load point displacement
Δ_p	plastic component of Δ
Δ_T	total displacement including system
ν	Poisson's ratio
ϵ	strain
σ	stress
σ_Y	yield stress

η constant which is geometry dependent

γ surface energy

ψ function of geometry and loading

θ co-ordinate axis

δ crack opening displacement

δ_c critical value of δ

APPENDIX A

EVALUATION OF STRUCTURAL COMPONENTS BY J-INTEGRAL TECHNIQUES

The evaluation of structural components by J-integral methods requires that a material J-resistance curve be obtained which is representative of the component in question. A standard method for obtaining such a curve shall be briefly reviewed in Section 1. Included is a short discussion on the merits of using a J-T curve, as opposed to the J-resistance curve, to evaluate a structural component.

Section 2 provides an overview of how to obtain the J-driving curve (and T-driving curve) for a particular component, with a graphical description of how these curves compare with those obtained in Section 1. Quantitative methods for analyzing these curves are presented in Section 3; these include methods to assess whether stable crack propagation is possible, and the mode of ultimate failure. In Section 4, comments are provided on the limitations of this analysis method, and the range of tests required before these techniques can be appropriately used.

1. Development of a J-Resistance Curve*

A J-resistance curve can be derived from the load-displacement curves of a number of test specimens, each identical in shape and loading configuration, but precracked to different crack lengths "a". Due to uncertainties regarding the dependence of J on various parameters, the material, geometry, heat treatment, etc. should be as close as possible to those of the component in question, and the range of crack sizes should be representative of those under investigation (Ref. 40). (For our purposes, an appropriate crack size would be one that leads to an easily detectable leakrate from a pipe, including some factor of safety (Ref. 45) Suggested criteria for selecting the number of test specimens needed for either archival or fresh material, are given in Ref. 45.

For each load displacement test, the value of J, henceforth subscripted as J_{mat}, can be calculated from (Ref. 38,53):

$$J_{mat} = \frac{2U}{B(w-a)} \qquad \text{A-1}$$

where U is the area under the load-displacement curve up to the point of first crack extension, B is the specimen thickness, and (w-a) is the length of the uncracked ligament. A graph is then constructed of J_{mat} versus crack length, or J_{mat} versus Δa, where Δa is the difference in crack length between the current and first specimen.

---

* Refer to Standard Test Method for Determining J-R Curves, 12th Draft, 25 July 1985, ASTM Committee on Testing.

An idealized graph, shown in Figure A-1, will initially rise very steeply at a constant slope and then abruptly shift to a much smaller slope at $J_{mat} = J_{Ic}$, where stable tearing begins. (Brittle materials may abruptly fail without showing any stable tearing. Materials with a small thickness B will not start to tear until $J_{mat} > J_{Ic}$.) In practice, a smooth curve is normally observed, also shown in Figure A-1 (Ref. 42).

Rather than use this figure to evaluate actual structures, a graph of the material tearing modulus T_{mat} versus J_{mat} is constructed as presented in Figure A-2, where:

$$T_{mat} = \frac{E}{\sigma_Y^2} \frac{dJ_{mat}}{da} \qquad \text{A-2}$$

There are two primary motivations for introducing the tearing modulus:

(1) T_{mat} shows less temperature dependence than does J_{mat}, and therefore, testing temperatures may be somewhat different from operating temperatures (Refs. 12,45).

(2) The stability of a structure is assessed by comparing $\frac{dJ_{mat}}{da}$ with $\frac{dJ}{da}$ of the applied load. It is far easier to visually compare the magnitudes of two plots than to compare their derivatives.

2. Evaluation of J-Loading Curves

The J-loading or driving force curve must be obtained by approximate analytical techniques. The usual approach is to separate J into elastic and plastic components. The elastic component can easily be calculated (Ref. 42), and is normally much smaller than the plastic component. The plastic component can be determined from modified fully-plastic solutions for simple geometries, using numerical techniques. Note that the J-loading curve depends not only on crack geometry, but also on the global geometry of the component, e.g., length-to-radius ratio of a pipe. Either load or displacement controlled loading may be considered, depending primarily on the system's method of restraint (Ref. 40).

Typical J-loading and tearing modulus curves are superimposed on their respective material property curves in Figures A-1 and A-2. Figure A-1 illustrates that as Δa increases, the crack driving force (for load-controlled configurations) escalates rapidly while the material resistance to crack growth fails to keep pace.

3. Crack Stability Analysis

Use of Figures A-1 and A-2 to assess crack stability is assisted by a physical understanding of what happens as the load is increased on a cracked specimen. There will be no crack extension until $J_{applied}$ is equal to J_{mat} (for a sharp crack in a thick specimen, this will occur at J_{Ic} (Ref. 38)). If at this equilibrium point, one has $T_{applied} < T_{mat}$, then a

small crack extension will result in $J_{applied}$ being less than J_{mat}, so that crack propagation will cease until the load is further increased.

After a certain amount of extension, however, $T_{applied}$ will increase to approach T_{mat}. At this point, any further increase in applied load will cause catastrophic failure, because no amount of further crack extension can return J_{mat} to equilibrium with $J_{applied}$. The value of J at which T_{mat} equals $T_{applied}$ provides the amount of stable growth before instability occurs.

It is important to note that failure of a component can occur not only through crack propagation, but also through plastic collapse. This situation normally arises when the plastic zone surrounding the crack tip extends to the component's boundary. Such failures lie beyond the domain in which J-integral techniques are considered valid, as illustrated in Figure A-2.

The question of crack stability can also be addressed by considering the various regions of the graph in Figure A-2:

Region A: This section corresponds to $J_{applied} < J_{Ic}$; no crack extension is possible and stability is therefore not an issue.

Region B: To the left of T_{mat}, in the region lying between the J_{Ic} line and the value of J corresponding to plastic collapse, there will be stable crack growth. Note that J-integral techniques are highly suspect near conditions of plastic collapse.

Region C: To the left of T_{mat}, in the area lying above the plastic collapse line, the component will fail by plastic collapse of the remaining ligament.

Region D: To the right of the T_{mat} line, and above the J_{Ic} line, failure will occur by rapid unstable crack growth.

The amount of stable crack growth preceding failure can also be determined from Figures A-1 and A-2. For example, considering the applied load-controlled curve of Figure A-2, stable crack growth will occur up to the point "P". The value of J corresponding to "P" is then used to determine the amount of crack extension from Figure A-1 (Ref. 42).

4. Limitations

The theory of crack stability analysis based on J-integral methods is based on the premise that J_{mat} is dependent only on the amount of crack extension. Tests have shown, however, that there is a measurable dependence on specimen geometry and original crack size (Ref. 40). For this reason, tests should be conducted on specimens whose geometry and load configurations duplicate or bracket those of the actual component to the extent possible. When this is not feasible, specific tests can be done that yield conservative values of J_{mat}, where use is made of general trends observed over extensive testing programs. For example, tests on stainless steel piping (Ref. 42) indicated that the extent of stable crack growth is increased by:

(a) decreasing the pipe length

(b) increasing the pipe diameter

(c) increasing the initial crack length

Other trends, such as the conservative effect of using sidegrooves in the measurement of J_{mat} on CT specimens, should enable the extrapolation of laboratory results to a plant environment.

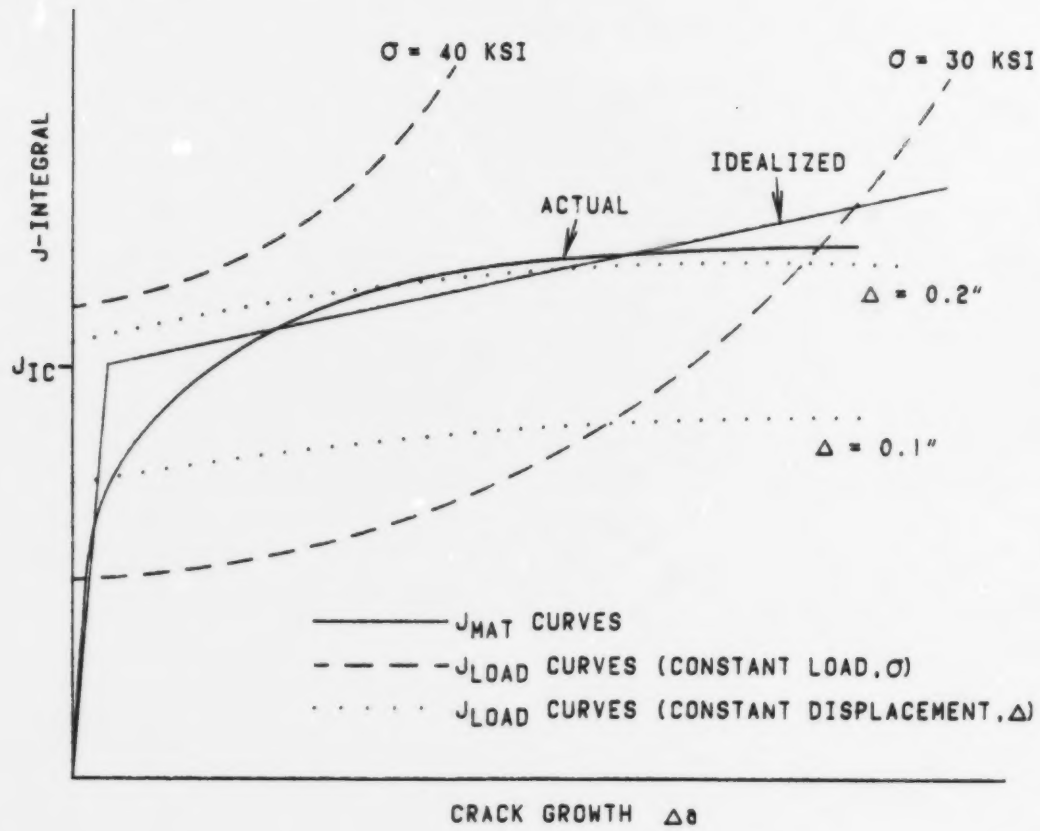

FIGURE A-1: REPRESENTATIVE J_{MAT} AND J_{LOAD} CURVES. (ADAPTED FROM REF. 42)

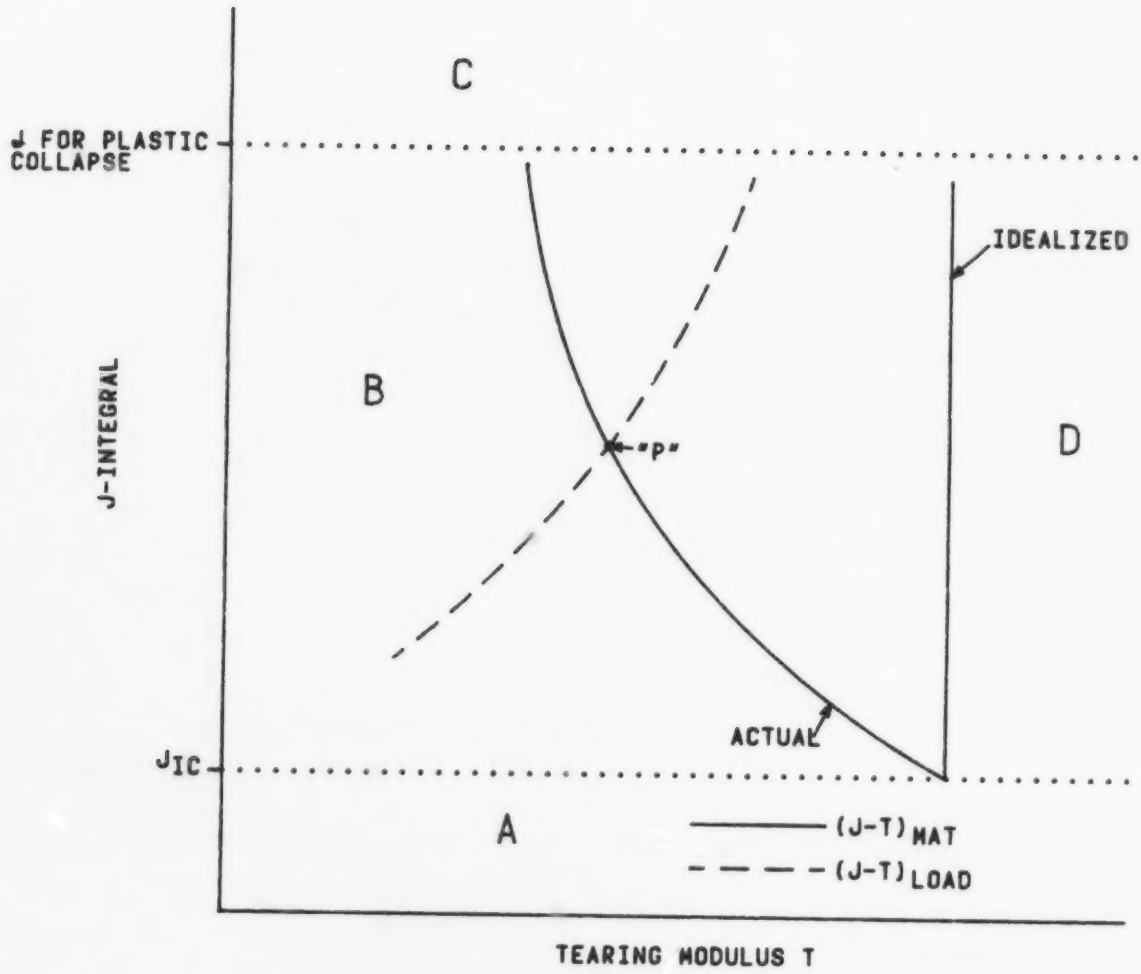

FIGURE A-2: REPRESENTATIVE J-INTEGRAL VERSUS TEARING MODULUS PLOTS. (ADAPTED FROM REFS. 42 AND 45)

APPENDIX B

FATIGUE CRACK PROPAGATION

1. Introduction

For many years the design community has been searching for a life prediction method for dealing with the portion of the fatigue process known as the fatigue crack propagation process. In a more general sense, "damage" is known to develop under cyclic loading that results in either formation of a discontinuity or propagation of a discontinuity that is inherent to a component. In the first instance, if a single discontinuity is propagating, and if it can be modelled with fracture mechanics, then in today's technology the generation of data, modelling of data, and application of data to life estimation (for total life or propagation of cycles between inspection intervals) are straightforward for LEFM conditions only. In the section that follows, a brief discussion of the LEFM techniques is provided. As a future activity, it is recommended that an extended review of fatigue crack propagation lifing techniques be prepared.

Figure B-1 shows the the conceptual divisions of the fatigue process. Region 1 deals with the areas where a discontiniuity must form, if not present initially. Region 2 deals with propagation but the structure of the material influences the propagation and thus fracture mechanics cannot currently be used to model this portion of the process. Regions 3 and 4 are where fracture mechanics can be used as indicated in Figure B-1(a) and presented in columns 3 and 4 on Figure B-1(b). Figure B-2(a) depicts a more general representation of crack growth while Figure B-2(b) shows the general plot of data that results after processing the data as described in Ref. 54 and the ASTM E647 standard for fatigue crack propagation testing.

The evaluation of fatigue crack propagation behaviour is performed to compare materials and to experimentally (empirically) and analytically develop fatigue-crack propagation predictive capability. Numerous fatigue-crack propagation "laws" have been proposed and are discussed in Ref. 54. The number of relationships put forth is obviously large. This is in part due to the possibility of presenting a relationship in one of a number of forms dependent on the variables introduced. Thus, to present a tractable relationship could involve many different variables.

Most analytical approaches to the problem have attempted to relate the growth rate (da/dN) with crack length, plastic enclave size, material parameters, stress, and specimen dimensions. The relationships differ primarily in the emphasis placed on the variables and the concomitant assumptions.

It is now generally agreed that fatigue crack-growth can be prediced by some form of one of the following equations

$$\frac{da}{dN} = C_1(a)^n \qquad \text{B-1}$$

$$\frac{da}{dN} = C_2\sigma(a)^n \qquad \text{B-2}$$

$$\frac{da}{dN} = C_3 f(K) \qquad \text{B-3}$$

At the present time, equations of the form given by Equation B-3 are preferred because of the relative simplicity with which they relate gross stress and crack length by the stress intensity parameter. Thus, the prediction of fatigue life or initial flaw size between inspection intervals depends on the application of an equation similar to those above. However, more advanced fitting functions are being used as well as direct use of actual data from fatigue crack propagation experiments.

Refs. 54-57 give detailed examples of the application of data to life prediction. For purposes of this brief summary, Table B-1 is provided showing one example of such an application. Different procedures can be used depending on the inputs and desired outputs. As indicated previously, the most reliable method to perform the analysis is to use actual data and perform stepwise integration. However, simple relationships, such as the Paris relationship $da/dN = C(\Delta K)^n$, can be used if, and only if, the boundary conditions for its use are satisfied.

(a)

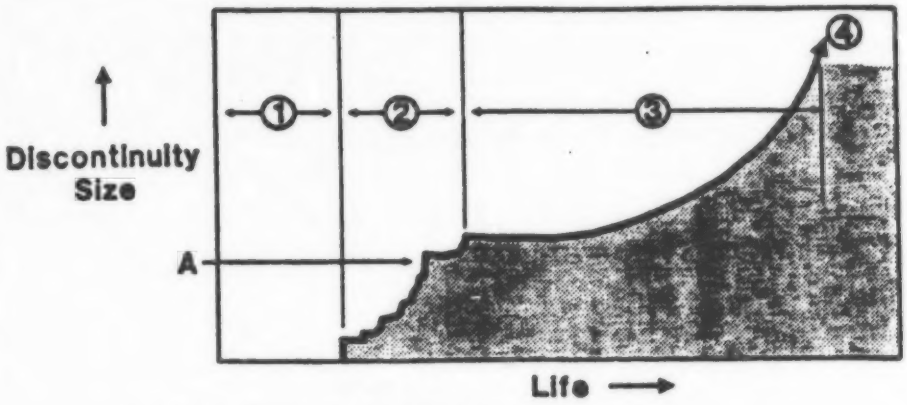

A: "FIRST" detectable crack
1: Nucleation phase, "NO CRACK"
2: "SMALL CRACK" phase - steps related to local structure (Anisotropy)
3: Stress dominated crack growth, LEFM ,EPFM
4: Crack at length to produce instability

(b)

METHODS FOR EACH LIFE PHASE

Nucleation	"SMALL CRACK" Growth	Stress Dominated Crack Growth	Failure (Fracture)
Material failure mechanism with appropriate stress/strain life data	Crack Prop. threshold related to structure (micro)	Fracture mechanics •similitude •boundary cond. ⟨ LEFM / EPFM ?	K_{Ic} etc.
Nucleated discontinuity (not inherent) type,size,location	Structure dominated crack growth	Data base **	C.O.D.
Presence of malignant D°,H°	Mechanisms, rate	Appropriate stress intensity factor	Tensile/ compressive buckling
Possibility of extraneous effects • Corrosion • Fretting • Creep • Mechanical damage	Onset of stress dominated crack growth	Initial D°,H° Size,location,type	
	Effects of •R ratio •Stress state •Environment •Spectrum-waveform ⟨ t / chem / T	Effects of •R ratio •Stress state •Environment •Spectrum -waveform ⟨ t / chem / T	

FIGURE B-1: THE DAMAGE PROCESS IN FATIGUE

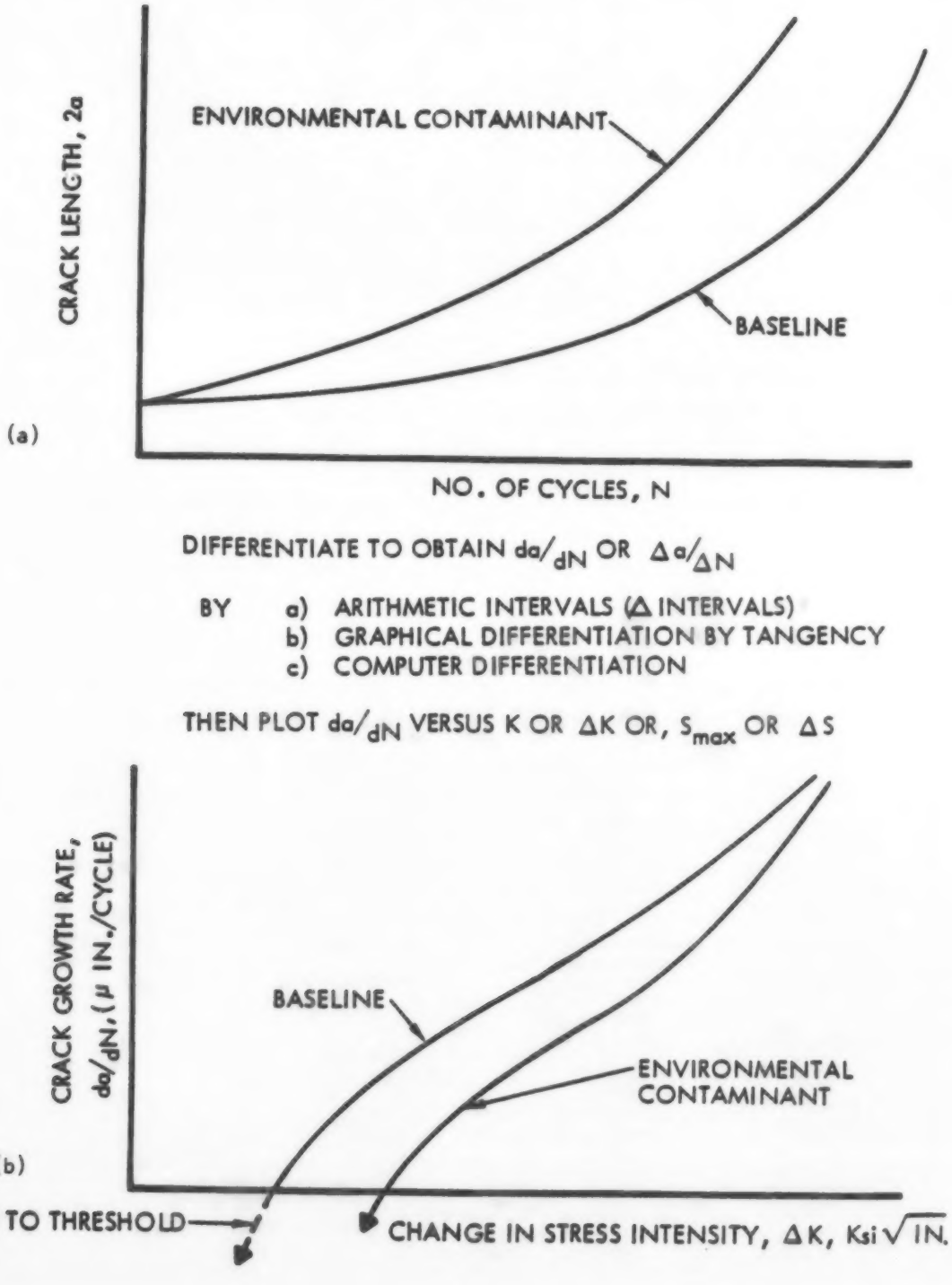

FIGURE B-2: TYPICAL FATIGUE CRACK GROWTH DATA.

TABLE B-1: Steps in Applying Fracture Mechanics Concepts to Fatigue-Crack Propagation Analysis

1. Establish Initial Flaw Size, a_i

   a) Maximum size flaw that can be missed in an inspection

   b) Establish reliability, confidence level

2. Define Failure Criterion and Determine Critical Flaw Size for Material/Thickness/Geometry Combination

   a) From K_{Ic} with thickness, B, greater than B_c use

$$a_c = \frac{1}{\pi \psi} \left(\frac{K_{Ic}}{\sigma}\right)^2$$

   b) If K_c greater than K_{Ic} for the thickness of interest, use

$$a_c = \frac{1}{\pi \psi} \left(\frac{K_c}{\sigma}\right)^2$$

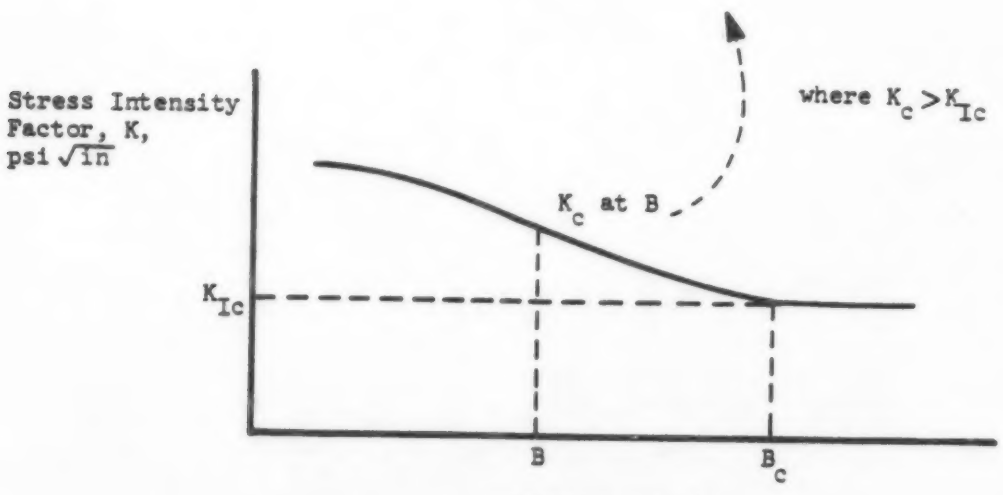

TABLE B-1 (Cont'd)

3. Calculate Cycles Required to Grow Crack from a_i to a_c from Fatigue-Crack Growth Law

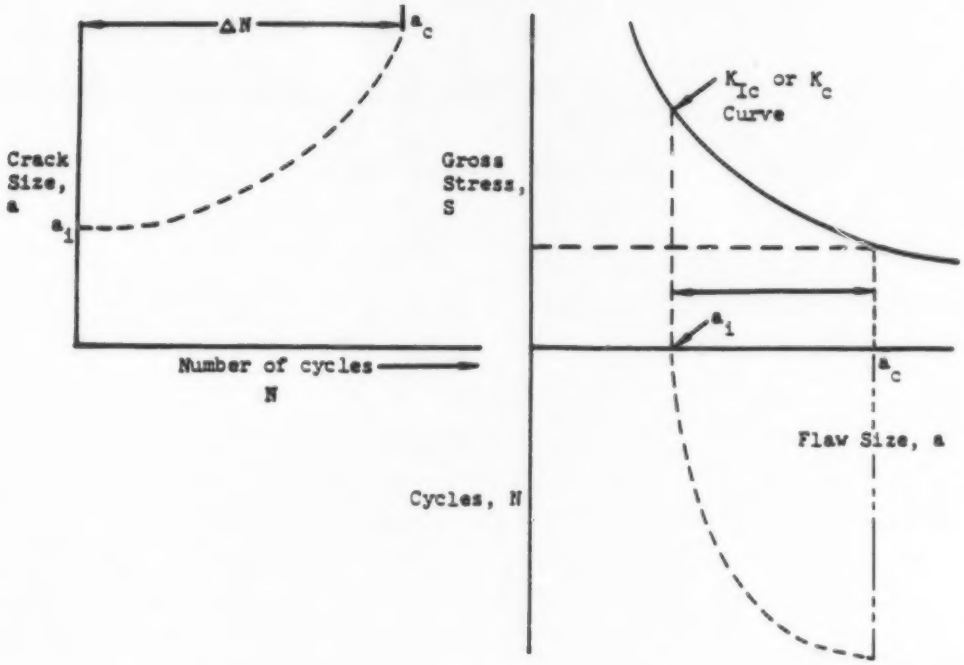

Inputs

a_i, B

K_{Ic} or K_c

a_c

Environment, Temperature or Contaminant (frequency, wave form)

basic material property data, C, N

Stress (Including Spectrum)

or

Life Requirement

Perform Analysis to Yield Output

$\frac{da}{dN} = f(\Delta K)$

or

$\frac{da}{dN} = \frac{C(\Delta K)^n}{(1-R)\,K_c - \Delta K}$

Outputs

Operating Stress Level (Allowable)

or

Life

2. Discussion of Fatigue Crack Propagation in EPFM

In crack propagation analyses, the correlation between stress intensity and fatigue crack growth rates from LEFM can be depicted as shown in Figure B-3. Moreover, within an intermediate stress intensity range, ΔK, a straight line is usually obtained on a log-log plot of ΔK versus cyclic crack growth rate, da/dN. According to the Paris law, the relationship between ΔK and da/dN follows from

$$da/dN = C(\Delta K)^n \qquad \text{B-4}$$

where C and n are constants for a given material and stress ratio. This relationship is particularly true for low toughness high strength structural materials.

However, it is essential to develop other criteria for fatigue crack growth which account for plasticity effects where crack growth rates cannot be simply expressed in terms of ΔK. This is especially necessary for ductile metals of high fracture toughness.

Dowling and Begley (Ref. 58) were the first to attempt investigations into elastic-plastic fatigue crack growth using CT specimen identical to that of the ASTM standard (ASTM E399). Cyclic J values were estimated from load versus deflection hysteresis loops taking cognizance of the effect of crack closure. A typical method of analysis is shown in Figure B-4, and test data results for an A533B pressure vessel steel is shown in Figure B-5. An analogous relationship to that of the LEFM approach was derived using a least squares fit through the data points and is given by

$$\frac{da}{dN} = 2.13 \times 10^{-8} (\Delta J)^{1.587} \qquad \text{B-5}$$

Equation B-5 expresses the rate of fatigue crack growth as a power function of the range of J-integral (ΔJ). A particular difficulty associated with the determination of the cyclic J is the type of control condition which is sufficiently adequate for crack growth studies during gross plasticity. This was partially alleviated in their work by controlling the deflection to a sloping line on a load versus deflection plot (Figure B-6), using an analog control circuit. When exercising load control conforming to the sloping line, the cyclic plastic deformations were small but large plastic deformation in the tensile directions accumulated during the tests. A consequence of load-controlled tests was that beyond a certain ΔJ value, crack growth rates increased without further increase in ΔJ. This behaviour, according to Dowling and Begley (Ref. 58) is related to the unstable increase in crack growth rate observed at the end of linear elastic crack growth tests on ductile materials.

Finally, in deriving correlations between da/dN and ΔJ, load range, elastic-plastic deflection range, crack opening deflection and crack length must be accounted for.

Later work by Dowling (Ref. 59) on CCT and large CT specimens using an A533B pressure vessel steel demonstrated the geometric independence of cyclic J. The results suggest that the J-integral is a valid geometry and size

independent correlation parameter for elastic-plastic fatigue crack growth rate. Recent investigations on a CT specimen of ASTM A516 Gr 70 steel by El Haddad and Mukherjee (Ref. 60) confirm the potential of the J-integral parameter in correlating fatigue crack growth, particularly in ductile materials at high load levels.

While these types of correlations are being investigated, it can be argued that the ΔJ parameter is indeed artificial and has very limited association with the fundamental definition of J.

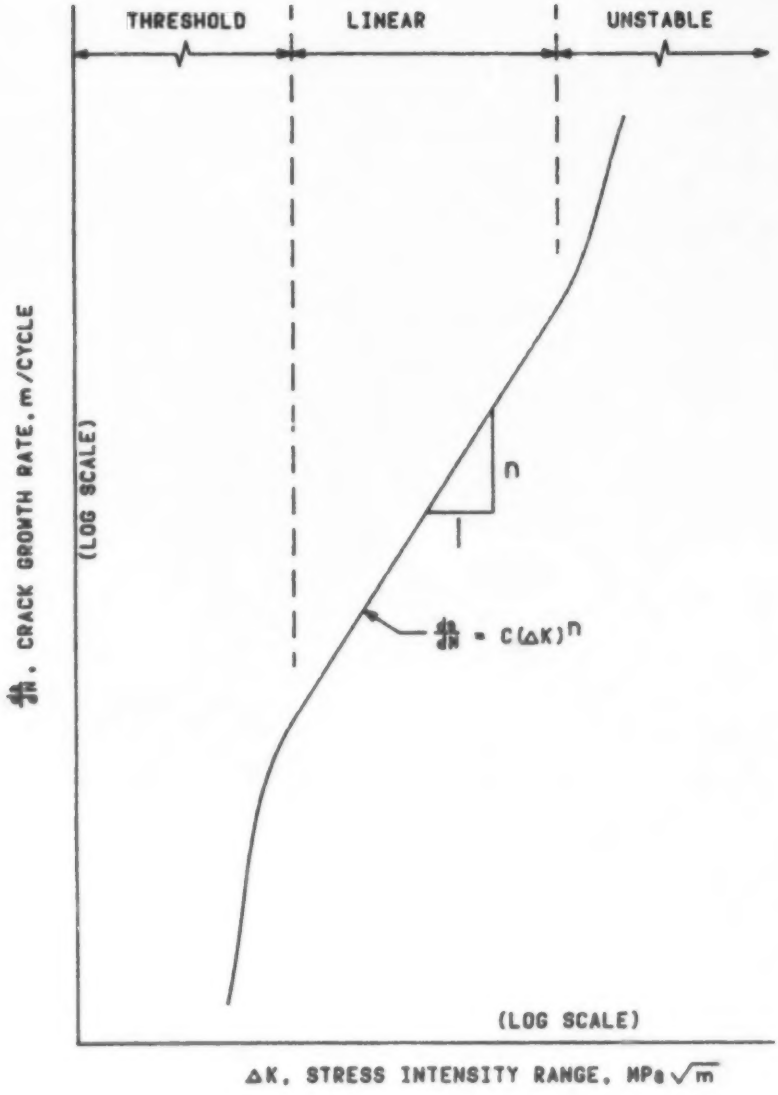

FIGURE B-3: RELATIONSHIP BETWEEN FATIGUE CRACK GROWTH RATE AND STRESS INTENSITY RANGE.

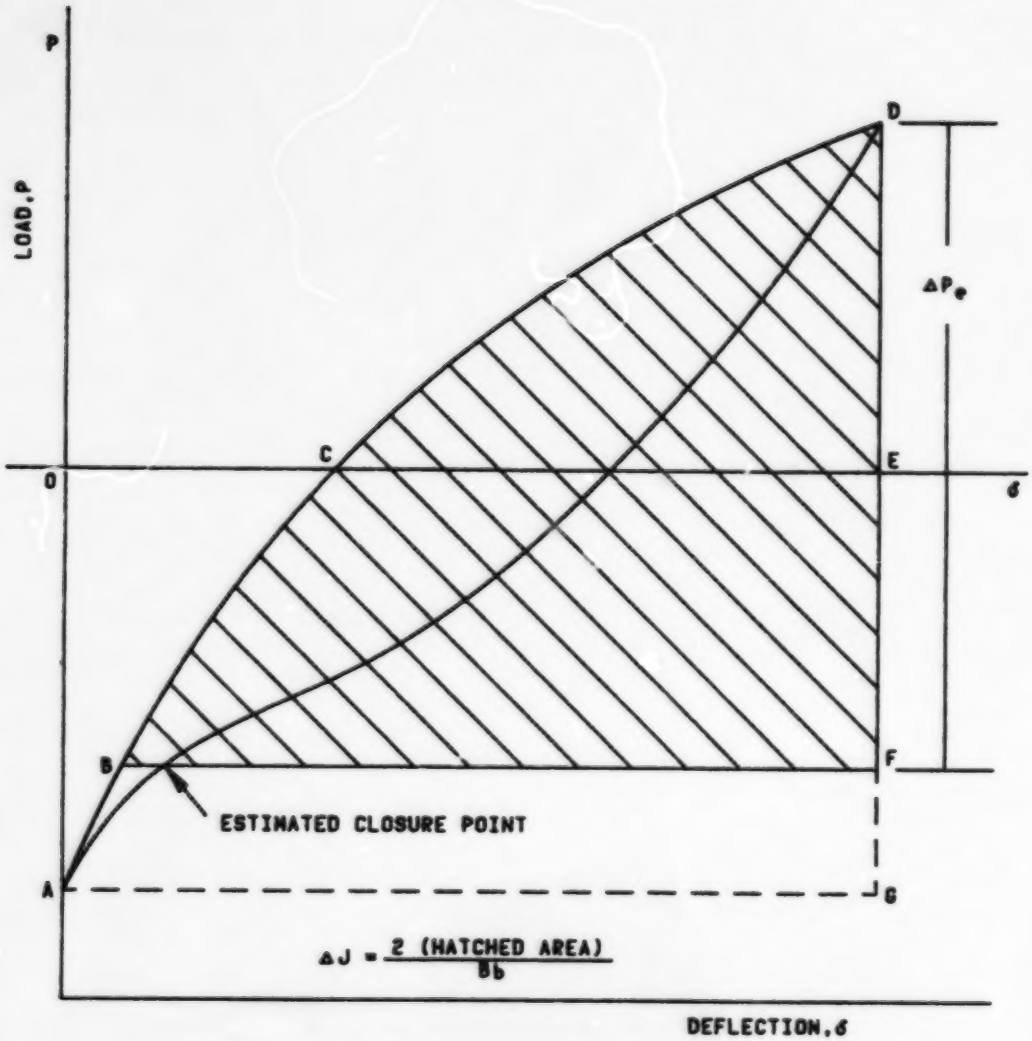

FIGURE B-4: OPERATIONAL DEFINITION OF CYCLIC J. (REF. 58)

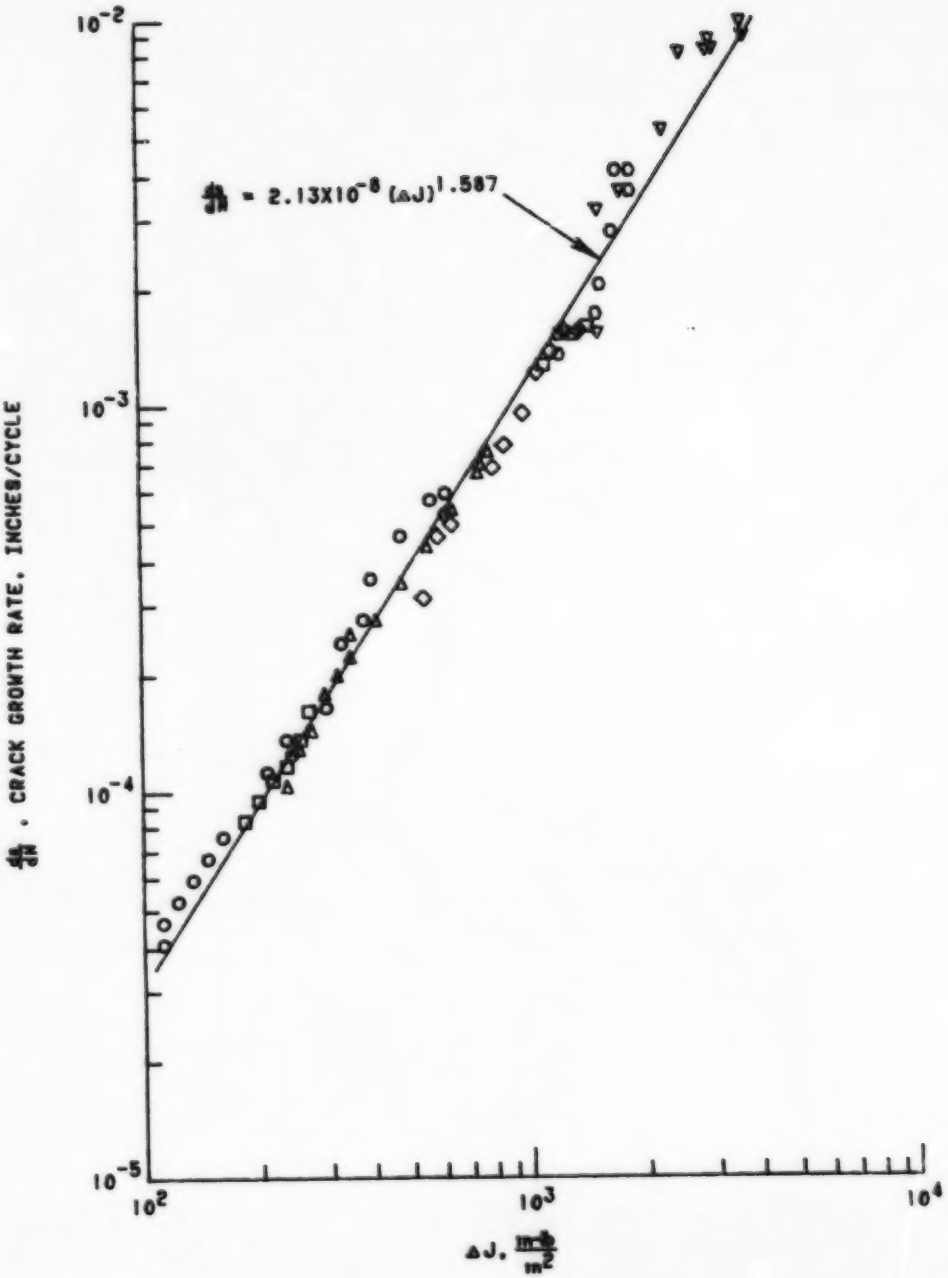

FIGURE B-5: FATIGUE CRACK GROWTH RATE AS A FUNCTION OF J FOR DEFLECTION CONTROL TO A SLOPING LINE. (REF. 58)

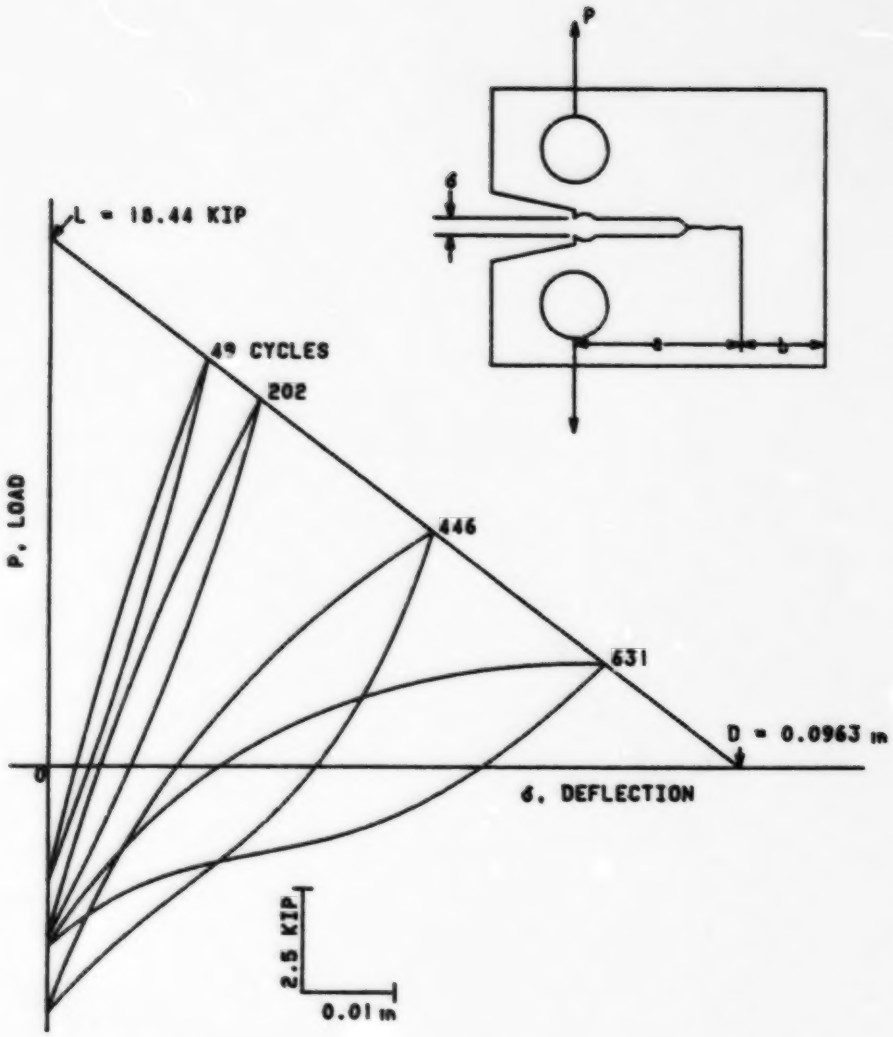

FIGURE B-6: LOAD VERSUS DEFLECTION HYSTERESIS LOOPS DURING DEFLECTION CONTROL TO A SLOPING LINE. (REF. 58) (L AND D ARE LOAD AND DEFLECTION INTERCEPTS RESPECTIVELY FOR MATERIAL A533B.)